TRACK TRAIN DYNAMICS
TECHNICAL DOCUMENTATION

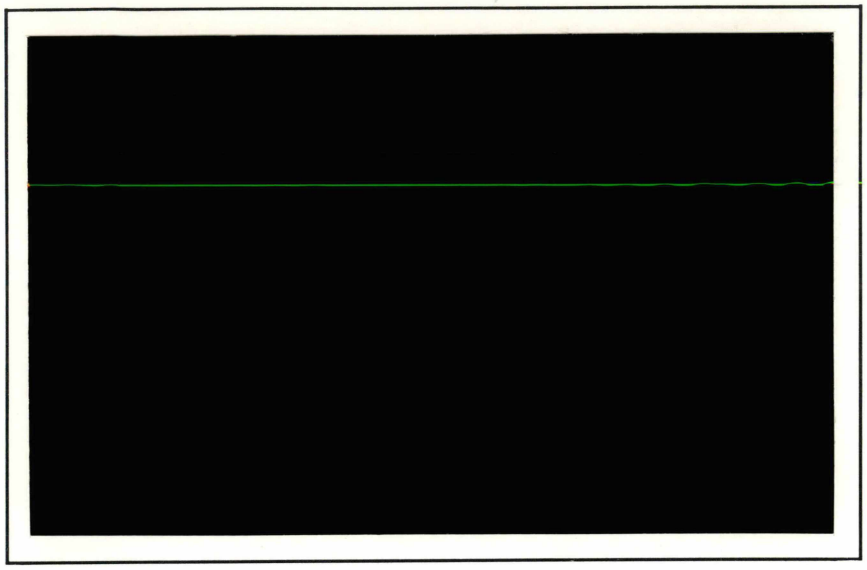

AAR

International Government-Industry
search Program on Track-Train Dynamics

03 - Rail Vehicles & Components

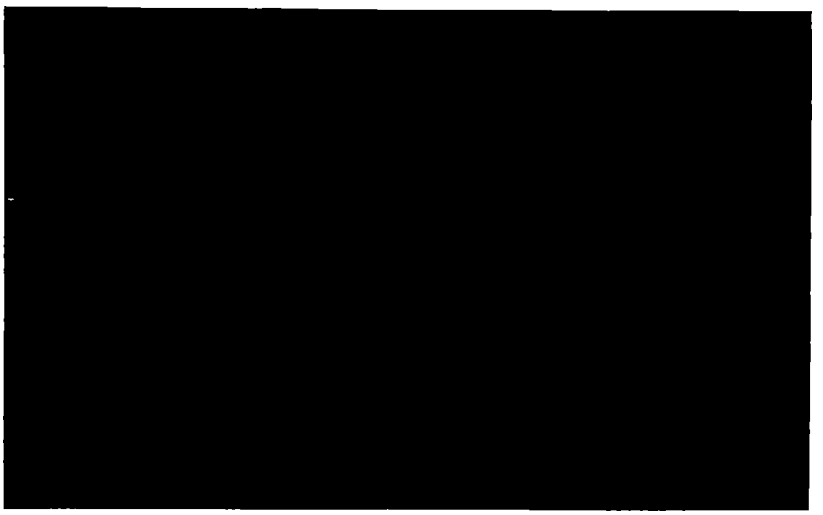

HIGH PERFORMANCE, HIGH CUBE COVERED HOPPER CAR PROGRAM, BASE CAR DYNAMIC PERFORMANCE TESTS

VOLUME 1 - ROCK-AND-ROLL AND BOUNCE

Report No. R-566

S. F. Kalaycioglu

S. K. Punwani

April, 1984

AAR Technical Center

Chicago, Illinois

1. REPORT NO.
R-566

2. REPORT DATE
April, 1984

3. PERIOD COVERED
Dec., 1982 through
Nov. 29, 1983

4. TITLE AND SUBTITLE
High Performance, High Cube Covered Hopper Car Program, Base Car Dynamic Performance Tests. Volume 1 - Rock-and-Roll and Bounce

5. AUTHOR(S)
Semih F. Kalaycioglu, Senior Engineer/Analyst
Swamidas K. Punwani, Asst. Manager., Applied Technology

6. PERFORMING ORGANIZATION NAME AND ADDRESS
Association of American Railroads
Track Train Dynamics
3140 South Federal Street
Chicago, Illinois 60616

7. TYPE OF REPORT
Research

8. CONTRACT OR GRANT NO.
DTFR 53-82-C-00251

9. SPONSORING AGENCY NAME AND ADDRESS
Federal Railroad Administration
400 7th Street, S. W.
Washington, D.C. 20590

10. NO. OF PAGES
105

11. NO. OF REFERENCES
11

12. SUPPLEMENTARY NOTES
Part of the Track Train Dynamics High Cube, High Performance Covered Hopper Car Program.

13. ABSTRACT
A series of dynamic performance tests were conducted on a 100-ton high cube (4750 cu. ft.) covered hopper car. This report describes the test program concerning the rock-and-roll and bounce tests, which were conducted on shimmed track sections at the Transportation Test Center in Pueblo Colorado.

The test results are presented for the base car, which will serve as the reference against which new prototype cars will be compared. This test program was part of the Track Train Dynamics High Cube, High Performance Covered Hopper Car Project.

14. SUBJECT TERMS
Bounce, Covered Hopper Car, Derailment, Pitch, Rock-and-Roll, Roll Angle, Track Perturbations, Wheel Unloading

15. AVAILABILITY STATEMENT
Assistant Vice President
AAR Technical Center
3140 S. Federal Street
Chicago, Illinois 60616

EXECUTIVE SUMMARY

The High Performance, High Cube Covered Hopper Car Project was initiated in 1980, as part of the Track Train Dynamics Program, with a view to promoting improved designs of cars. The supply industry was invited to develop and submit improved designs of covered hopper cars for test. Performance guidelines were issued for new car designs and included the outline for a test program. This document called for the testing of a current design (base line case) covered hopper car, against which each prototype car would be compared. A test base car was obtained on loan from the Missouri Pacific Railroad. A series of reports will describe in detail the base car test series. This particular report describes the rock-and roll and bounce regime tests.

The rock-and-roll and bounce tests were conducted on shimmed track sections in the Linear Induction Motor (LIM) track and Balloon Loop at the Transportation Test Center in Pueblo, Colorado. Both empty and loaded car tests were conducted.

For the rock-and-roll regime, the measurements of primary interest were the car body roll angles and vertical wheel loads, with particular regard to wheel lift and suspension system spring travel.

For the bounce regime, the vertical accelerations at the car body center plate and wheel loads were of primary interest.

The bounce and rock-and-roll test runs were conducted in such a manner that the resonance condition could be determined within 1 mph of the true resonant speed.

It was found from the results that track curvature did not affect the resonant roll speed of the vehicle. The maximum roll response was attained when the car body roll natural frequency coincided with that of the rail joint input frequency. The resulting maximum peak-to-peak roll angles on tangent track ranged from 9.3 degrees for the empty car to 10.6 degrees for the loaded car. The results from the curved track tests were comparable. It should be noted that the maximum peak-to-peak roll angle recommended in the AAR Guidelines is about 6 degrees.

The vertical wheel loads, measured on the leading wheel set of the empty car, were also comparable in both the tangent and curved track tests. Dynamic load factors exceeding twice the static wheel load were found in all of the test runs.

In the case of the loaded car, the maximum wheel loads were developed at speeds near the resonant speed of the vehicle. Dynamic load factors of more than 2.0 and sustained wheel unloadings, with a distance duration of 6 feet, were noted in the critical speed range of 15.5 to 19 mph.

The results of the bounce tests indicated that the car body vibrated at its input excitation frequencies and their harmonics. The vehicle experienced its bounce and pitch resonances near 56 mph, for which the natural frequency of the car body on its suspension system coincided with the

frequency at which the car passed the 39-foot rail joints.

A brief summary of the results is as follows:

Rock-and-Roll Tests

Track	Vehicle Configuration	Critical Speed (mph)	Peak-to-Peak Roll Angle (degrees)	Vertical Wheel Load Minimum (lb)	Vertical Wheel Load Maximum (lb)
Tangent	Empty	24.8	9.3	0	21,000
	Loaded	16.7	10.6	0	78,000
Curved	Empty	24.4	9.3	0	22,500
	Loaded	18.0	9.8	0	68,500

Bounce

Vehicle Configuration	Critical Speed (mph)	Vertical Acceleration [rms g's]	Vertical Acceleration [peak g's]	Vertical Wheel Load Minimum (lb)	Vertical Wheel Load Maximum (lb)
Empty	70 mph*	*	*	*	*
Loaded	56.3mph	0.4	1.2	9,500	58,000

* Not determined, because the critical speed was above the maximum speed tested.

The wheel loads shown here are the "peak" minimum and "peak" maximum values, and represent the absolute minimum and maximum values. Other statistical characterizations are discussed in the report.

ACKNOWLEDGEMENTS

The authors sincerely acknowledge their indebtedness to the Federal Railroad Administration for funding the Covered Hopper Car Test Program and for providing invaluable technical support during all phases of the test program. Special appreciation is expressed to Ms. Clare Orth and Mr. Alfred G. Bowers of the Federal Railroad Administration for their technical inputs.

The authors also wish to acknowledge Mr. Keith L. Hawthorne, Technical Director - A.A.R. Technical Center, and Mr. Roy A. Allen, Manager - Applied Technology, for their helpful guidance and encouragement throughout the test program.

The authors extend their appreciation to Mr. Nirangan Harralolka for his assistance in the data reduction and preparation of this report.

Special thanks to the crew members of the AAR-100 Research Car, Messrs. Frank Hirsh, Bill Sneed, Ron Bidweell, Jim Rzonca, Don Waldo and Alex Harrell.

Thanks are also expressed to Messrs. Osman Ahmad, Sean Judd and Bill Drish for their help in the test data reduction.

The authors thank the Missouri Pacific Railroad for the loan of the base covered hopper car to the Track Train Dynamics Program for use in the test program.

The authors also wish to express their appreciation to Dr. Robert F. Breese, for his editorial assistance and suggestions, and to Ms. Valerie Giles and Ms. Rita Potts for their hard work and patience in the preparation of the manuscript.

LIST OF SYMBOLS AND ABBREVIATIONS

Symbol (or) Abbreviation	Definition
AR4	A-end (leading), right side, fourth axle of the vehicle.
AL4	A-end (leading), left side, fourth axle of the vehicle.
L/V	Ratio of lateral to vertical wheel load.
AL	A-end (leading), left side.
AR	A-end (leading), right side.
ALD	Automatic location detector.
LIM	Linear Induction Motor (the name of the track where the rock-and-roll tests were conducted).
CG	Center of gravity.
L5*	The level that is exceeded ninety-five percent of the time.
L95*	The level that is exceeded five percent of the time.
LTD6MIN*	The minimum of all levels that are continuously sustained over a six foot length of track.
LTD6MAX*	The maximum of all levels that are continuously sustained over a six foot length of track.
RMS*	Root mean square.
STD*	Standard deviation.

* See Appendix A for more detailed descriptions.

TABLE OF CONTENTS

LIST OF TABLES

LIST OF FIGURES

LIST OF FIGURES (Continued)

LIST OF FIGURES (Continued)

LIST OF FIGURES (Continued)

1.0 INTRODUCTION

The cooperative international Track Train Dynamics Program initiated a High Performance, High Cube Covered Hopper Car Project in 1980 with the objective of encouraging the development of an improved covered hopper car. Industry derailment statistics pointed to the need for improving the performance of this car type, particularly the roll stability. After careful review of available dynamic performance test data, a set of performance guidelines were developed. These were described [1]* in terms of dynamic performance regimes, such as hunting, curving, curve entry, rock-and-roll and bounce.

These guidelines were published and railway industry suppliers were encouraged to develop cars with improved performance that would meet the provisions of the performance standards. After a review of industry-published test data, it was concluded that sufficient data were not available for the conventional 100-ton high cube covered hopper car. Thus, the project plan called for testing of a current design (base line case) covered hopper car, against which each new prototype car would be compared. The base car was obtained on loan from the Missouri Pacific Railroad for use in the test program.

---

* Numbers in square brackets [] refer to the References, listed in Section 10.0 of this report.

This report describes the dynamic test program and results for the roll, pitch and bounce regimes. The rock-and-roll performance of a covered hopper car is one of the major elements of the program, because of its relationship with operational safety.

The overall test series also examined other performance aspects of the base car, and these are reported in a total of four volumes. This report is Volume 1. Volume 2 [2] describes the hunting performance, Volume 3 [3] describes the curving performance and Volume 4 [4] presents a summary of all of the base car performance tests.

2.0 TEST CAR

Figure 1 shows the base car, a 100-ton covered hopper car with a capacity of 4750 cubic feet. The car is 57 ft., 4 in. over strikers and with a truck center distance of 45 ft., 9 in. The estimated center of gravity height is 95 inches loaded and 61 inches empty, above the top of rail. The car was equipped with conventional three-piece trucks, with constant-column friction damping and double roller conventional side bearings. Each spring group had seven AAR D-5 outer coil springs and nine AAR D-5 inner coil springs, with a capacity (at solid height) of 95,698 lb.. Other pertinent car dimensions are shown in Figure 2.

The test car was selected to be generically representative of a class which have exhibited performance deficiencies during revenue service operations.

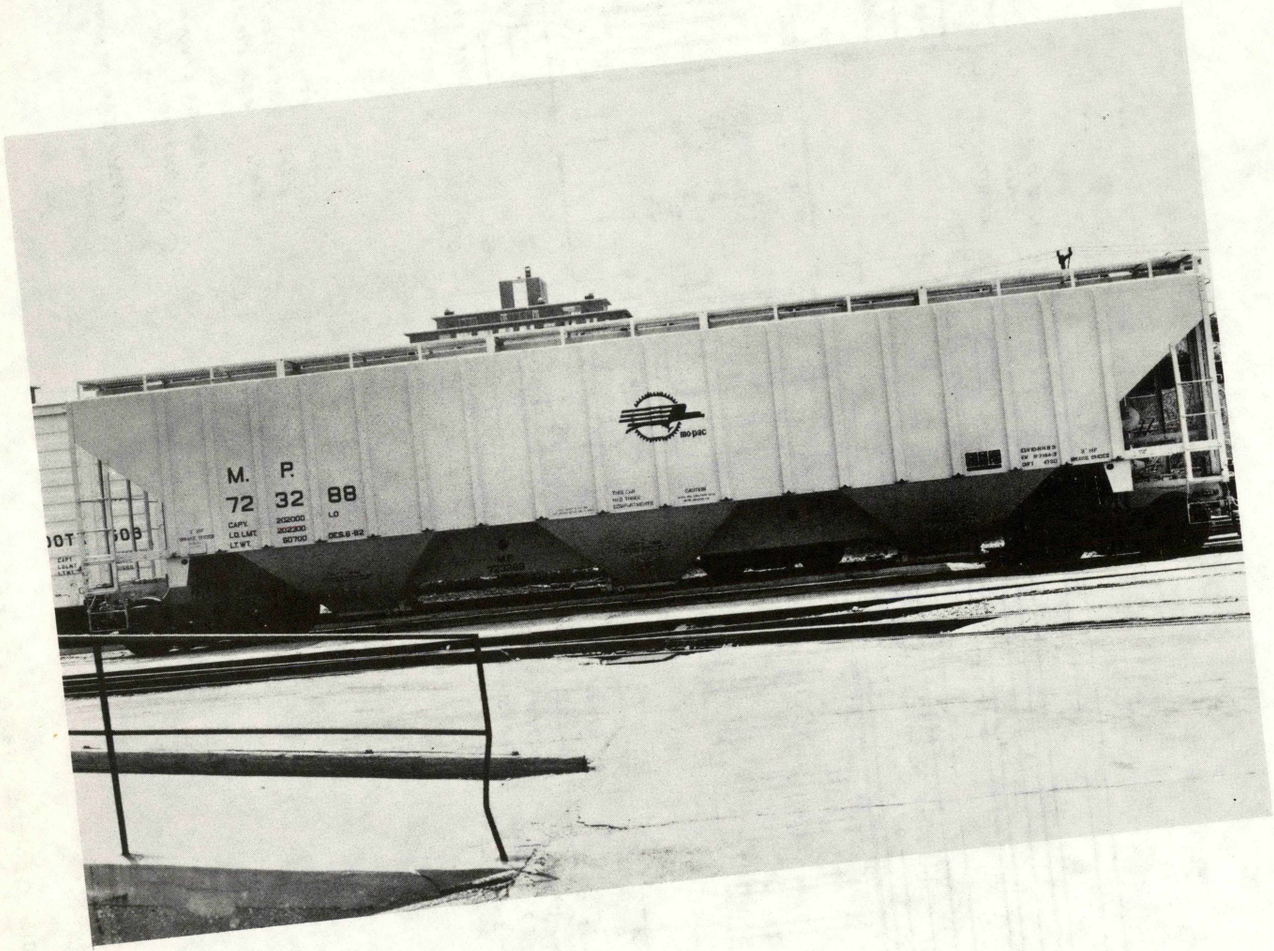

Figure 1. 100-ton High Cube (4750 cu. ft.) Covered Hopper Car, Used for the Dynamic Performance Tests.

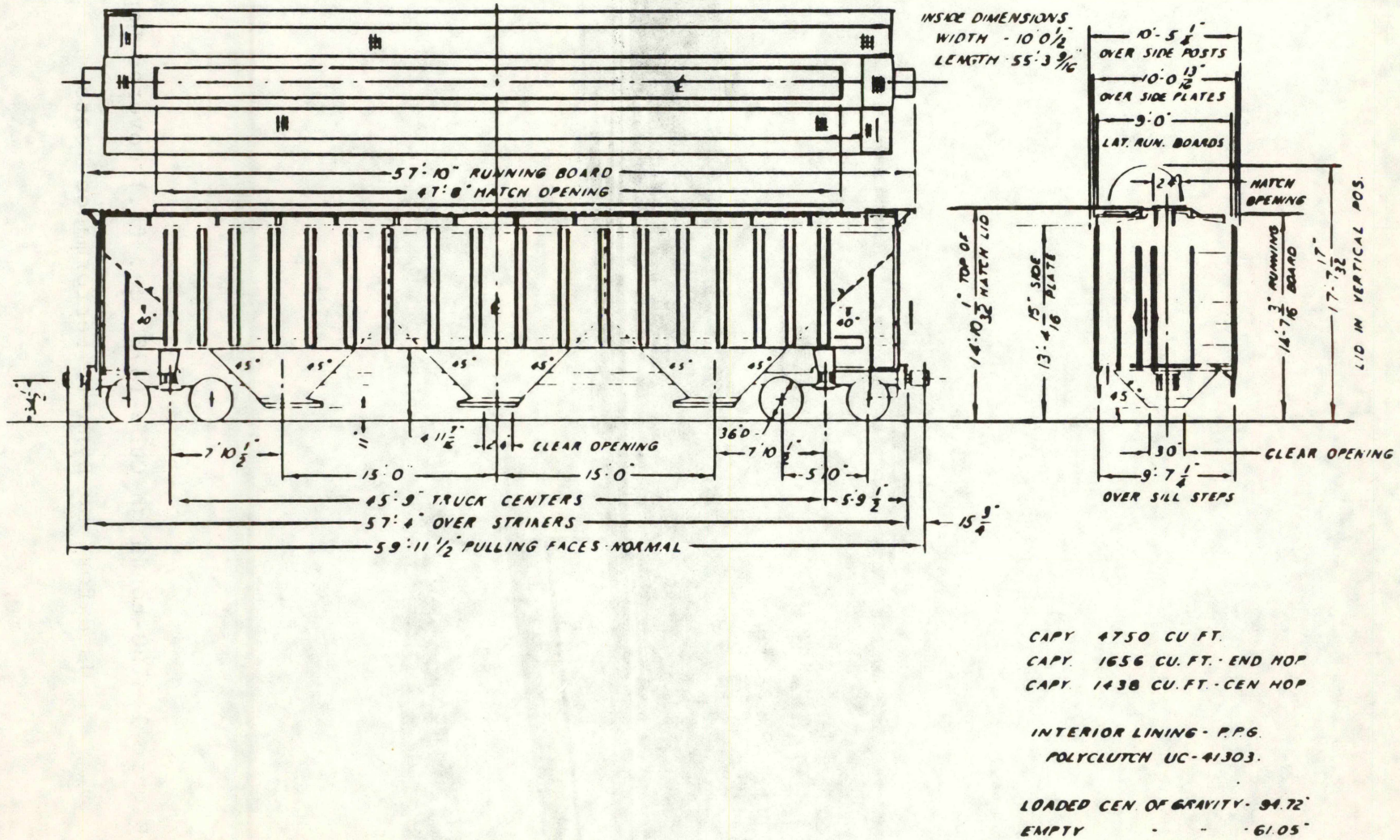

CAPY 4750 CU FT.
CAPY. 1656 CU. FT. - END HOP
CAPY. 1438 CU. FT. - CEN HOP

INTERIOR LINING - P.P.G.
POLYCLUTCH UC-41303.

LOADED CEN. OF GRAVITY - 94.72"
EMPTY - - 61.05"

Figure 2. General Dimensions of the Base (Reference) 100-ton Covered Hopper Test Car.

3.0 TEST PROGRAM

The Dynamic Performance Test Program was designed to quantify the essential parameters, for each dynamic performance regime, with which the base car could be judged and compared in relationship to any new prototype car. The dynamic performance regimes that are neccessary to characterize the performance of a car are related to wear and stability, and include curving, curve entry, hunting, rock-and-roll and bounce. The test program was designed around available track sites at the Transportation Test Center in Pueblo, Colorado, as shown in Figure 3. A Test Matrix summary for the rock-and-roll and bounce tests, including the test tracks that were used, is shown in Table 1. The rock-and-roll tests utilized perturbed track sections in the LIM (Linear Induction Motor) track and the Balloon Loop, which were shimmed in accordance with the pattern shown in Figure 4. Automatic location detectors (ALD) were placed on each of the test tracks to identify the various track loops and test sections. This system uses retroreflective markers on the track, and an infrared light emitting source and receiver system on the test car. For the LIM tangent track rock-and-roll section, ALD markers were placed at both ends of the shimmed section, which was approximately 400 feet in length. The curved track rock-and-roll section on the Balloon Loop was 400 feet long and was designated, for data reduction purposes, as Section 3 of the Balloon Loop. A guard rail was provided to prevent derailments. The Balloon Loop is a 7-1/2 degree curve with a 4-1/4 inch superelevation,

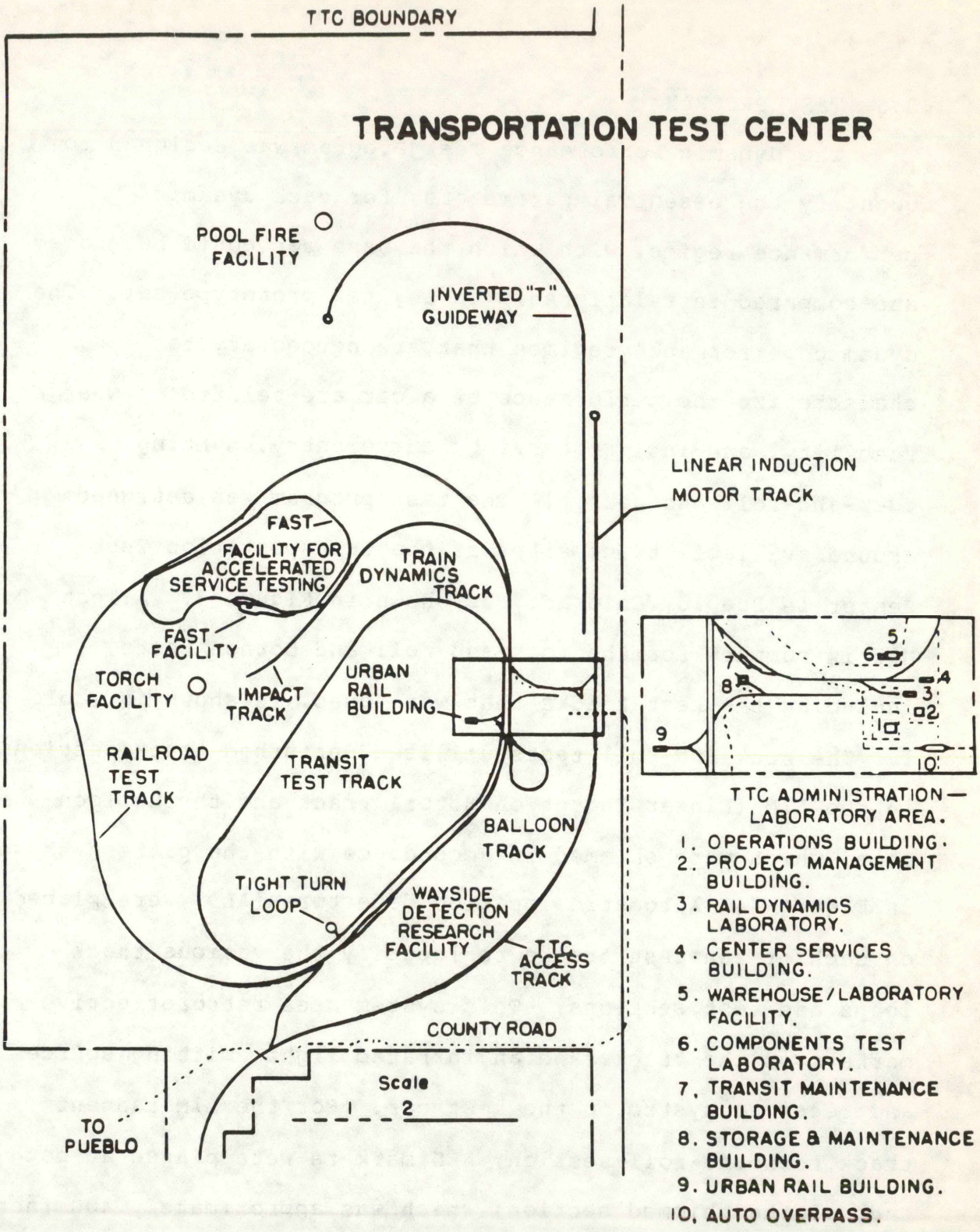

Figure 3. Schematic Diagram of the Transportation Test Center at Pueblo, Colorado, Showing Various Test Track Locations.

Table 1

Test Matrix Summary for the Base Covered Hopper Car Tests

DYNAMIC PERFORMANCE REGIME	LOADED	EMPTY	TEST TRACK USED
TANGENT ROCK-AND-ROLL	X	X	LIM
CURVE ROCK-AND-ROLL	X	X	BALLOON
BOUNCE	X	X	LIM

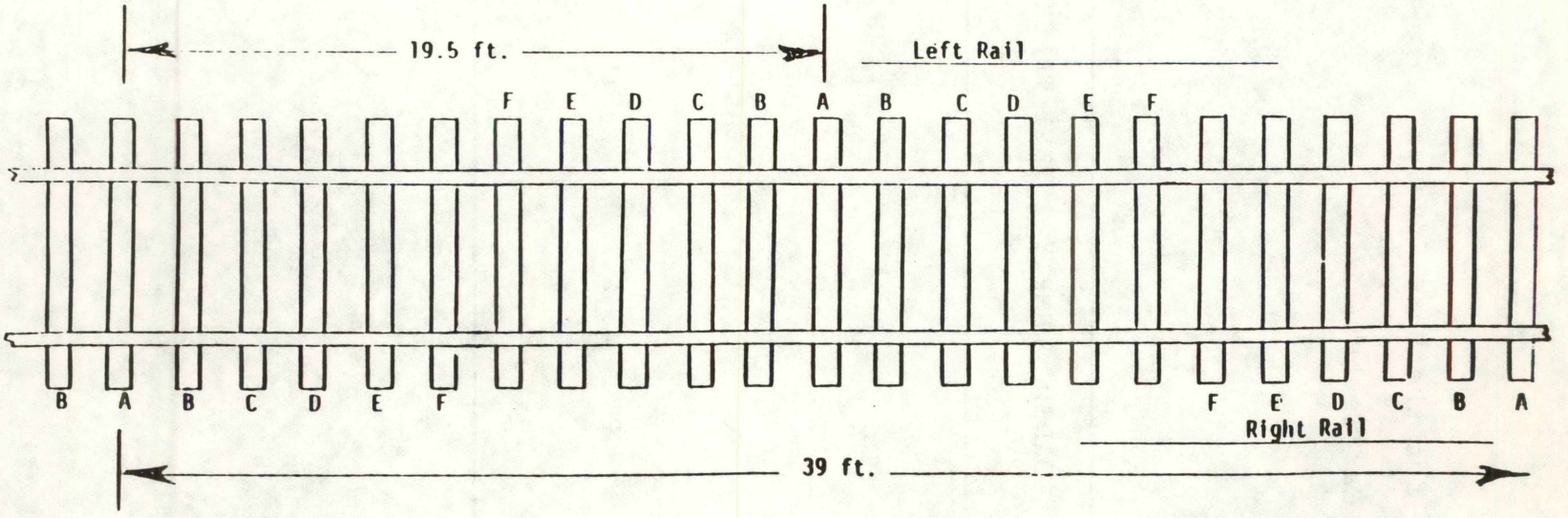

RAIL SHIMMING PATTERN (INCHES ± 0.1 INCH)

Tie A:	3/4	Tie D:	3/8
Tie B:	5/8	Tie E:	1/4
Tie C:	1/2	Tie F:	1/8

Tangent Track: At least 20 rail lengths total, each shimmed as indicated.
7-1/2° Curve. Balloon Loop: At least 10 rail lengths, starting at Station 3086 CCW, and shimmed as indicated.

Figure 4. Shimming Pattern for the Rock-and-roll Test Track Section.

resulting in a balance speed of about 30 mph.

4.0 TEST RUNS FOR ROCK-AND-ROLL AND BOUNCE

The test runs were made in one direction only over the perturbed sections. The general methodology was to locate the resonance condition within 1 mph, and to quantify the performance throughout a reasonable range of operating speeds. For the rock-and-roll tests, a speed increment of 2 mph was initially chosen. After bracketing the resonant speed range within 2 mph, intermediate speeds were then run. The runs started at 12 mph for the loaded car and 20 mph for the empty car. In each case, the runs continued until it was determined that resonance had been reached and passed, and the resonant speed was accurately located. The procedures were identical for both the curved and tangent track rock-and-roll runs.

The test runs for empty and loaded car bounce were conducted in a similar manner. The speed increments were 5 mph, starting at 20 mph, until the resonance condition had been achieved or the limiting track speed was reached.

5.0 TEST CONSIST AND INSTRUMENTATION

The test consist included, in order, a four-axle locomotive, the AAR-100 Research Car, a loaded 100-ton open-top hopper car, serving as a buffer car, the test car, and a follow-on buffer car. The A-end of the test car was the leading end in all of the tests.

The AAR-100 Research Car has been designed for data

collection, and includes a PDP 11/34 computer and associated hardware which was recently installed. An instrumentation block diagram for the on-board data collection system and transducer input cable connections is shown in Figure 5.

The data acquisition system was under the control of a general purpose data acquisition software program, described in Section 6. In all cases, a sampling rate of 256 samples/sec was used for each of the channels.

The transducers used for the rock-and-roll and bounce performance tests included two instrumented wheel sets, an angle-of-attack measurement device on the A-end (leading) truck and roll gyros. The vertical and lateral force measurement strain gages on each instrumented wheel, and the roll gyros were the principal transducers for the rock-and-roll tests. They were selected so as to directly evaluate the rock-and-roll performance. Other transducers were used to obtain supplementary information, that would be useful for modeling purposes, and for gaining insights into the effects of possible parametric variations of the design hardware. These parameters included spring displacements, side bearing forces and side frame/bolster relative displacements.

The instrumented wheel sets were of the IIT Research Institute design [5], in which each wheel had strain gages mounted on the wheel plate and electrically connected so as to form six separate full Wheatstone bridges: three vertical, two lateral and one position (lateral). After cross-channel corrections, the output from each was used to provide

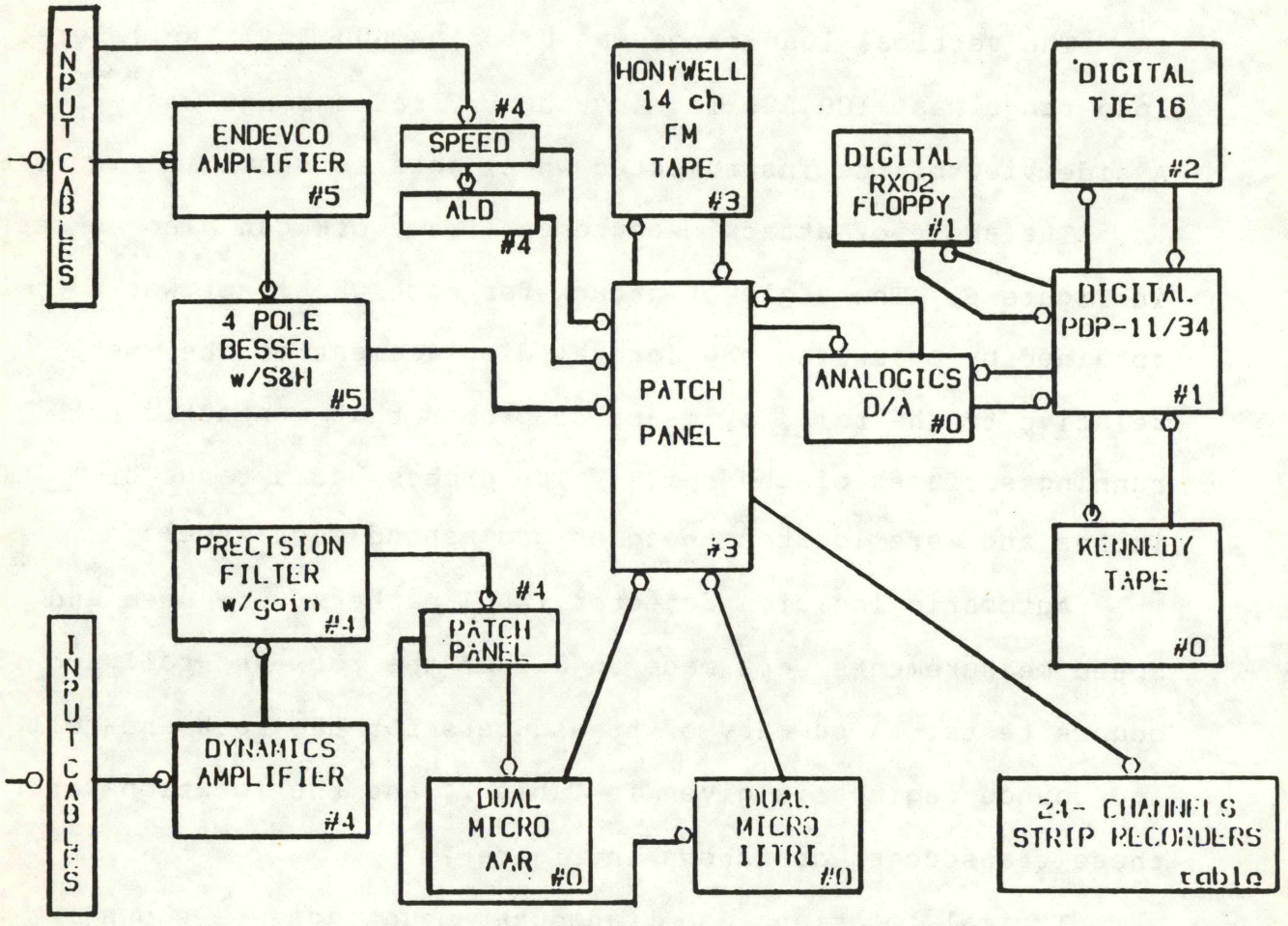

Figure 5. Block Diagram Showing the Data Collection System on the AAR-100 Research Car.

continuous vertical and lateral load measurements. This was done in real time by use of a dedicated microprocessor for each wheel set. A lateral to vertical load (L/V) ratio measurement was also provided continuously. Each microprocessor handled twelve channels of data (from one wheel set) and had its own analog-to-digital converter. It could also convert the digital data back into an analog format, for display on a strip chart recorder.

The vertical load range was 0 to 100,000 lb., the lateral load range was ±100,000 lb. and the L/V ratio range was ± 10. A side view of the instrumented wheel sets is shown in Figure 6.

The angle-of-attack measurement framework can also be seen in Figure 6. The angle-of-attack for each wheel set was obtained by measuring the lateral displacement of the wheel relative to the rail, by means of probes that contacted the running surfaces of the rails. The probes had a range of ± 2.0 inches and were located ahead of and behind each wheel.

Automatic location detector (ALD) markers were used and speed measurements were made in all of the rock-and-roll and bounce tests. A summary of transducers for the rock-and-roll and bounce regimes is given in Table 2, and the locations of these transducers are shown in Figure 7.

Typical locations and transducer mountings are shown in Figures 8, 9 and 10. Figure 8 shows the rate gyro for roll angle measurements, which incorporated an integrator in the associated signal conditioner to provide roll displacements directly in degrees. Figure 9 shows a vertical spring group displacement transducer, of the bending-beam-type, equipped

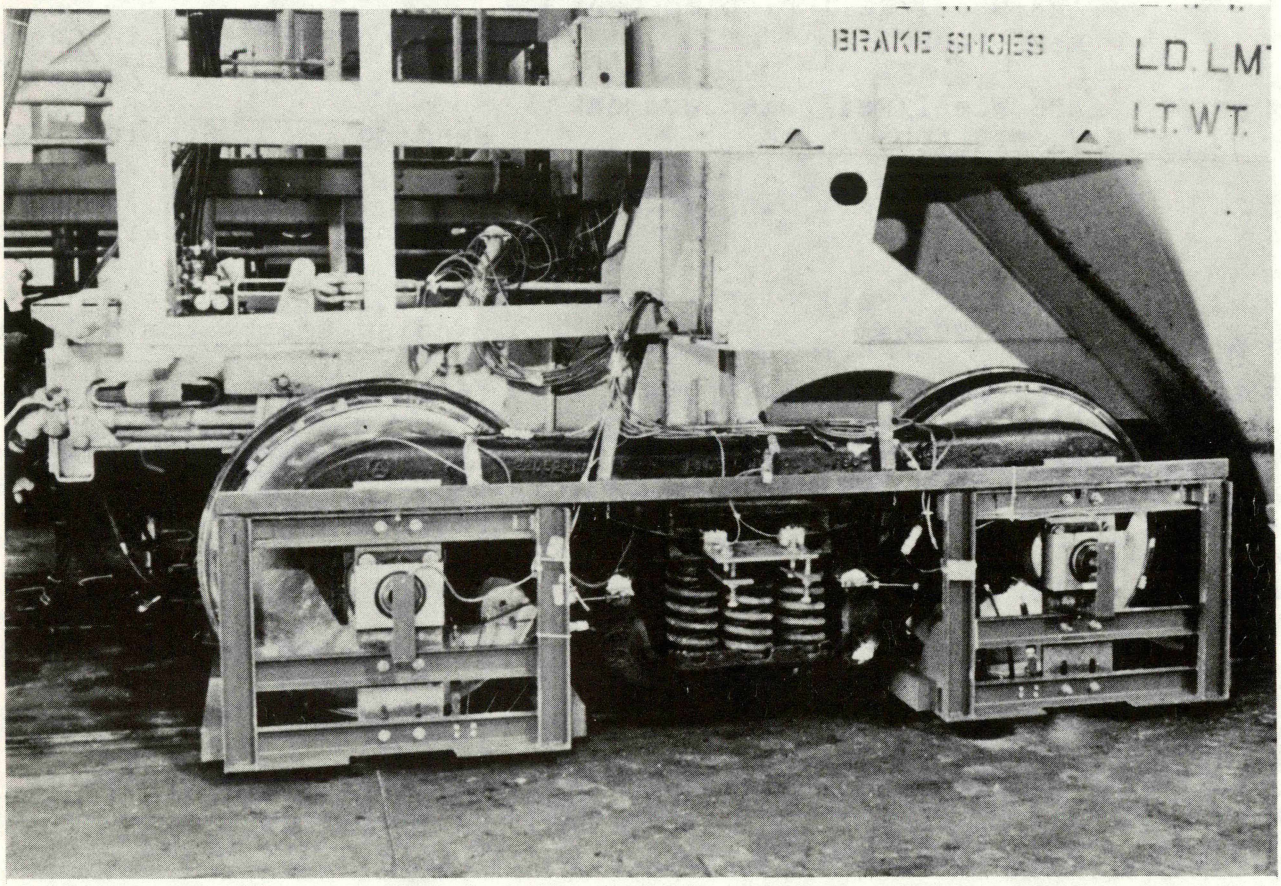

Figure 6. Instrumented Wheel Sets and Associated Angle-of-attack Measurement Frame for the A-end (Leading) Truck.

Table 2

Summary of Instrumentation for the Base Car Performance Tests.

Measurement No.	Parameter and Location	Transducer Type
1	Automatic Location Detector	--
2	Research Car Speed	--
3	AR3 Wheel/Rail Displacement Rear Probe	Bending Beam, Strain Gaged.
4	AR3 Wheel/Rail Displacement Front Probe	Bending Beam, Strain Gaged.
5	AR4 Wheel/Rail Displacement Rear Probe	Bending Beam, Strain Gaged.
6	AR4 Wheel/Rail Displacement Front Probe	Bending Beam, Strain Gaged.
7	AR3 Vertical Wheel Load	Instrumented Wheel Set.
8	AR3 Lateral Wheel Load	Instrumented Wheel Set.
9	AR3 L/V Ratio	Instrumented Wheel Set.
10	AL3 Vertical Wheel Load	Instrumented Wheel Set.
11	AL3 Lateral Wheel Load	Instrumented Wheel Set.
12	AL3 L/V Ratio	Instrumented Wheel Set.
13	AL4 Vertical Wheel Load	Instrumented Wheel Set.
14	AL4 Lateral Wheel Load	Instrumented Wheel Set.
15	AL4 L/V Ratio	Instrumented Wheel Set.
16	AR4 Vertical Wheel Load	Instrumented Wheel Set.
17	AR4 Lateral Wheel Load	Instrumented Wheel Set.
18	AR4 L/V Ratio	Instrumented Wheel Set.
19	AL3 Spring Travel	Bending Beam, Strain Gaged.
20	AL4 Spring Travel	Bending Beam, Strain Gaged.
21	BL Side Bearing Load	Load Cell.
22	BR Side Bearing Load	Load Cell.

Table 2 (Continued)

Measurement No.	Parameter and Location	Transducer Type
23	A-end Roll Gyro	Rate Gyro with Integrator Circuit.
24	B-end Roll Gyro	Rate Gryro with Integrator Circuit.
25	AL3 Side Frame-to-Bearing Adaptor, Longitudinal Displacement	Bending Beam, Strain Gaged.
26	AR3 Side Frame-to-Bearing Adaptor, Longitudinal Displacement	Bending Beam, Strain Gaged.
27	AL4 Side Frame-to-Bearing Adaptor, Longitudinal Displacement	Bending Beam, Strain Gaged.
28	AR4 Side Frame-to-Bearing Adaptor, Longitudinal Displacement	Bending Beam, Strain Gaged.
29	AL3 Side Frame-to-Bearing Adaptor, Lateral Displacement	Bending Beam, Strain Gaged.
30	AR3 Side Frame-to-Bearing Adaptor, Lateral Displacement	Bending Beam, Strain Gaged.
31	AL4 Side Frame-to-Bearing Adaptor, Lateral Displacement	Bending Beam, Strain Gaged.
32	AR4 Side Frame-to-Bearing Adaptor, Lateral Displacement	Bending Beam, Strain Gaged.
33	A-end Lateral Acceleration at Car Body Center of Gravity	Bell & Howell Accelerometer.
34	B-end Lateral Acceleration at Car Body Center of Gravity	Bell & Howell Accelerometer.
35	AL Side Sill Lateral Acceleration	Bell & Howell Accelerometer.

Table 2 (Continued)

Measurement No.	Parameter and Location	Transducer Type
36	AR Side Sill Lateral Acceleration	Bell & Howell Accelerometer.
37	BL Side Sill Lateral Acceleration	Bell & Howell Accelerometer.
38	BR Side Sill Lateral Acceleration	Bell & Howell Accelerometer.
39	AR3 Bearing Adapter Lateral Acceleration	Setra Accelerometer.
40	AR4 Bearing Adapter Lateral Acceleration	Setra Accelerometer.
41	BR1 Bearing Adapter Lateral Acceleration	Setra Accelerometer.
42	BR2 Bearing Adapter Lateral Acceleration	Setra Accelerometer.
43	A-end Center Plate Vertical Acceleration	String Potentiometer.
44	B-end Center Plate Vertical Acceleration	String Potentiometer.
77	A-end Left Truck Swivel	String Potentiometer.
78	A-end Right Truck Swivel	String Potentiometer.
79	A-end Right Spring Travel	String Potentiometer.

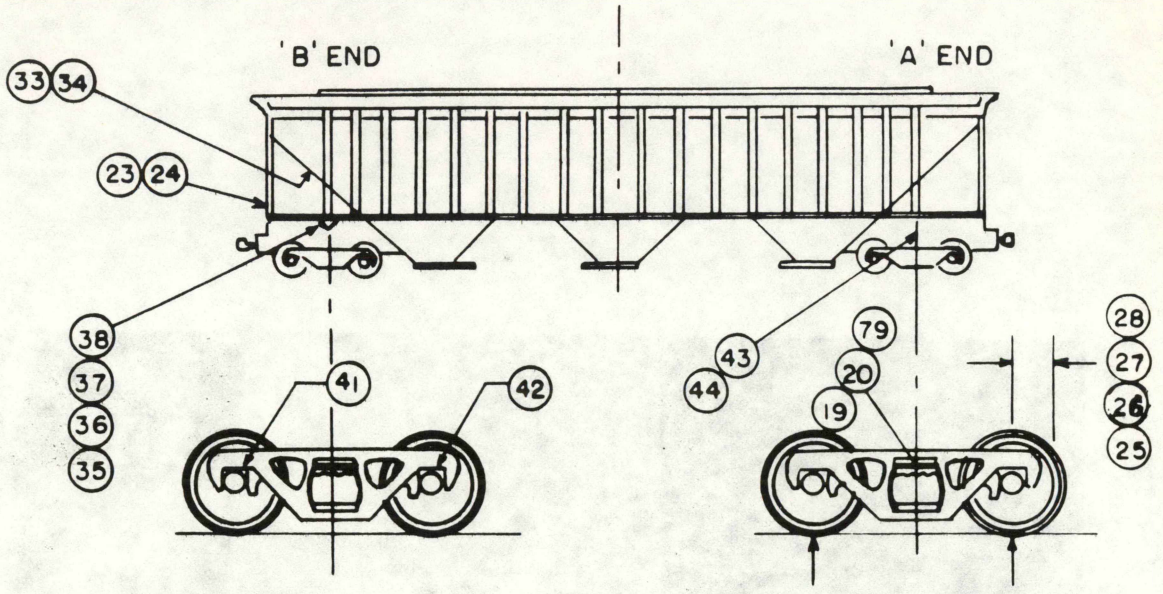

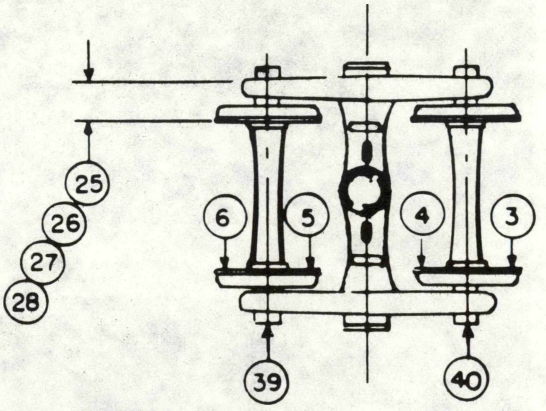

(1) AUTOMATIC LOCATION DETECTOR (ALD).
(2) SPEED.
(3) (4) (5) (6) ANGLE-OF-ATTACK PROBES TO MEASURE WHEELSET DISPLACEMENT RELATIVE TO RAIL.
(7) thru (18) VERTICAL, LATERAL, L/V: AL3, AL4, AR3, AR4 WHEELS.
(19) SPRING TRAVEL, ARL.
(20) " " "
(79) " " AR.
(21) SIDE BEARING LOAD, BL and BR.
(22) " " " " " "
(23) GYRO ON ℄ CAR (AT EACH END).
(24) " " " " " " "
(25) (26) (27) (28) SIDE FRAME/WHEELSET LATERAL and LONGITUDINAL DISPLACEMENT. 'A' END TRUCK ONLY.

(33) (34) LATERAL ACCELEROMETER AT C.G. HEIGHT. (BOTH ENDS.)
(35) (36) (37) (38) LATERAL ACCELEROMETER ON SIDE SILL AL, AR, BL, BR.
(39) (40) LATERAL ACCELEROMETER ON ROLLER BEARING
(41) (42) ADAPTER BR1, BR2, AR3, AR4.

(77) TRUCK YAW
(78) SWIVEL AL, AR.

Figure 7. Transducer Locations for the Base Car Tests.

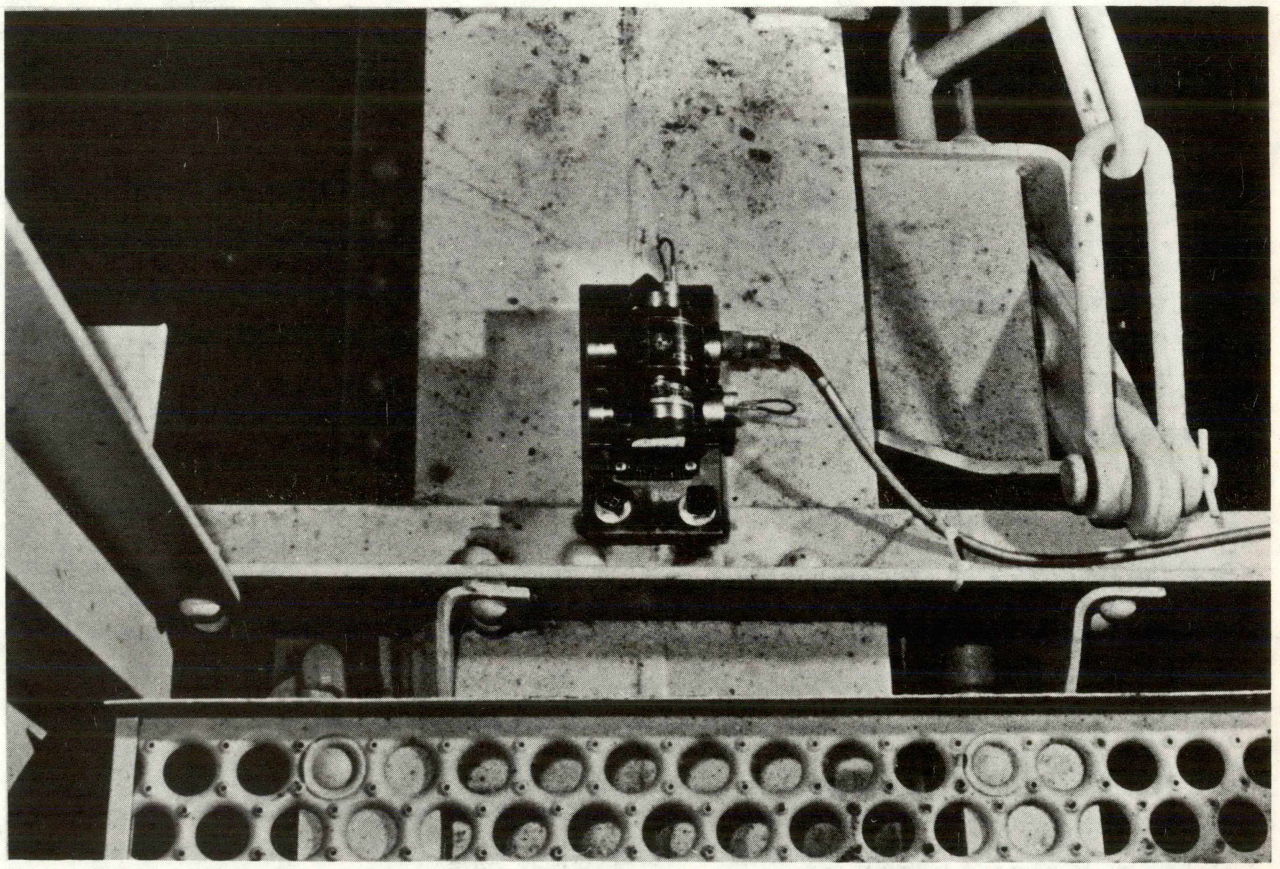

Figure 8. Rate Gyro for Measuring Car Body Roll Angles, Mounted on the Centerline of the Test Car Center Sill, Near the End Sill.

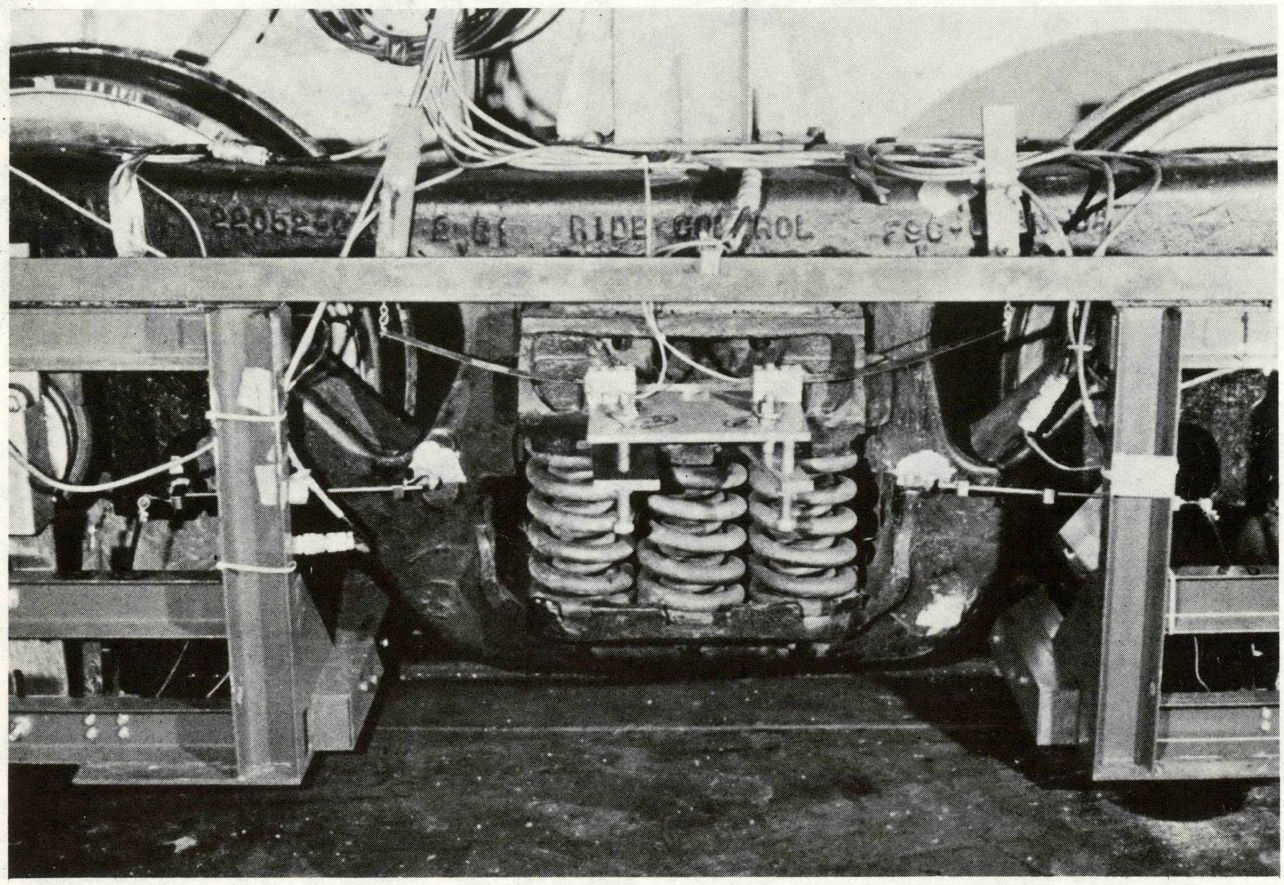

Figure 9. Strain-gaged Bending-beam-type of Transducer, for Measuring Test Car Spring Travel (Deflection).

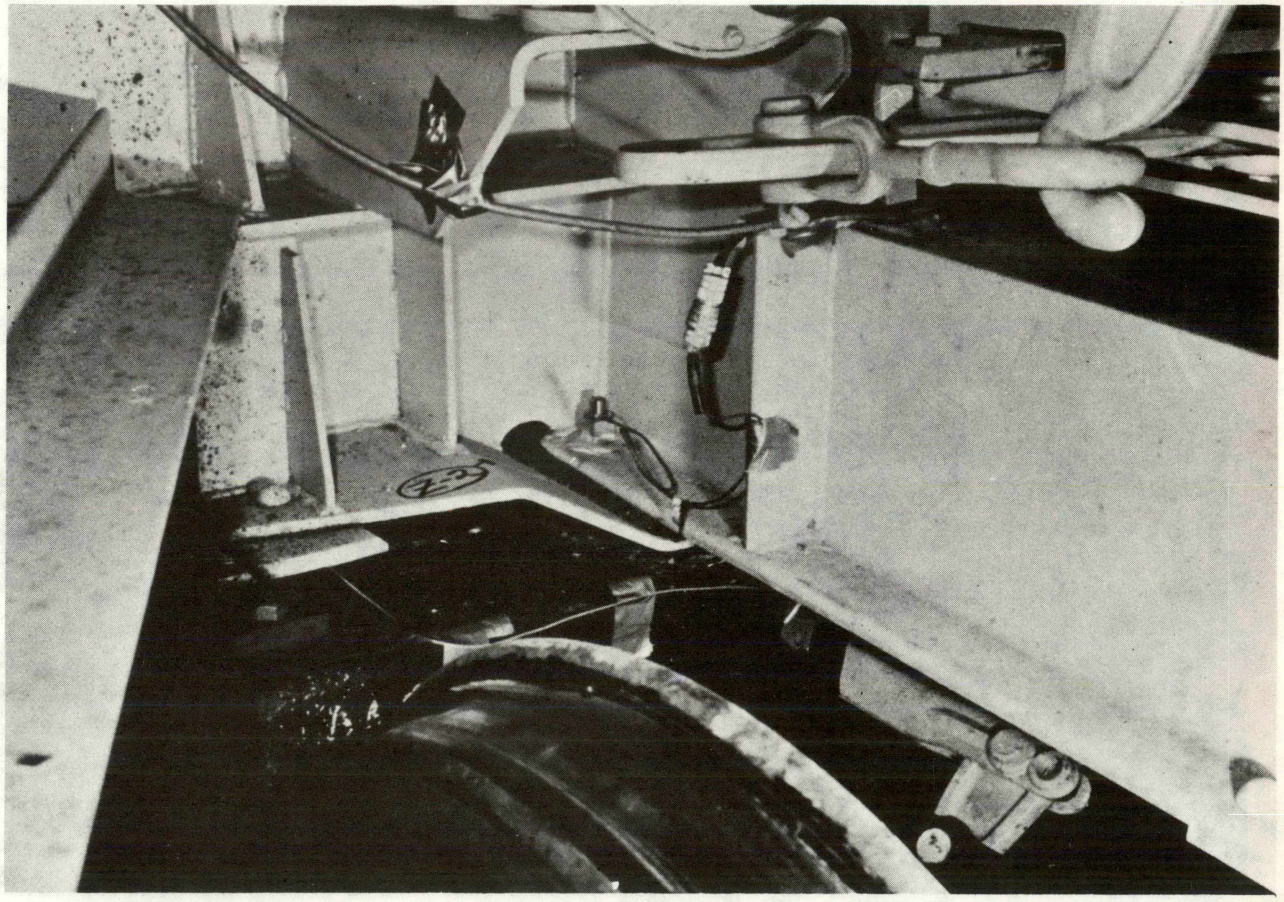

Figure 10. Vertical Acceleration Transducer, Mounted on the Center Sill Flange Near the Car Body Center Plate.

with strain gages and having an effective linear range of ± 4 inches. Figure 10 shows a typical vertical accelerometer near the body center plate. These were of the strain-gage-type, with a range of ± 6.0 g.

6.0 DATA ACQUISITION

The digital data acquisition software was comprised of five program modules, each dedicated to a specific part of the data acquisition.

An initialization file was created by one of the program modules and provided system runtime information, such as the sample rate, channels to be acquired and tape record length, to the data collection modules. For additional test condition information, test and channel descriptor records were written to this file. The channel descriptor record provided information on each data channel, including the characteristics of the transducer used and its calibration values.

At the beginning of the data acquisition process, the test and channel descriptor records were written onto tape. Communications among the various data acquisition peripherals, data collection and transfer were controlled by the acquisition program data collection modules.

The outputs from the transducers were sent first to the associated signal conditioners. In order to prevent aliasing of the high frequency information, the signals were filtered at about 100 Hz. The filtered signals were then amplified to a level suitable for the analog-to-digital conversion process.

Next in line was the patch panel, by means of which the conditioned signals were sent to the analog-to-digital converter. The ANDS 5400 analog-to-digital converter digitized the high-level analog input signals and the resulting data were transferred by direct memory access techniques to the tape recorder buffers in the computer. The digitized data were recorded on magnetic tape until the data acquisition was terminated. During data collection, four simultaneous channels of digital-to-analog output monitoring on strip chart recorders could also be supported by the program.

The remaining program modules were dedicated to playing the digitized data back after data collection. In this mode, the digital data were converted back into analog signals for display on a strip chart recorder.

A Quick-look Program could be used to check the statistical properties of the data (in engineering units) for selected test runs, in order to permit the test crew to examine the integrity of the data.

7.0 DATA REDUCTION AND ANALYSIS

The data were collected on digital tapes for each of the test runs in each performance regime. The tapes were copied at the Transportation Test Center in Pueblo, Colorado, and then sent to the AAR Chicago office for data reduction and analysis on the DECSYSTEM-2060 mainframe computer.

The subsequent processing of the test data was accomplished in three categories, as follows:

1) Data re-formatting,

2) Data pre-processing and

3) Data analysis.

The first phase in the data reduction was the preparation of the raw data for detailed examination. The data (in binary format) were first converted to the DECSYSTEM-2060 format. The calibration signals recorded prior to data collection were compared with the nominal calibration values for each measurement. The sensitivity factors (ratio of mechanical input to electrical output) were recalculated, and the data (in volts) were then converted into engineering units. Before storing the data in the data base, the ALD photocell voltage time history was processed for section identification, by using a routine which interpreted the specific time intervals between the recorded pulses.

The next step in data reduction was to prepare the data for analysis. During data collection activities, many problems can arise for a variety of reasons and spurious values can be injected into the data. Failure of the analog-to-digital converter, resulting in high bit dropouts, failure of the magnetic tape drive, causing a temporary record loss, transducer malfunction and extraneous noise picked up in the test environment are all examples of some of these problems. As an example, random points present in the data may introduce spurious frequencies into the power spectral density (PSD) plots, show false peaks, bias the probability density function (PDF) plots and subsequently alter the

characteristics of the physical phenomenon inherent in the data. It is, therefore, necessary to detect and eliminate "outliers" in the overall data reduction process, before a detailed data analysis can begin.

The key parameters of interest, such as wheel loads and accelerations, were plotted and hard copies of these plots were studied. An interactive pre-processing program was then used to remove any detected level shifts and trends, outliers and other types of errors. This program also allowed the user to examine the probability and power spectral density plots, as well as to digitally filter the data within a specified frequency bandwidth. Finally, all of the selected portions of data were made ready for analysis.

In the last phase of the data reduction, programs were used to determine maxima, minima, rms and mean values, standard deviations and other statistical descriptors that are used to determine the exceedences of various threshold levels. The data reduction and analysis procedures are described in Appendix A. The key parameters that were selected to quantify the performance of the vehicle in the prescribed test regime are described in the following sections.

8.0 TEST RESULTS FOR THE ROCK-AND-ROLL REGIME

The primary objective of the data reduction and analysis in the rock-and-roll regime was to determine the effects of extreme car body roll on the low speed operation of the base covered hopper car, running over a perturbed track section

with staggered rail joints. The key parameters, used to describe the dynamic performance of the vehicle, were:

1) Peak-to-peak car body roll angles, used to identify the critical rock-and-roll speed of the vehicle, and

2) Vertical wheel loads.

As a result of excessive car body roll, significant dynamic loads are imposed on the truck components, particularly after the car body rolls onto the side bearings. Depending upon the magnitude of the roll, the weight of the car may, in effect, be shifted onto the side bearings, resulting in spring bottoming and wheel lifts. The vertical load distribution on all four wheels of a truck may also vary considerably.

Maximum and minimum levels of the wheel loads, as measured at the leading wheel set of the leading truck, along with their associated time durations, were obtained, and the dynamic wheel loadings and unloadings calculated. The statistical descriptors used to quantify the maximum wheel load levels were the peak and L95 values. The L95 value of a parameter is defined as the level which is exceeded only 5 percent of the total time [6]. The wheel unloading is described in terms of a minimum "peak" load and a minimum load level, called the LTD6MIN, that is sustained continuously over a 6-foot-long track segment.

8.1 Rock-and-roll on Tangent Track

The test data were reduced and analyzed for the

base car in the empty and loaded conditions. In order to determine the critical speed of the empty base car, the roll angle time histories were plotted and studied for all of the test runs. Two of these traces are shown in Figures 11 and 12, which represent the response of the vehicle for an extreme case of rock-and-roll. A steady state response was observed at speeds below the resonant roll condition. At 20.77 mph, an average peak-to-peak roll angle of 4.5 degrees was experienced. As the speed of the vehicle increased, the response of the vehicle changed. At 30.5 mph, the roll response was no longer a steady state one, since the amplitudes of the motion varied with time, as found in nonlinear systems. A maximum peak-to-peak roll angle of 7.3 degrees was noted in this case.

The resonance condition, occurring at a speed where the car body experienced its maximum roll angle, was determined to be between 24 and 25 mph. The roll angle time history (Figure 13) for the leading end of the carbody at 24.84 mph showed a maximum peak-to-peak roll angle of 8.9 degrees. The corresponding value for the trailing end was 9.3 degrees (Figure 14).

To illustrate the peak roll response and show the location of the critical rock-and-roll speed, the maximum roll angles are plotted as a function of vehicle speed for the leading and trailing ends in Figure 15. As seen in this figure, the trailing end of the car body rolled slightly more than the leading end.

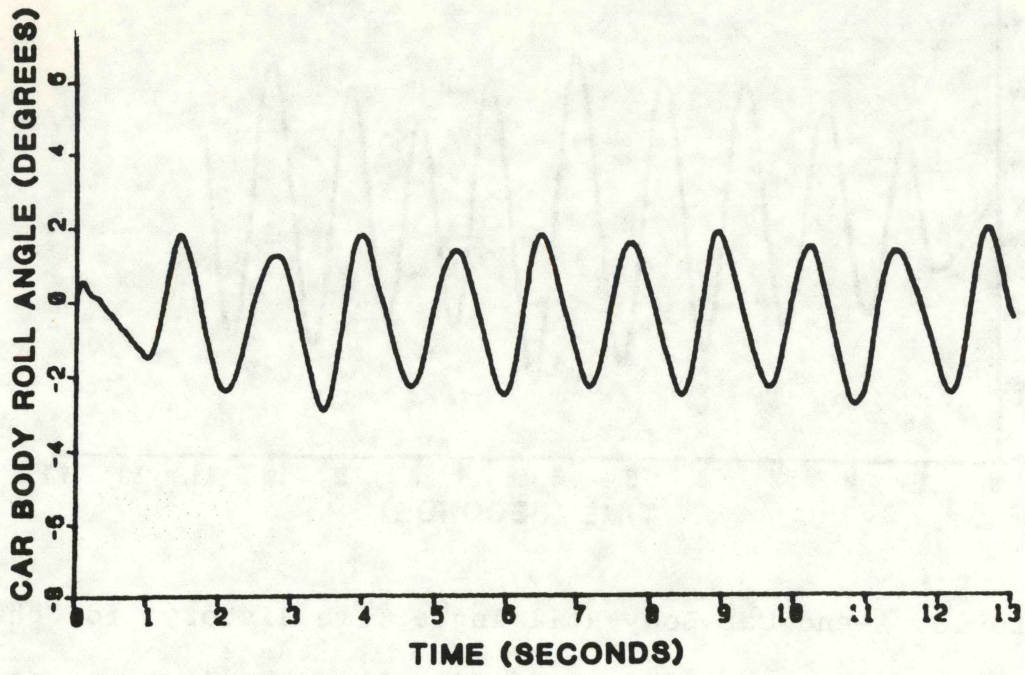

Figure 11. A-end Car Body Roll Angle Time History, for the Empty Base Car at 20.77 mph in the Rock-and-roll Regime on Tangent Track.

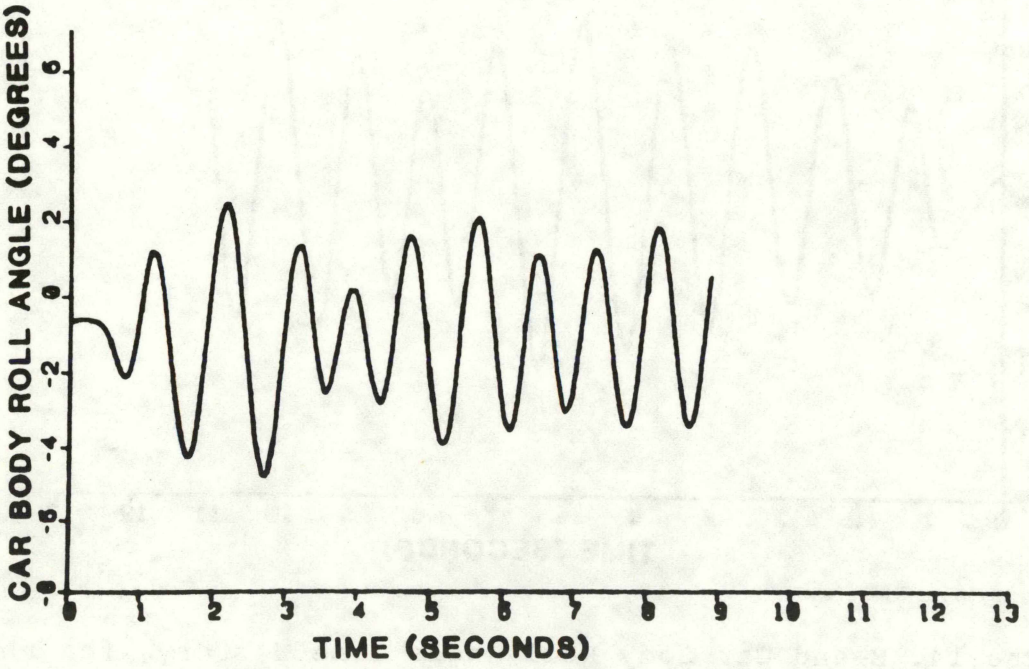

Figure 12. A-end Car Body Roll Angle Time History, for the Empty Base Car at 30.53 mph in the Rock-and-roll Regime on Tangent Track.

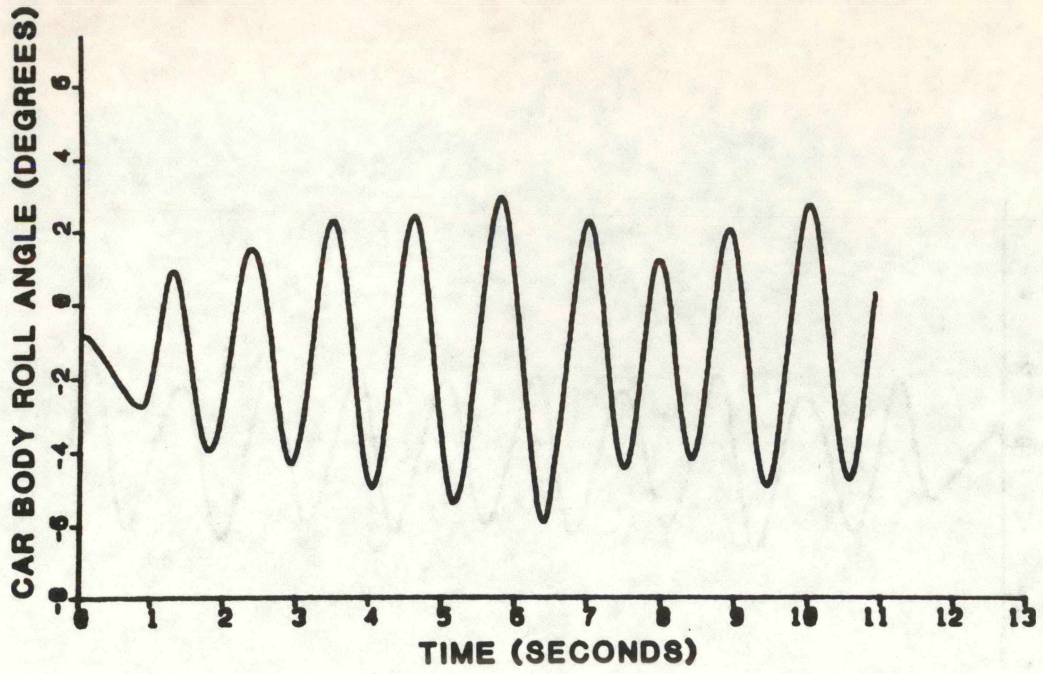

Figure 13. A-end Car Body Roll Angle Time History, for the Empty Base Car at 24.84 mph in the Rock-and-roll Regime on Tangent Track.

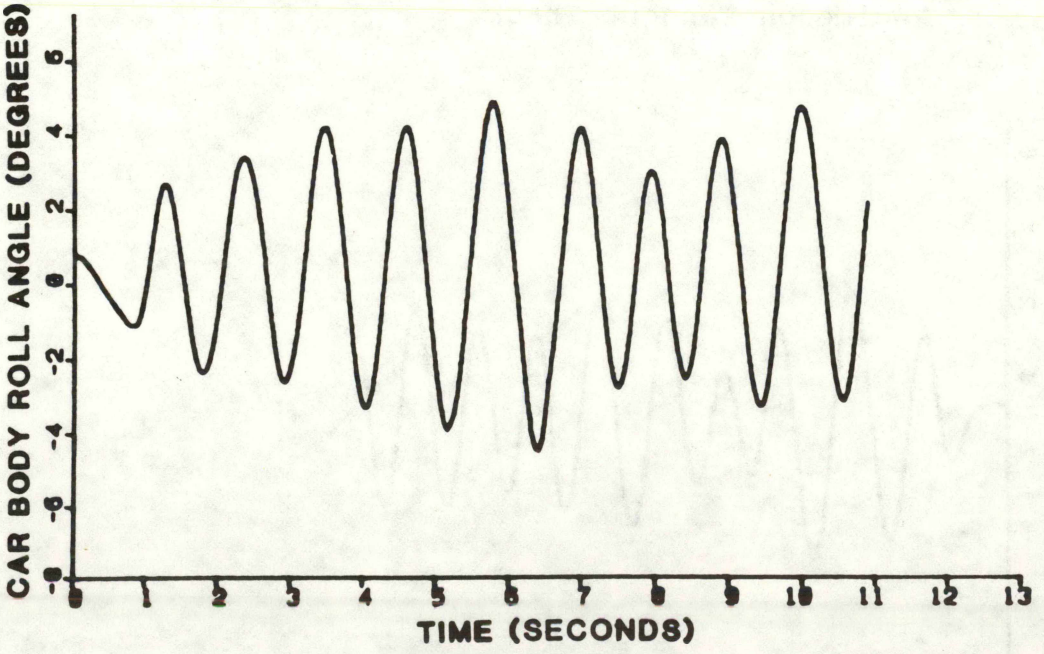

Figure 14. B-end Car Body Roll Angle Time History, for the Empty Base Car at 24.84 mph in the Rock-and-roll Regime on Tangent Track.

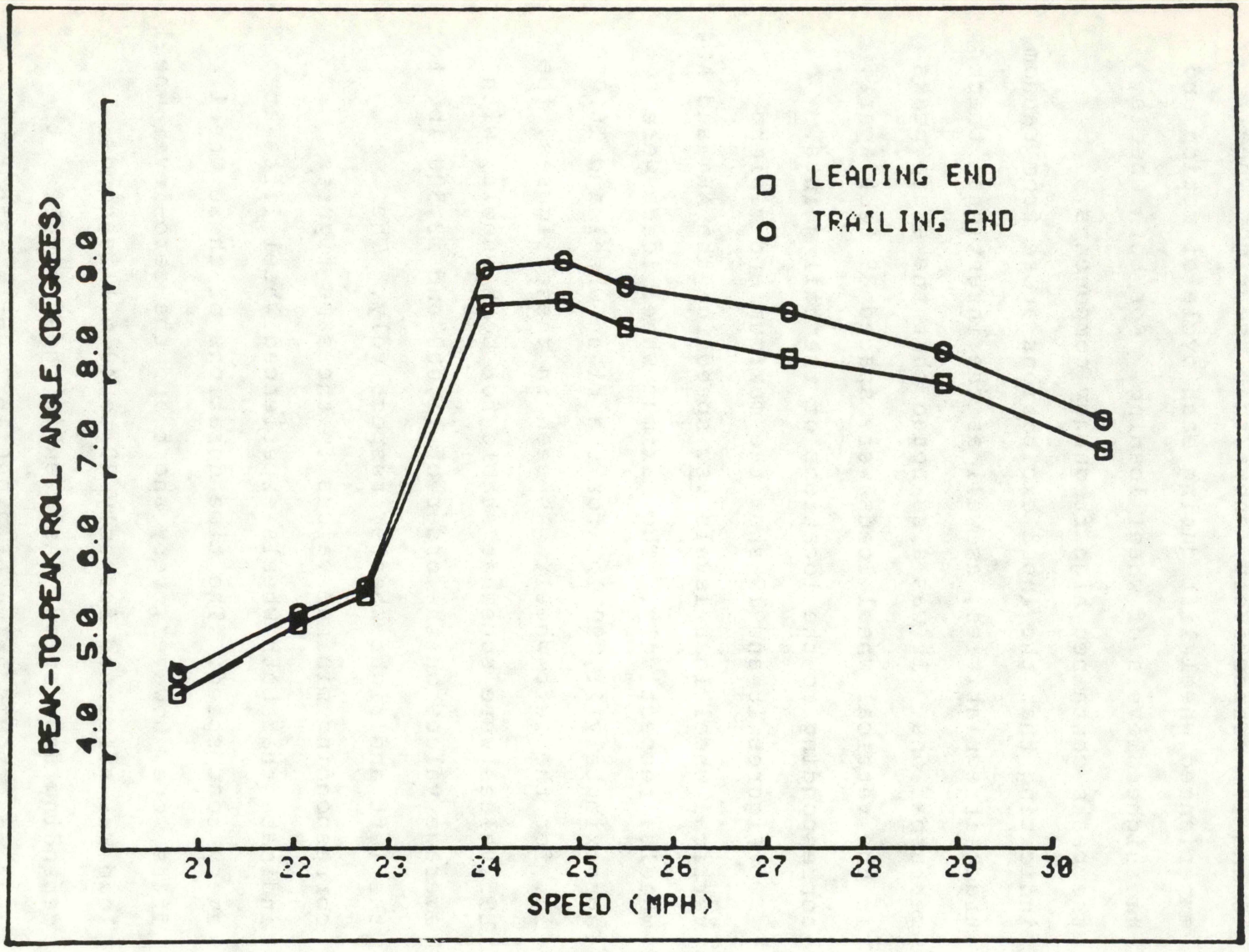

Figure 15. Car Body Roll Angle vs. Speed, for the Empty Base Car in the Rock-and-roll Regime on Tangent Track.

An examination of the vertical wheel load time histories for the AR4 (leading end, right side) and AL4 (leading end, left side) wheels at 24.84 mph, in Figures 16 and 17, respectively, shows that the right wheel experienced wheel lift during each cycle of motion and had higher levels of wheel loading. For both wheels, the peaks contained high frequency components, indicating that the input excitations arose from random track irregularities, as well as the intentional track perturbations. It was also noted that the sharp peaks in the vertical wheel loads were spaced 39 feet apart, corresponding to the locations of the rail joints.

Figures 18 and 19 show the maximum and minimum vertical wheel load levels vs. speed for the AR4 and AL4 wheels, respectively. The maximum wheel loads were approximately 21,000 lb. for the right wheel and 16,000 lb. for the left wheel. As seen in these figures, the L95 values were somewhat stable for both wheels, with average values on the order of 11,000 and 13,500 lb. for the left and right wheels, respectively. The corresponding minimum values in the same figures indicate that both wheels experienced wheel lifts at every test speed. The time durations of these wheel lifts were, however, very short and the zero-level wheel load was sustained for only 20 to 40 milliseconds, depending upon speed. As seen in these figures, the average LTD6MIN value of 2,000 lb. over a 6-foot distance indicated that there was, assuming a static

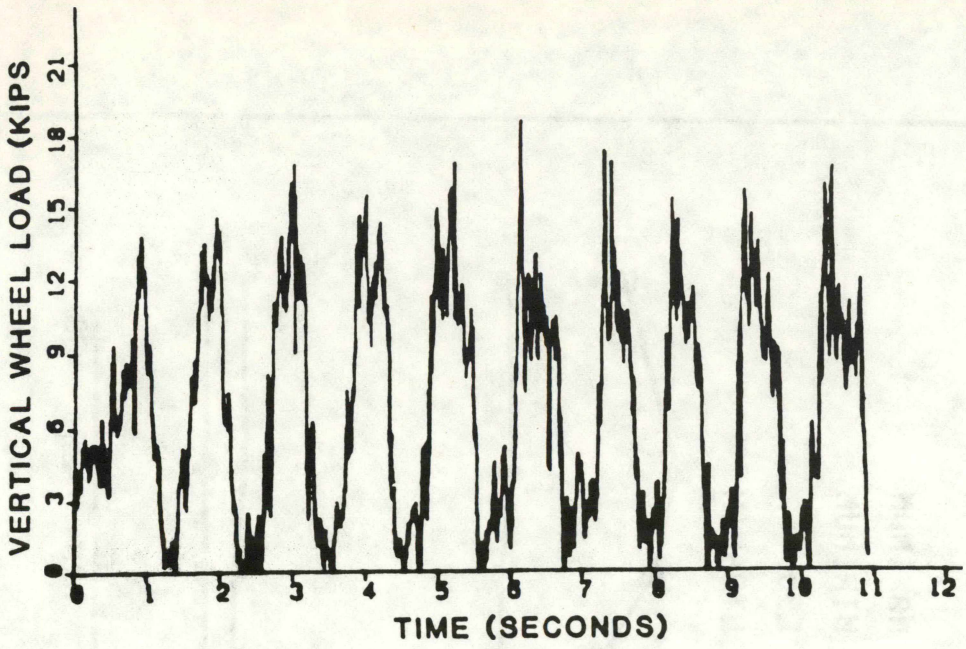

Figure 16. AR4 Vertical Wheel Load Time History, for the Empty Base Car at 24.84 mph in the Rock-and-roll Regime on Tangent Track.

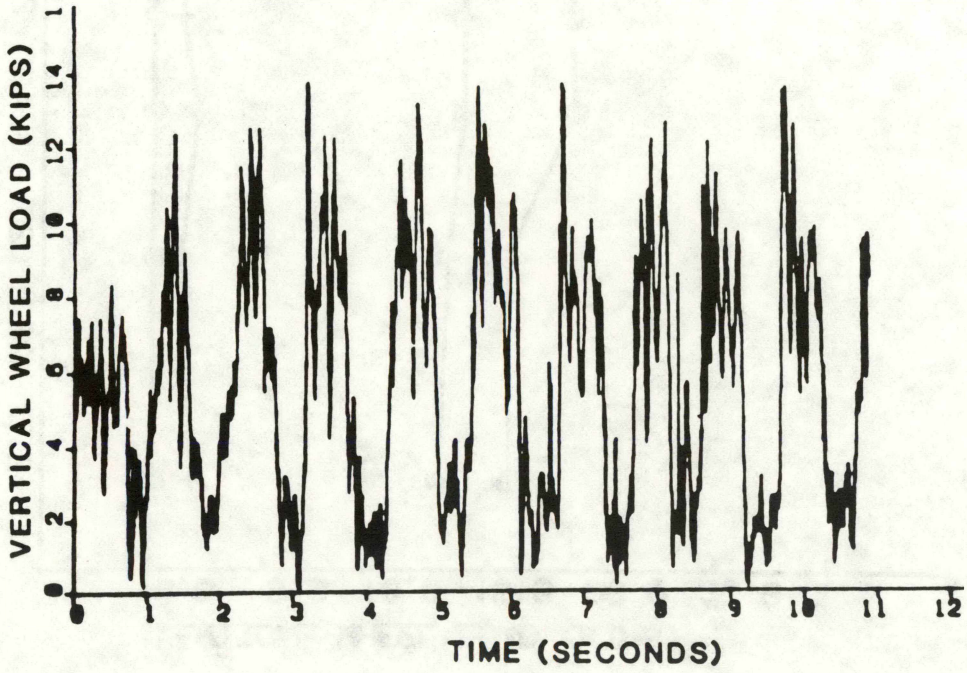

Figure 17. AL4 Vertical Wheel Load Time History, for the Empty Base Car at 24.84 mph in the Rock-and-roll Regime on Tangent Track.

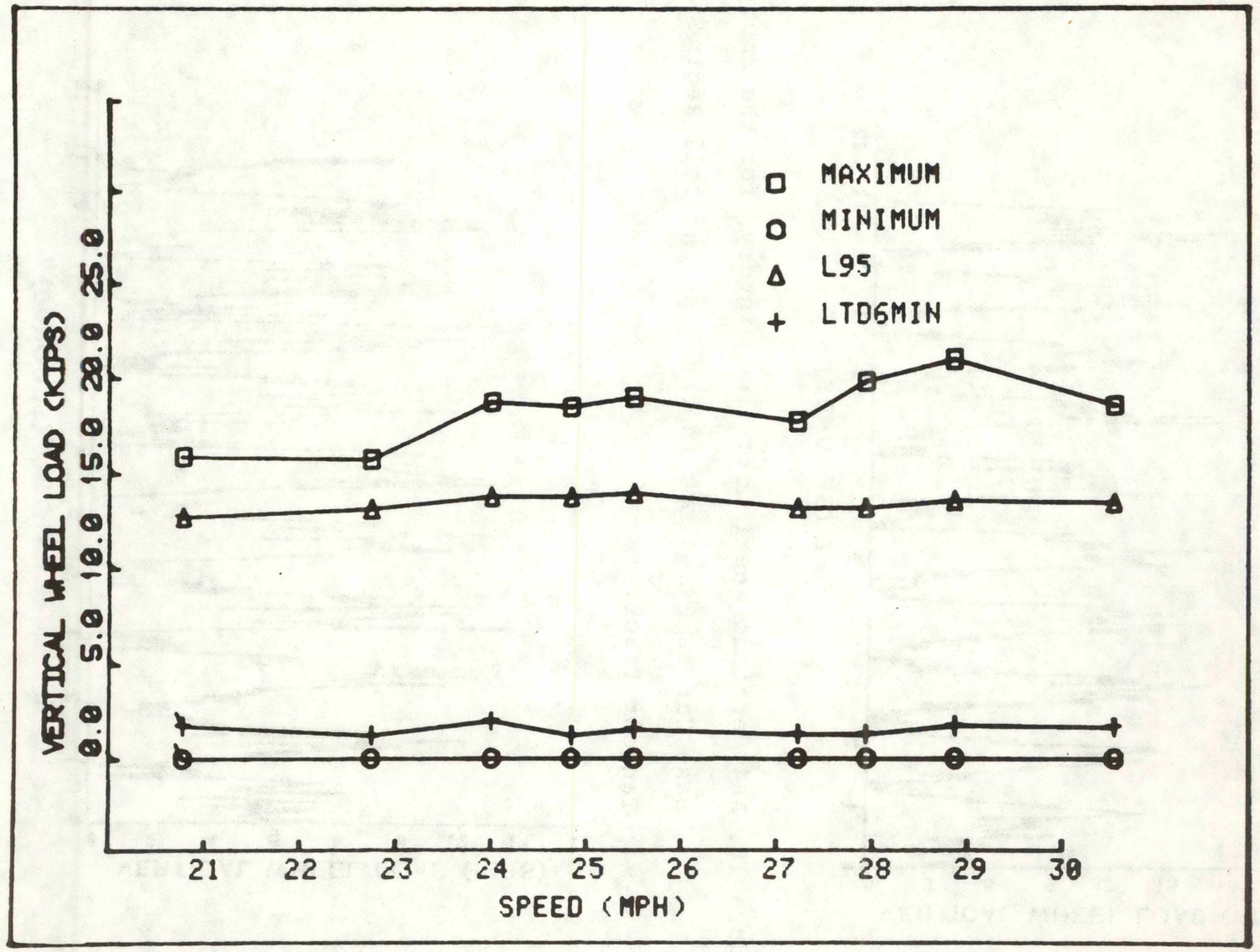

Figure 18. AR4 Vertical Wheel Load vs. Speed, for the Empty Base Car in the Rock-and-roll Regime on Tangent Track.

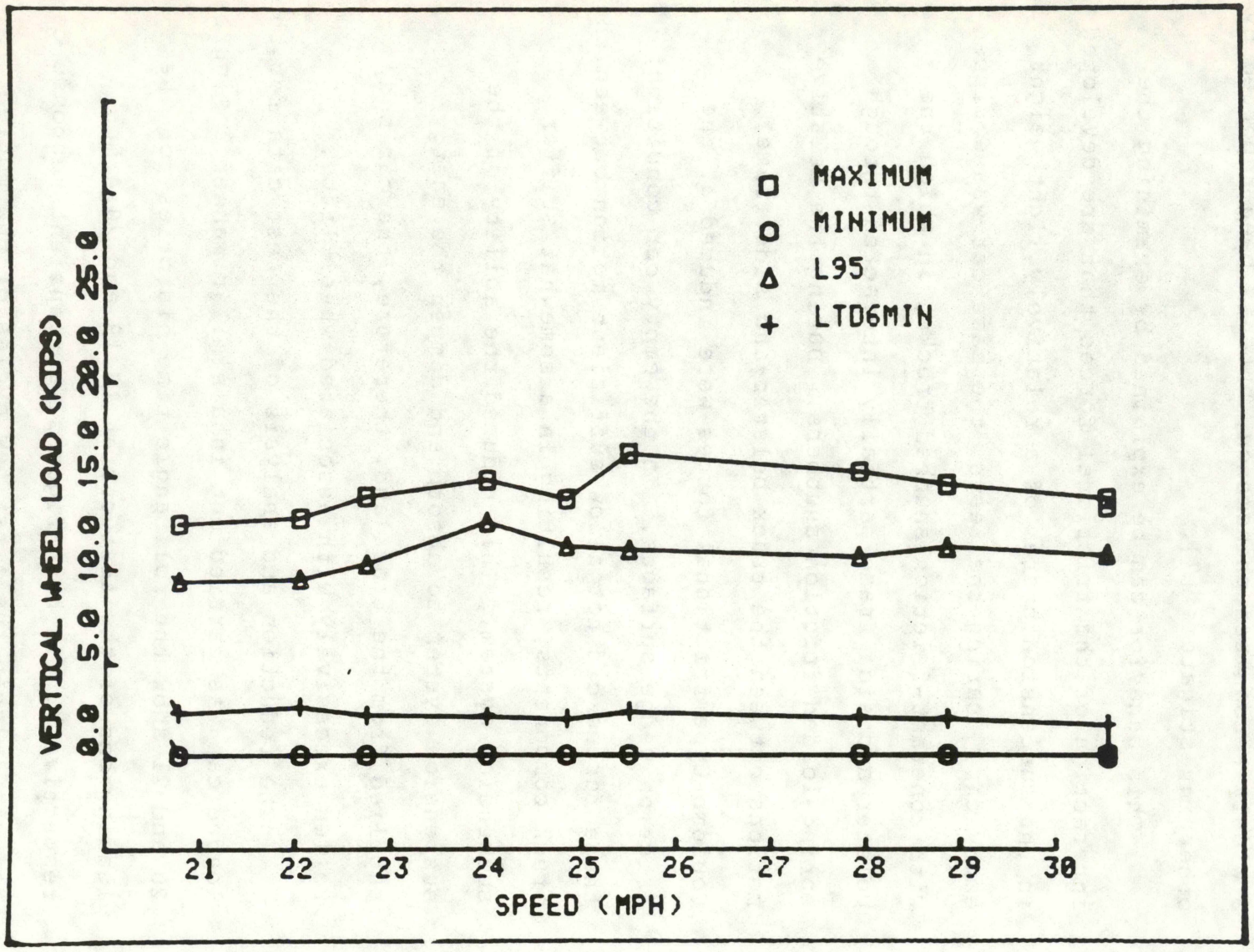

Figure 19. AL4 Vertical Wheel Load vs. Speed, for the Empty Base Car in the Rock-and-roll Regime on Tangent Track.

wheel load of 7,800 lb., a continuous 70% wheel unloading during most of the test runs. Extensive wheel unloading resulting from empty car rock-and-roll is not a widely recognized phenomenon, but has been reported by other investigators [7].

This behavior can be explained by examining the interaction of the frictional forces that are developed in the suspension system of a relatively light weight empty car. During the tests, the base car was equipped with constant-friction snubbed trucks, in which the bolster and side frame partially interacted through spring-loaded friction snubbers. During the relative motions between the truck bolster and side frame, Coulomb-type frictional forces were induced at the friction wedge surfaces. In the empty car condition, these forces did not allow sufficient motion between the truck components, resulting in a somewhat stiffer suspension system. This reduced the ability of the suspension system to absorb and dampen the energy supplied from the track and, therefore, the car body rolled excessively with associated wheel lifts.

The reduction and analysis of the test data for the loaded car was carried out in a similar manner. Figures 20 and 21 show the roll angle time histories for the leading end of the test car at 13.19 and 20.4 mph, respectively. In both figures, a transient response can be noted within the first few cycles of the motion. At 13.2 mph, the vehicle quickly dampened this motion and a

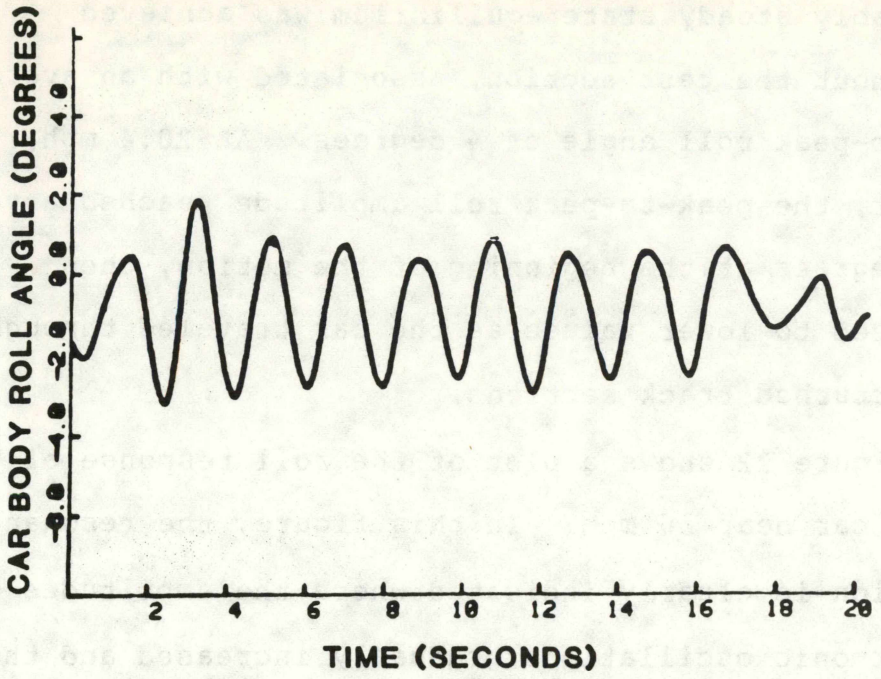

Figure 20. A-end Car Body Roll Angle Time History, for the Loaded Base Car at 13.19 mph in the Rock-and-roll Regime on Tangent Track.

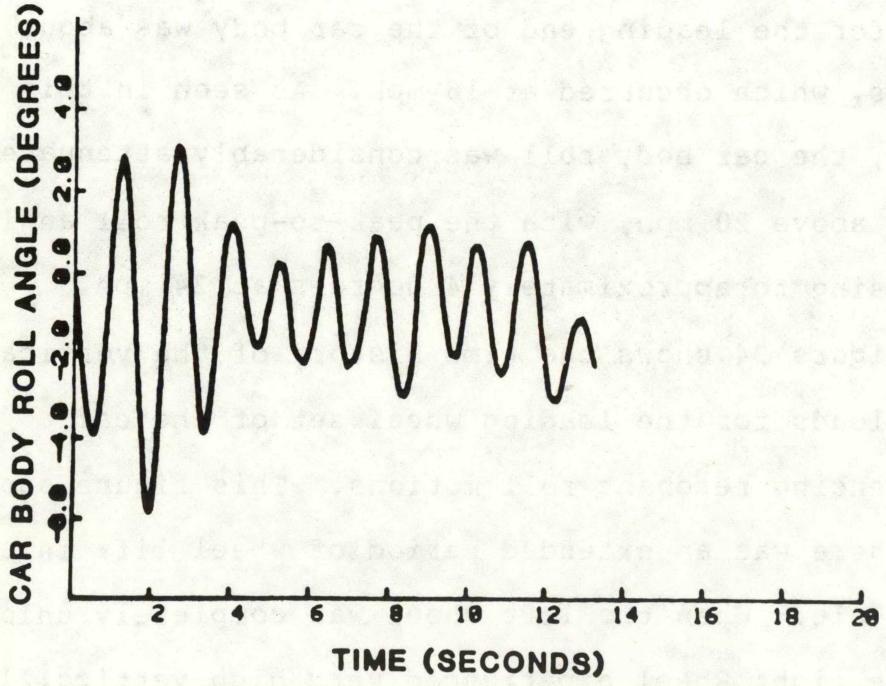

Figure 21. A-end Car Body Roll Angle Time History, for the Loaded Base Car at 20.4 mph in the Rock-and-roll Regime on Tangent Track.

reasonably steady state equilibrium was achieved throughout the test section, associated with an average peak-to-peak roll angle of 4 degrees. At 20.4 mph, however, the peak-to-peak roll amplitude reached a value of 8 degrees at the beginning of the motion, then decreased to lower values as the car traveled through the perturbed track sections.

Figure 22 shows a plot of the roll response of the loaded car near 16 mph. In this figure, the resonance condition is clearly indicated where the amplitudes of the harmonic oscillations gradually increased and then decreased, indicating a sufficient amount of damping inherent in the system to attenuate the oscillations.

Figure 23 shows the peak-to-peak car body roll angles with respect to vehicle speed. The maximum roll angle for the leading end of the car body was about 10.6 degrees, which occurred at 16 mph. As seen in this figure, the car body roll was considerably attenuated at speeds above 20 mph, with the peak-to-peak roll angle decreasing to approximately 4 degrees at 24 mph.

Figure 24 shows the time history of the vertical wheel loads for the leading wheel set of the car experiencing resonant roll motions. This figure shows that there was an extended period of wheel lift in each roll cycle. When the left wheel was completely unloaded, the right wheel experienced very high vertical loads and vice versa. This figure indicates that there were high frequency fluctuations about the peak values, due

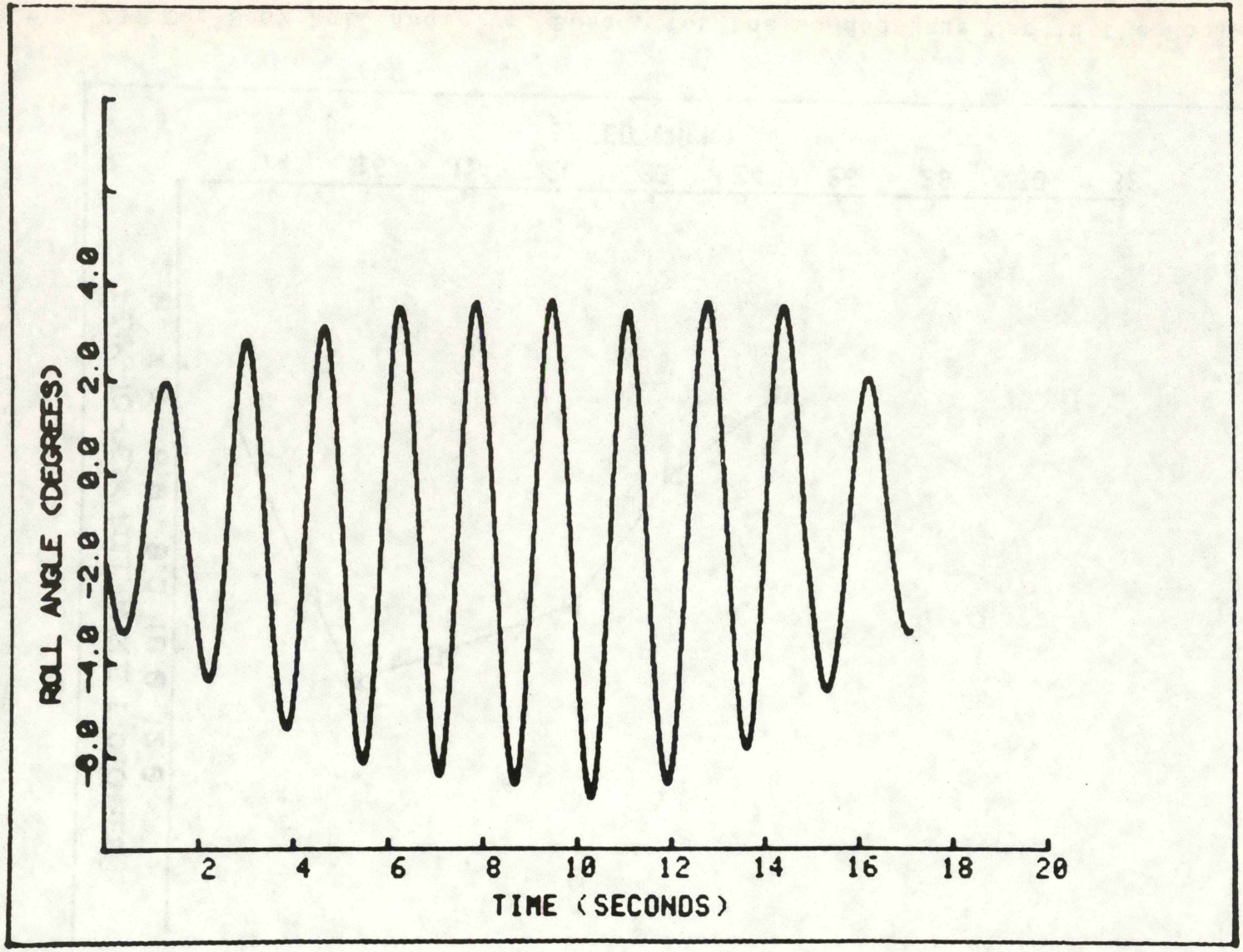

Figure 22. A-end Car Body Roll Angle Time History, for the Loaded Base Car at 16 mph in the Rock-and-roll Regime on Tangent Track.

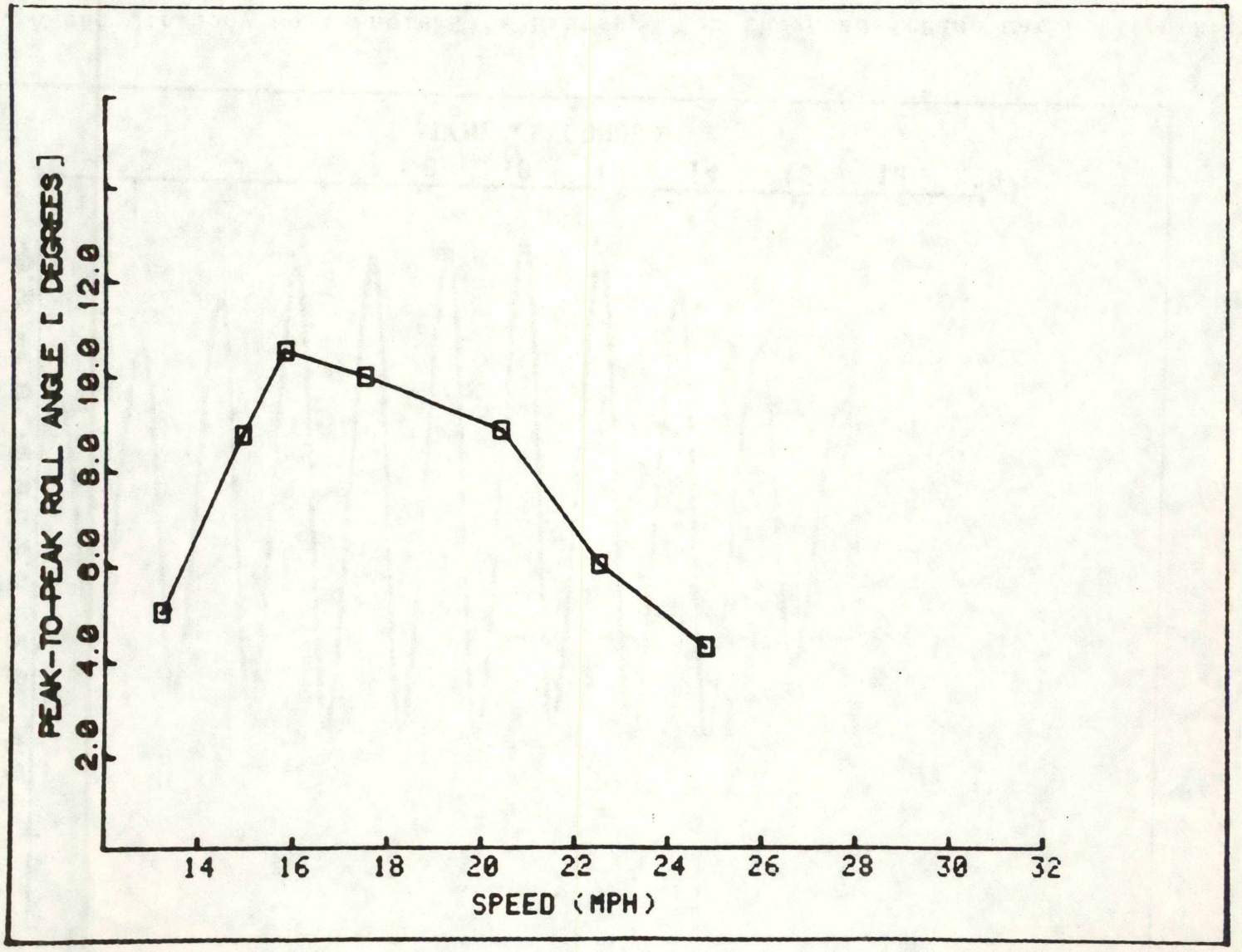

Figure 23. Car Body Roll Angle vs. Speed, for the Loaded Base Car in the Rock-and-roll Regime on Tangent Track.

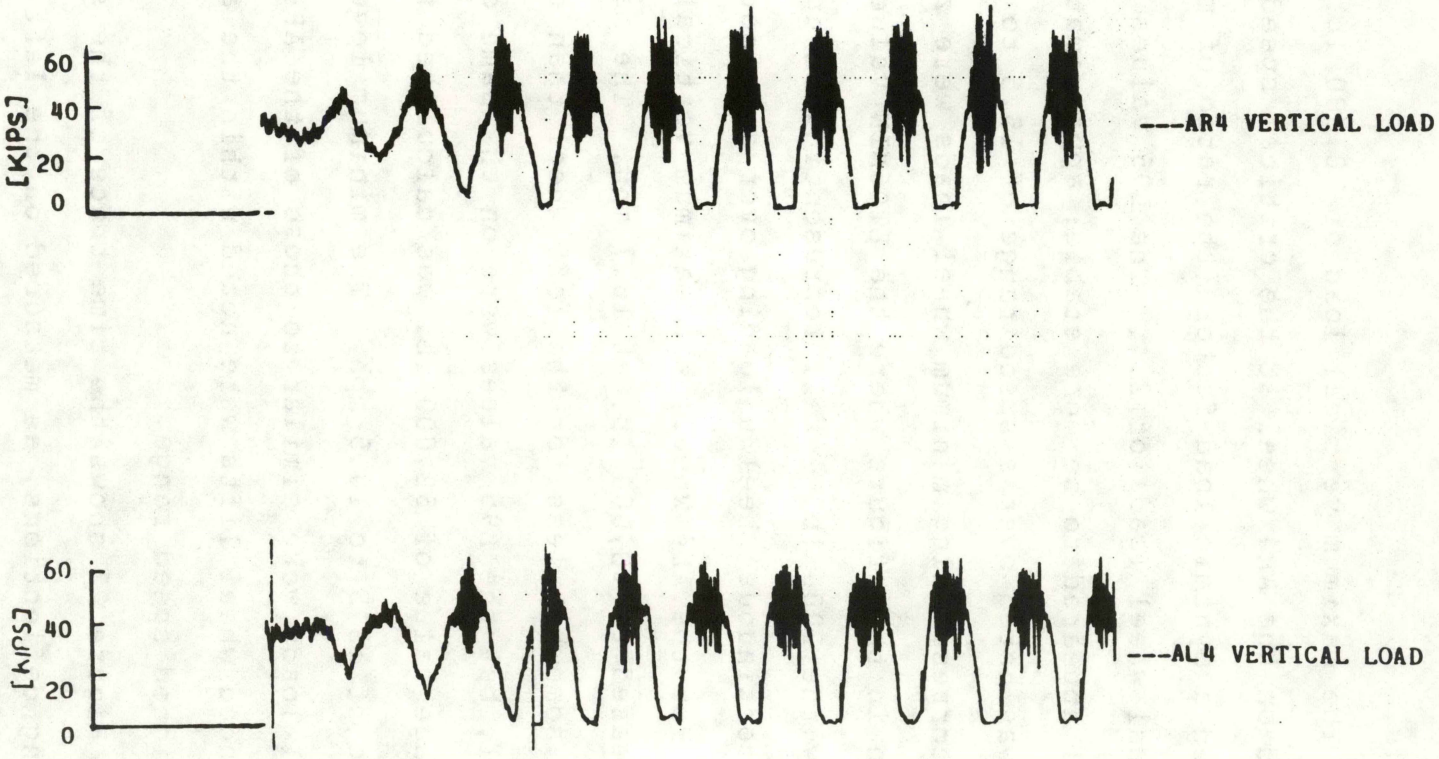

Figure 24. AR4 and AL4 Vertical Wheel Load Time Histories, for the Loaded Base Car at 16 mph in the the Rock-and-roll Regime on Tangent Track.

primarily to the wheel vibrations induced during extreme car body rolls.

Figures 25 and 26 illustrate the maximum and minimum levels of the wheel loads for the AR4 and AL4 wheels.

The maximum vertical load of 78,000 lb., experienced on the AR4 wheel at the critical speed, represented a dynamic load factor (the ratio of maximum to nominal wheel load) of 2.4. The L95 values for the same wheel appeared to be more stable; approximately 52,000 lb. was noted over a speed range of 15.5 to 18.5 mph. The corresponding minimum wheel loads were zero, as shown in this figure where the LTD6MIN values remained below the 2000 lb. level, representing an approximately 93% continuous wheel unloading over a 6-foot distance.

For the AL4 wheel, the maximum vertical load increased to 70,000 lb. at 16.7 mph. The maximum loads were somewhat less for the left wheel than the right wheel, but the L95 values were on the same order; an average value of 52,000 lb. was calculated for the speed range of 15.5 to 18.5 mph. The minimum levels of AL4 wheel loads were similar to those of the AR4 wheel, and extended wheel lifts were noted within the above-mentioned speed range.

Figure 27 shows the time trace of the suspension spring deflections, as measured on the left side of the leading truck at 16.70 mph, the resonant roll speed.

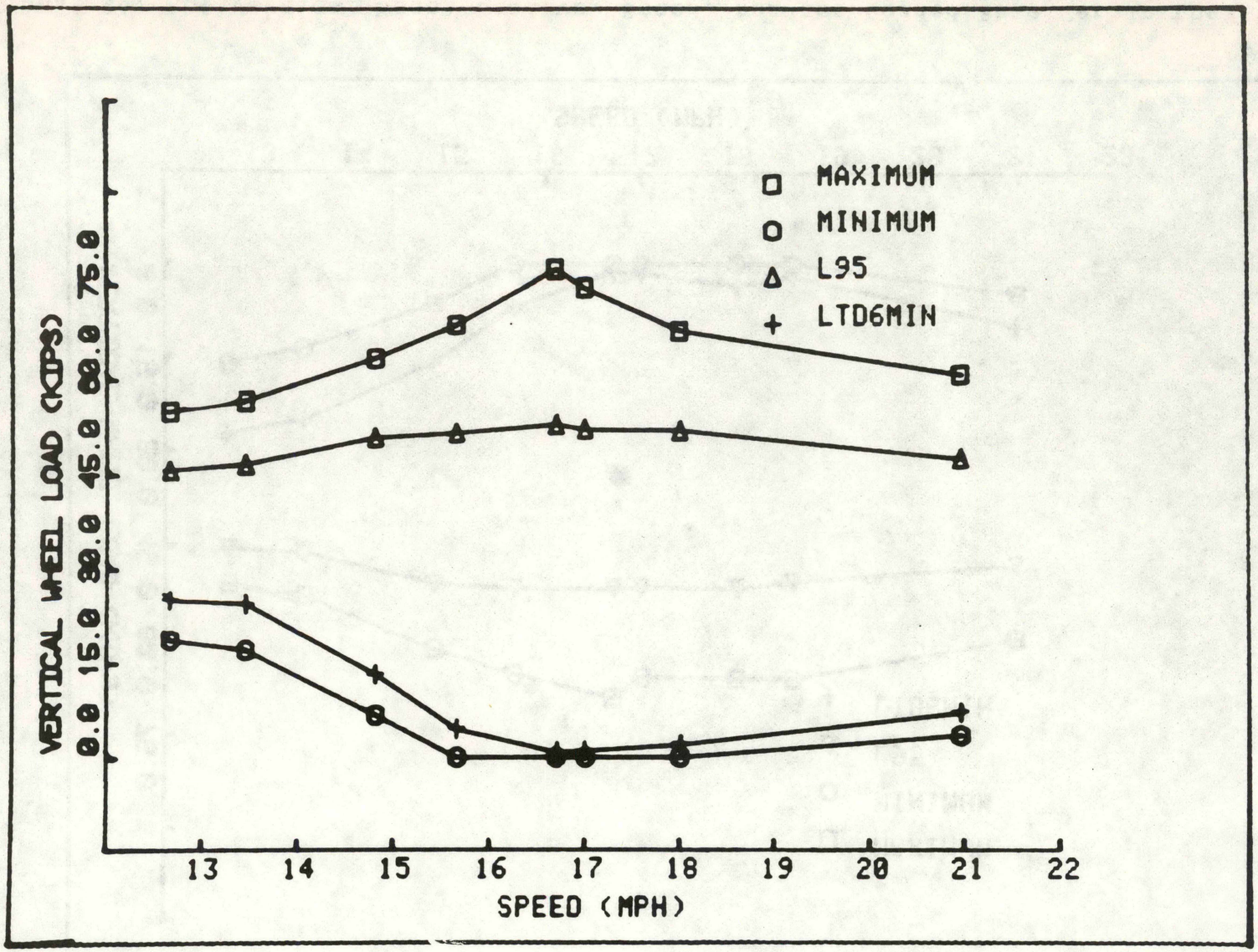

Figure 25. AR4 Vertical Wheel Load vs. Speed, for the Loaded Base Car in the Rock-and-roll Regime on Tangent Track.

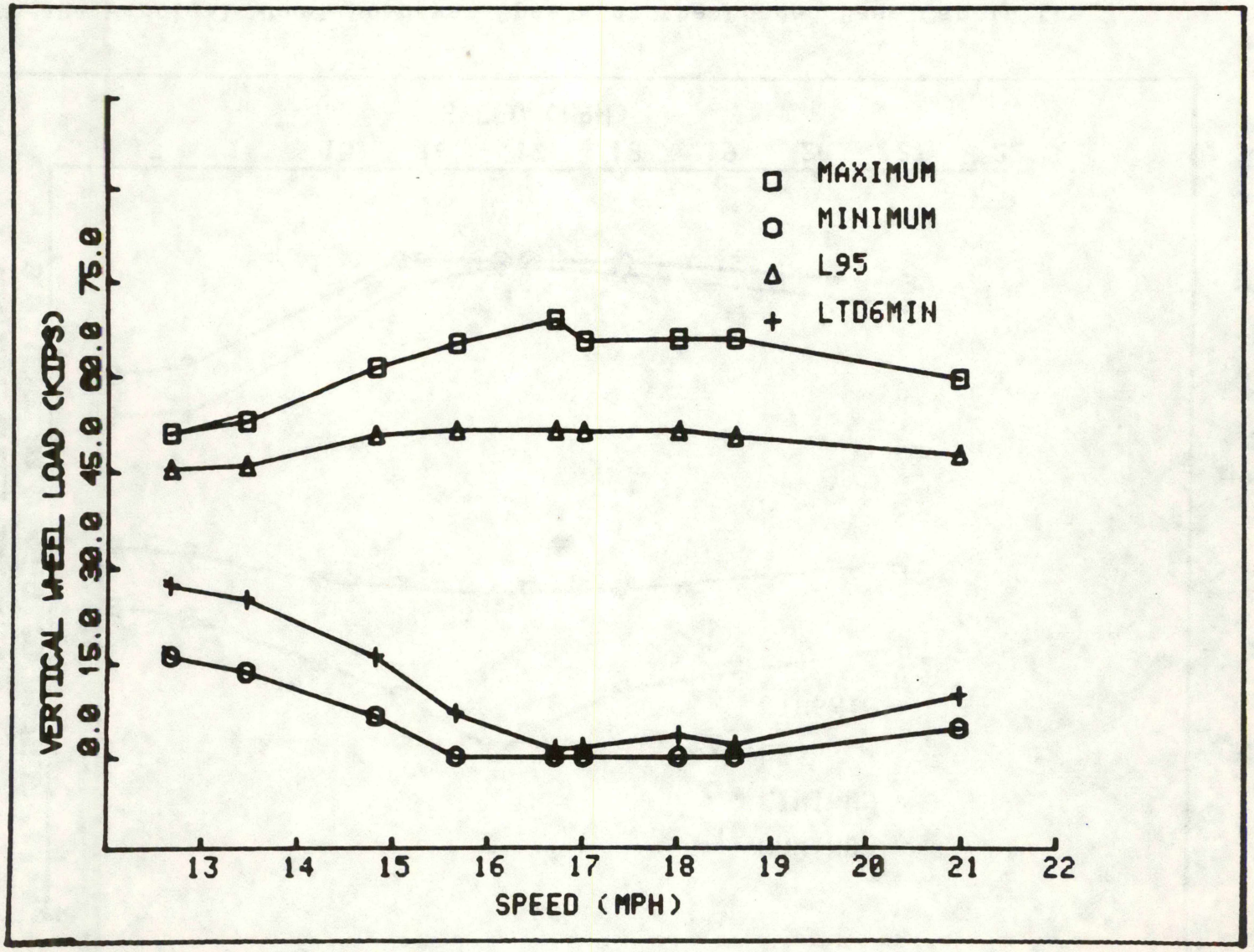

Figure 26. AL4 Vertical Wheel Load vs. Speed, for the Loaded Base Car in the Rock-and-roll Regime on Tangent Track.

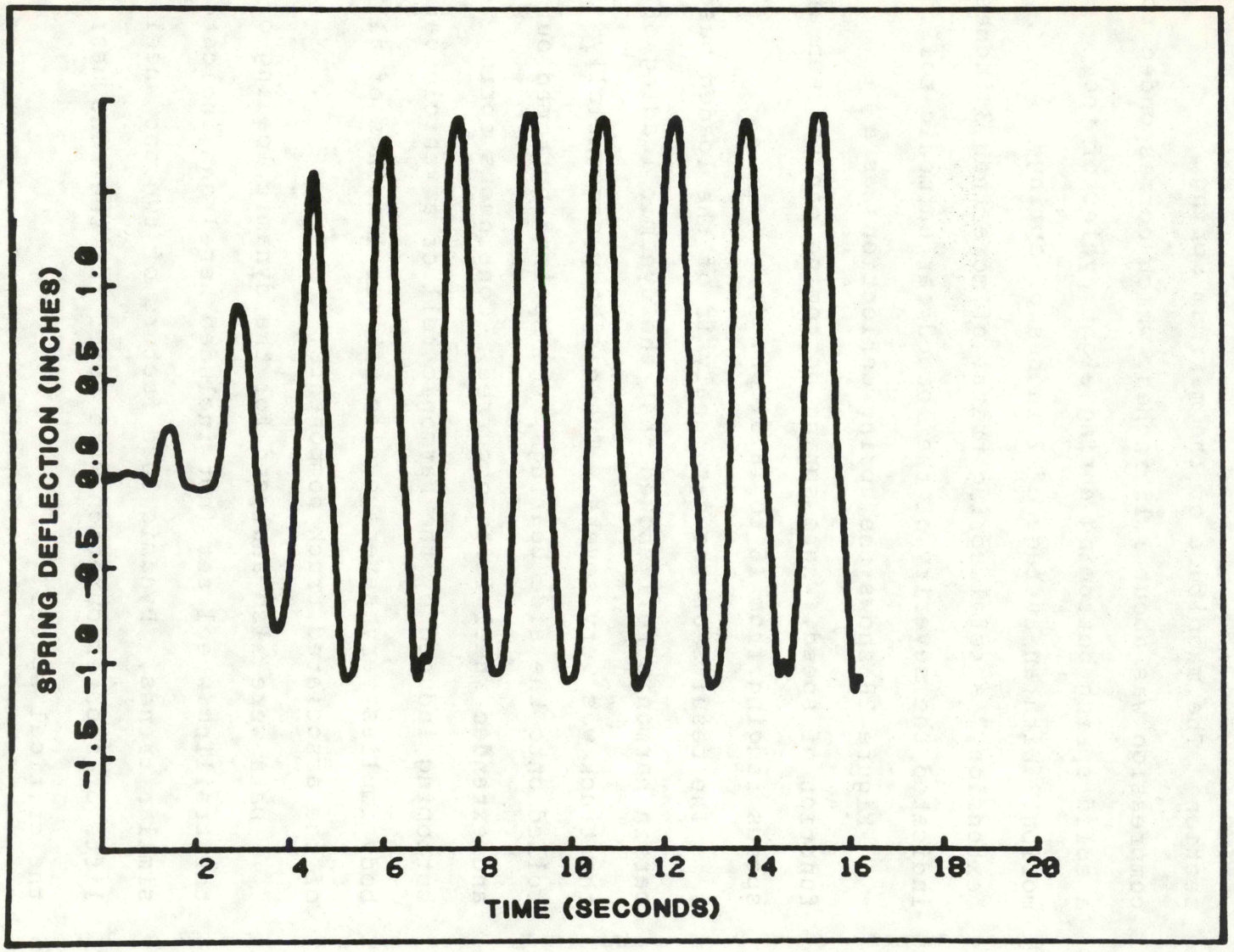

Figure 27. Spring Deflection Time History, for the Loaded Base Car at 16.7 mph in the Rock-and-roll Regime on Tangent Track.

The negative values of spring deflection correspond to spring compression, and the positive values to spring "extension." Steady state oscillations were noted after approximately six seconds into the perturbed track test section. The magnitude of the maximum spring compression was about 1.15 inches, which corresponded to a solid spring bottoming during eight cycles of the motion. With an average of 2 inches of spring "extension," a total spring travel of more than 3 inches indicated the severity of the loaded car harmonic roll.

Figure 28 shows the spring deflections as a function of speed, where spring bottoming can be seen at speeds ranging from 16 to 18.5 mph.

The results of the data analysis of the loaded base car in harmonic roll showed that the dynamic loading of the truck was very severe. The car body sequentially rolled onto the side bearings, the springs bottomed out and extended wheel lifts occurred. Continuous spring bottoming induced by the harmonic roll of a vehicle car body implies very severe cyclic fatigue loadings of all of the associated truck components.

Data were also analyzed for the dynamic loading of the trailing wheel set (not included here) and indicated similar trends. Dynamic load factors of two and wheel lifts of shorter duration were noted for the runs near the critical speed.

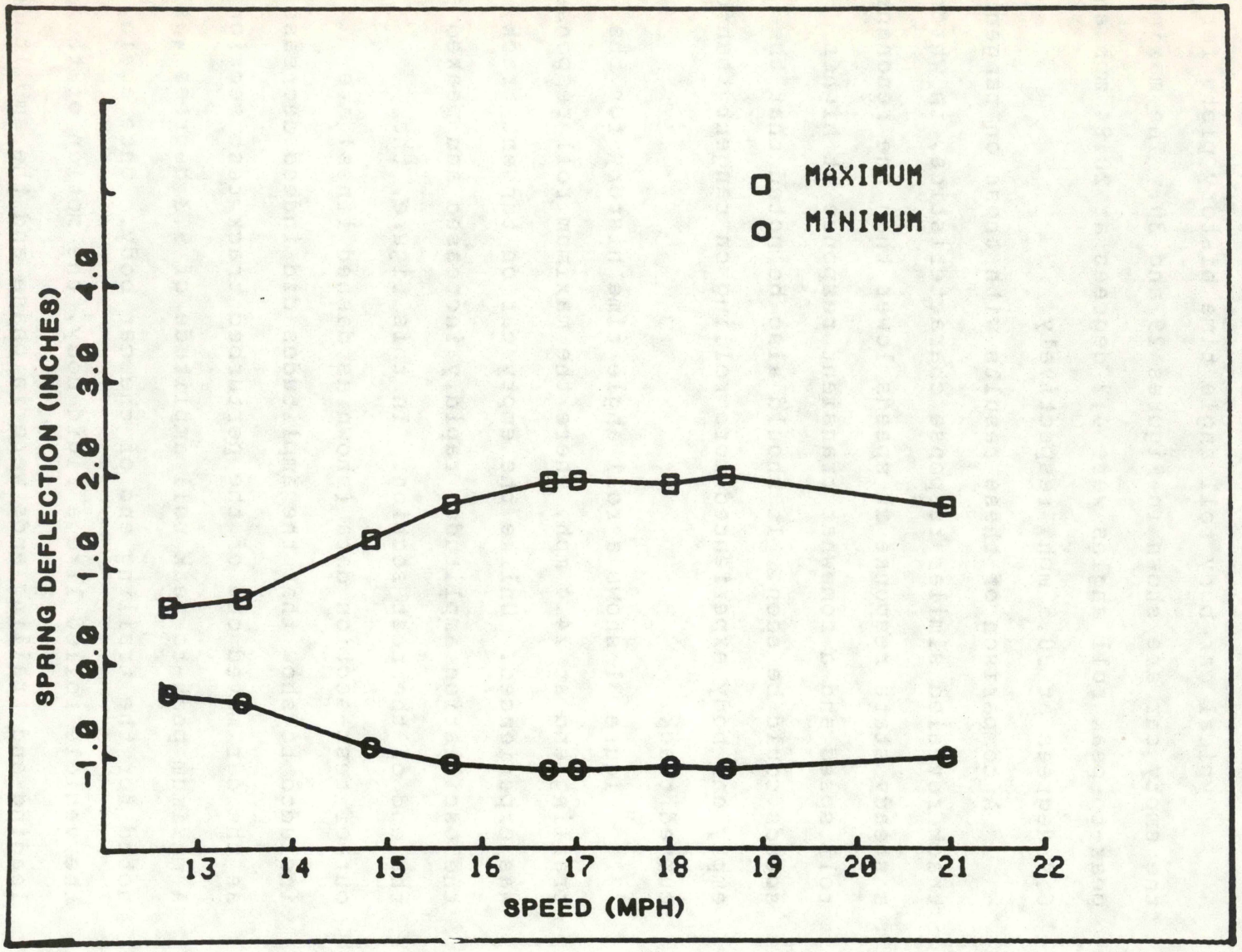

Figure 28. Spring Deflection vs. Speed, for the Loaded Base Car in the Rock-and-roll Regime on Tangent Track.

8.2 Rock-and-Roll on Curved Track

The data pertaining to the curved track rock-and-roll tests were analyzed to determine the effect of high curvature on the harmonic roll of the vehicle.

Typical car body roll angle time history plots for the empty car are shown in Figures 29 and 30. The maximum peak-to-peak roll angles were 4.2 degrees at 20.84 mph and 6.9 degrees at 30.5 mph, respectively.

A comparison of these results with those on tangent track revealed similar response characteristics, in which a steady state response at speeds lower than the resonant roll speed and a somewhat transient response at higher speeds could be seen. It should also be noted that the empty car body experienced more rolling on tangent than on curved track.

Figure 31 shows a roll angle time history for the trailing end at 24.4 mph, where the maximum roll response was experienced. Unlike the empty car on tangent track, the oscillation amplitudes rapidly increased and peaked at the end of the test section. In this figure, the out-of-test-section data (shown as dashed lines) are included to show that the amplitudes did indeed decrease as the car moved out of the perturbed track test section. A maximum peak-to-peak roll amplitude of 9.3 degrees was noted for the trailing end of the car body. Once again, the vehicle rolled like a rigid body, the motion of the leading and trailing ends were in phase and the amplitudes

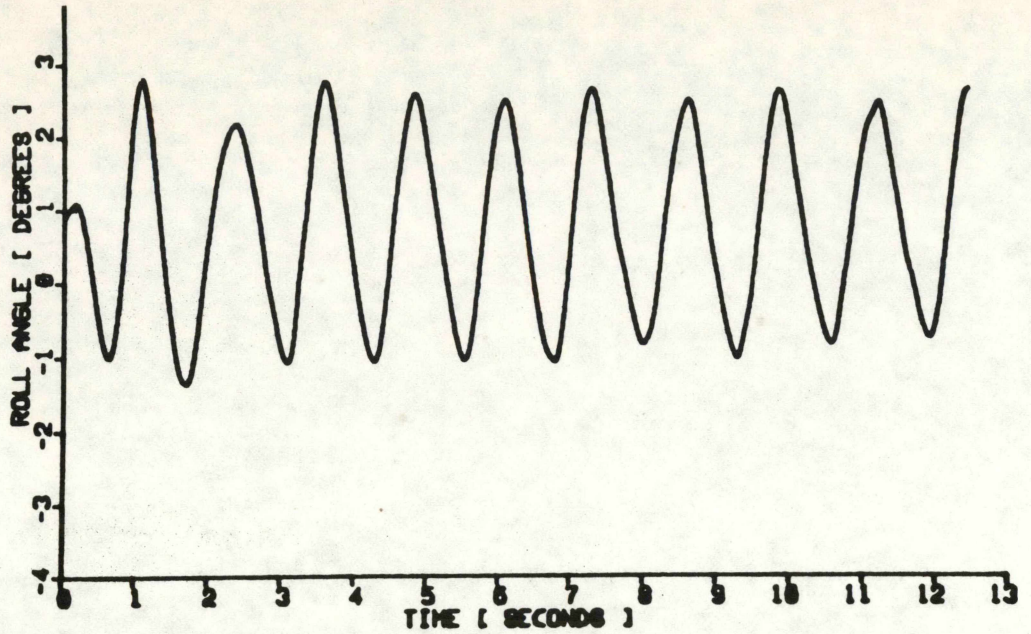

Figure 29. A-end Car Body Roll Angle Time History, for the Empty Base Car at 20.84 mph in the Rock-and-roll Regime on Curved Track.

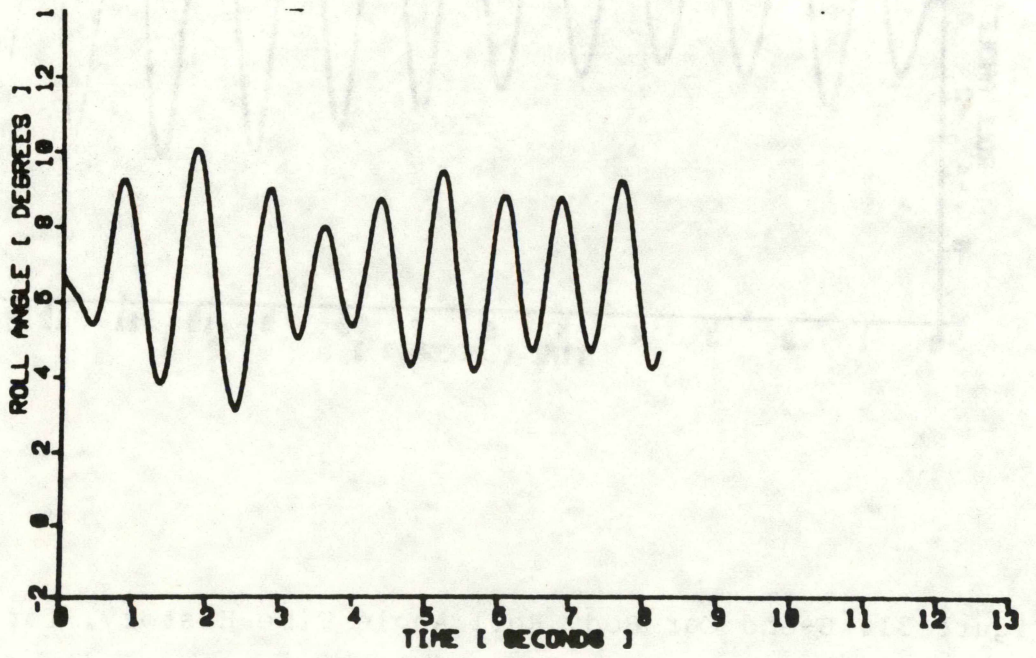

Figure 30. A-end Car Body Roll Angle Time History, for the Empty Base Car at 30.45 mph in the Rock-and-roll Regime on Curved Track.

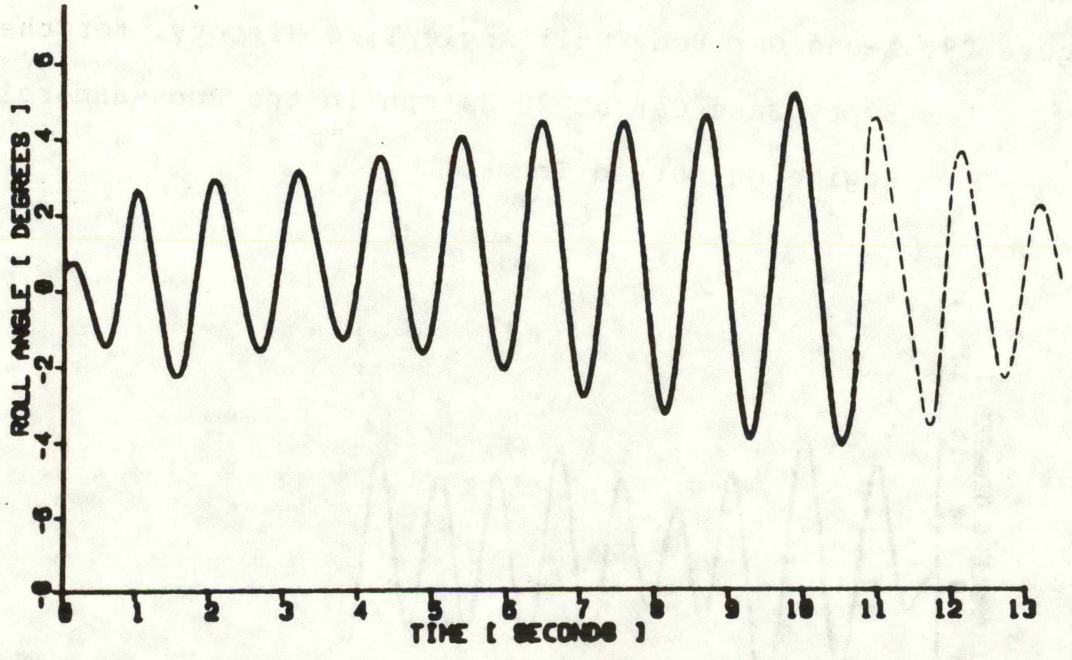

Figure 31. B-end Car Body Roll Angle Time History, for the Empty Base Car at 24.4 mph in the Rock-and-roll Regime on Curved Track.

of the oscillations were of the same order of magnitude.

The maximum peak-to-peak roll angles for the leading and trailing ends of the car body as a function of vehicle speed are shown in Figure 32. The roll amplitude abruptly increased to a peak value and then gradually decreased above the critical speed of the vehicle.

These high levels of car body roll angle above the critical speed may very well be indicative of a lack of effective damping. It can also be seen in this figure that the leading end car body roll angles were slightly lower than those for the trailing end; the maximum peak-to-peak roll angle was 8.9 degrees for the leading end at 24.3 mph. Time history plots for the AR4 (high rail) and AL4 (low rail) vertical wheel loads essentially demonstrated that the wheel load time histories in both tangent and curved track sections showed similar characteristics. In the curved track section, wheel lifts occurred during each cycle of motion, along with maximum loads that exceeded twice the static loads.

Figures 33 and 34 show the maximum and minimum loads for the AR4 and AL4 wheels, respectively, plotted as a function of speed. On the low rail, the peak maximum vertical wheel loads varied from 12,000 to 14,800 lb., and the L95 values were on the order of 10,000 lb., over the range of test speeds. Wheel lift was experienced during almost every cycle of motion for

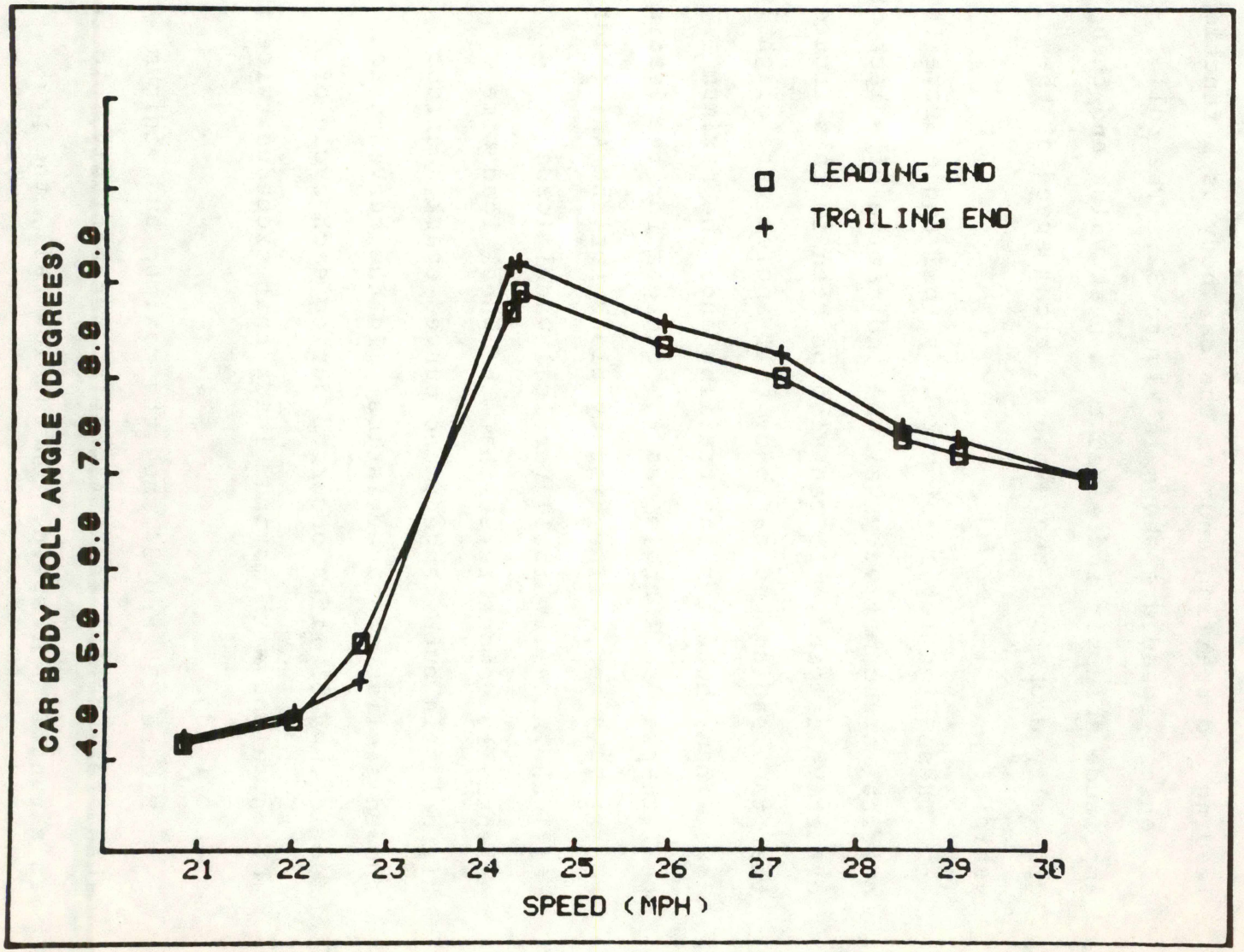

Figure 32. Car Body Roll Angle vs. Speed, for the Empty Base Car in the Rock-and-roll Regime on Curved Track.

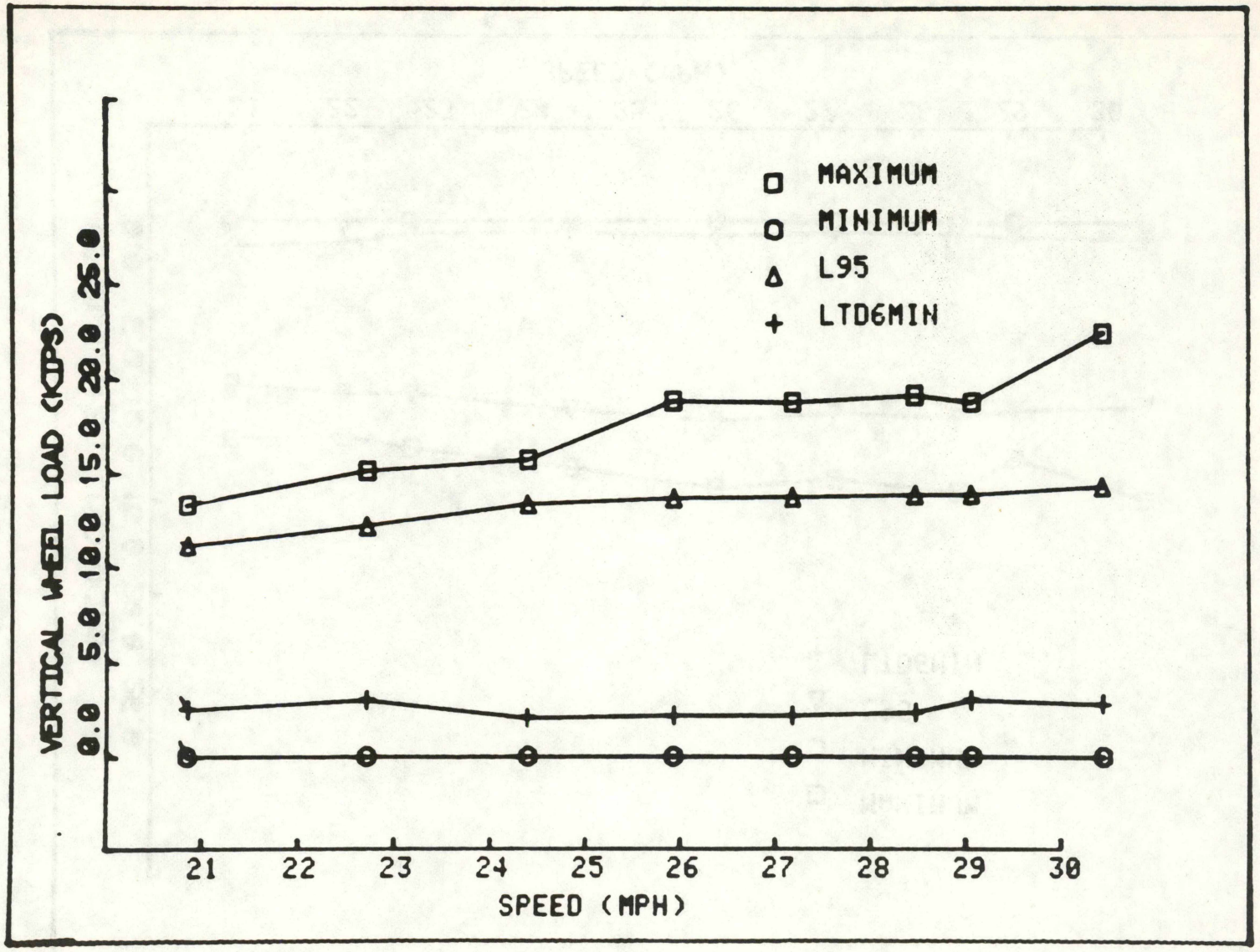

Figure 33. AR4 (High Rail) Vertical Wheel Load vs. Speed, for the Empty Base Car in the Rock-and-roll Regime on Curved Track.

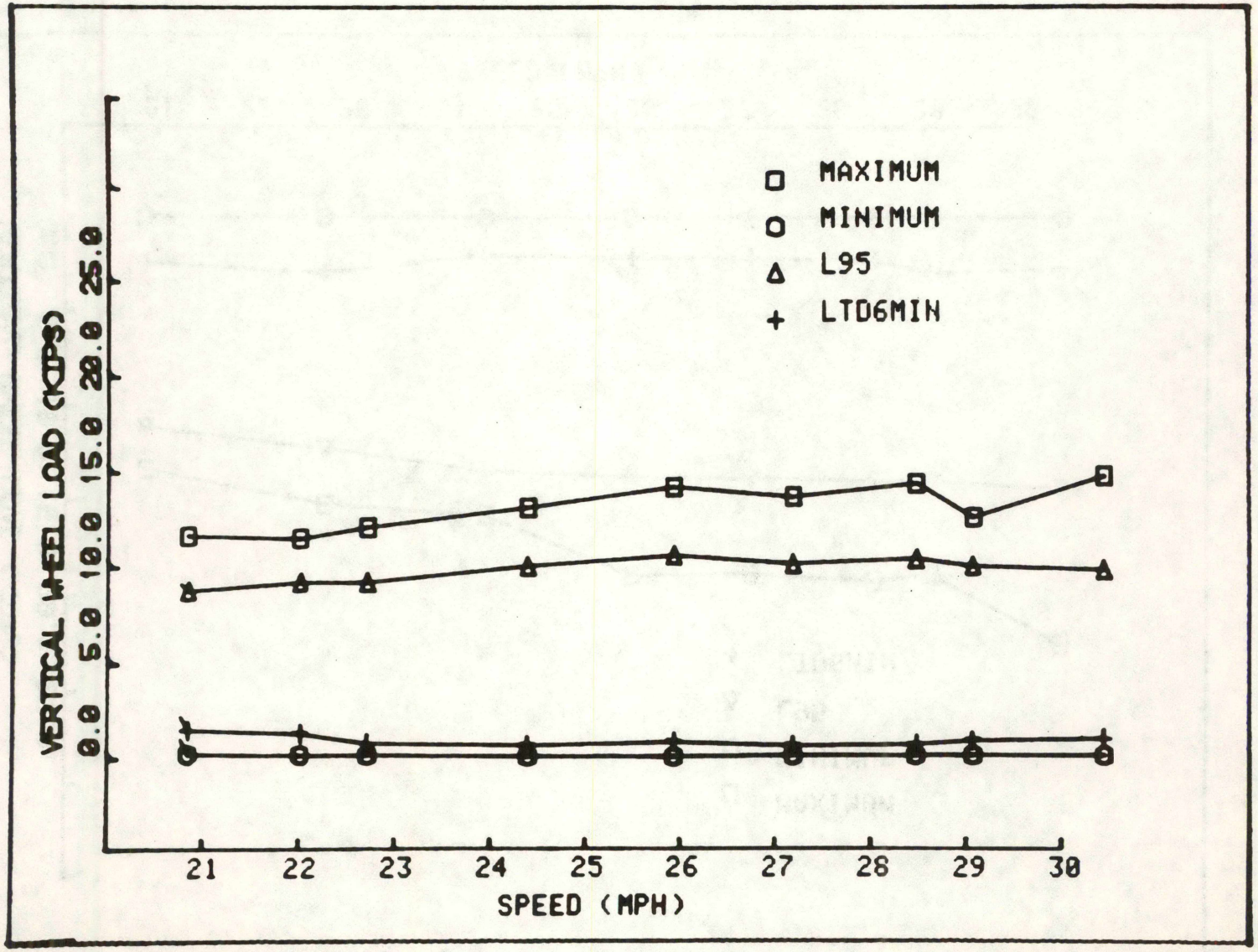

Figure 34. AL4 (Low Rail) Vertical Wheel Load vs. Speed, for the Empty Base Car in the Rock-and-roll Regime on Curved Track.

all of the test runs. As seen in Figure 34, the LTD6MIN values were less than 1,000 lb., for most speeds, indicating an 87% continuous wheel unloading.

For the high rail, the maximum wheel loads increased at the higher speeds and a maximum of 22,500 lb. was noted near 30 mph. The corresponding L95 value of the wheel load was 14,500 lb., representing a dynamic load factor of 1.9. Wheel lift was also noted on the AR4 (high rail) wheel for all test runs, with an average minimum value of 2,000 lb. sustained continuously over 6 feet of track, as shown in Figure 33.

The analysis of the loaded car rock-and-roll test data on the curved track section also showed similar response characteristics.

The maximum response of the car occurred near 18 mph. A roll angle time history for the leading end of the car body at this speed showed that large oscillations occurred, in which the amplitudes gradually increased to a maximum value towards the end of the track section and then decreased. Figure 35 shows the maximum peak-to-peak car body roll angle as a function of vehicle speed, and a maximum of 9.8 degrees was noted.

Figure 36 illustrates the vertical wheel load time histories for the leading wheel set at the resonant speed and the duration of the wheel unloading was much longer on the high rail than the low rail. Figure 37 shows the maximum and minimum levels of AR4 (high rail) wheel load with respect to vehicle speed.

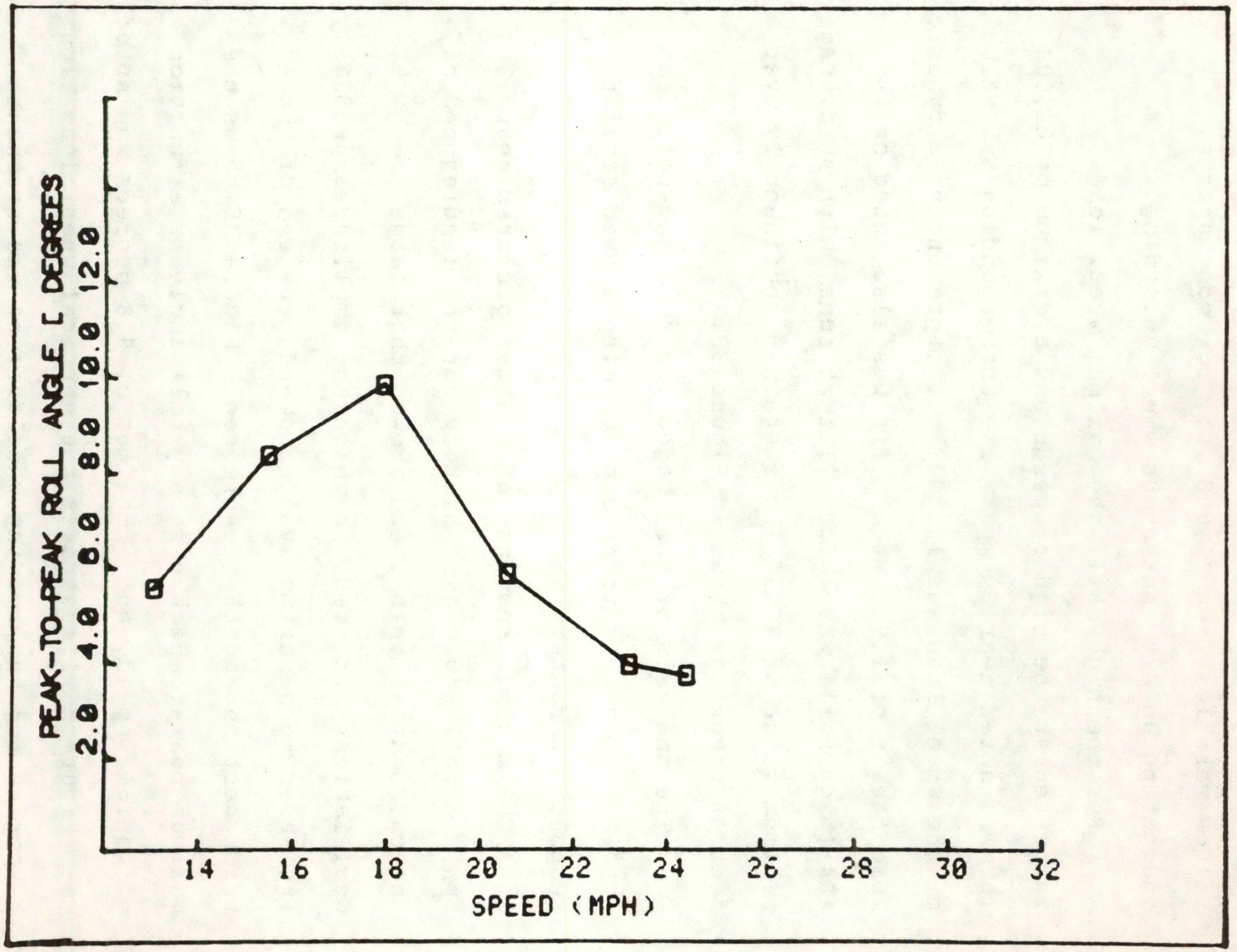

Figure 35. Car Body Roll Angle vs. Speed, for the Loaded Base Car in the Rock-and-roll Regime on Curved Track.

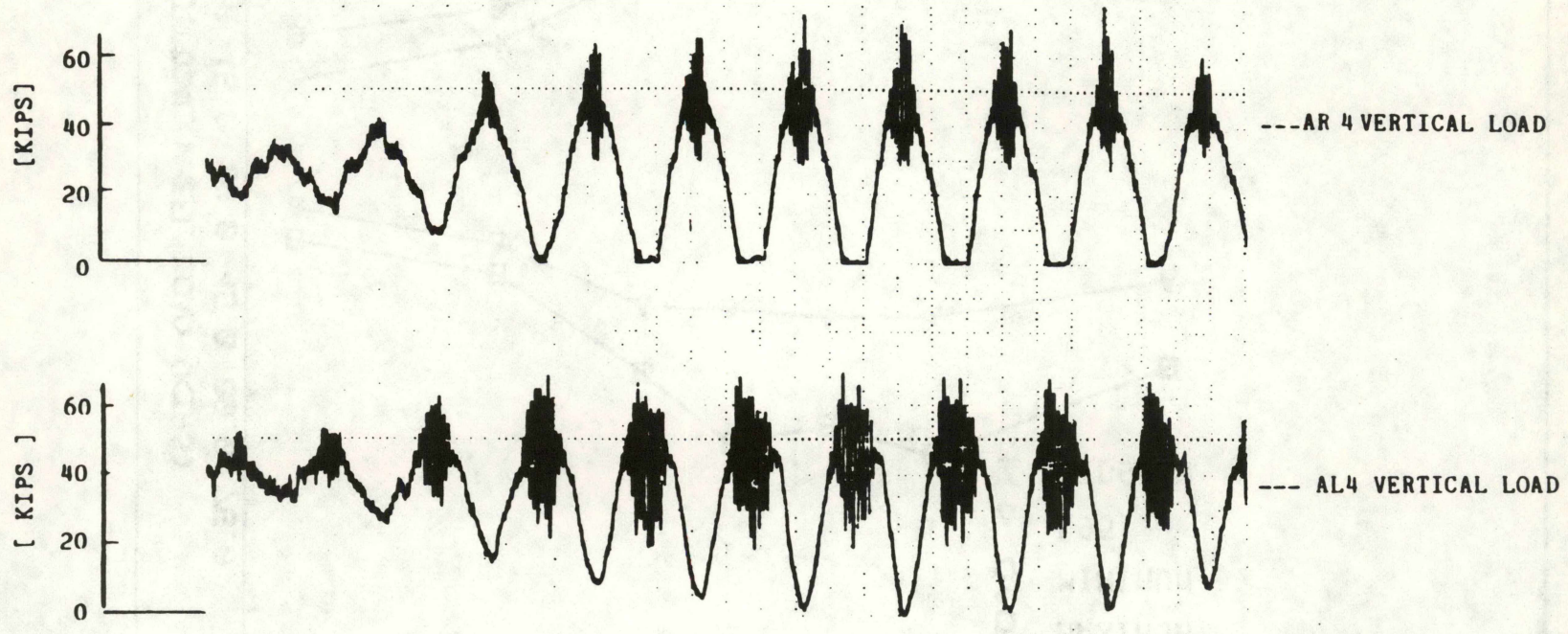

Figure 36. AR4 (High Rail) and AL4 (Low Rail) Vertical Wheel Load Time Histories, for the Loaded Base Car at 17.9 mph in the Rock-and-roll Regime on Curved Track.

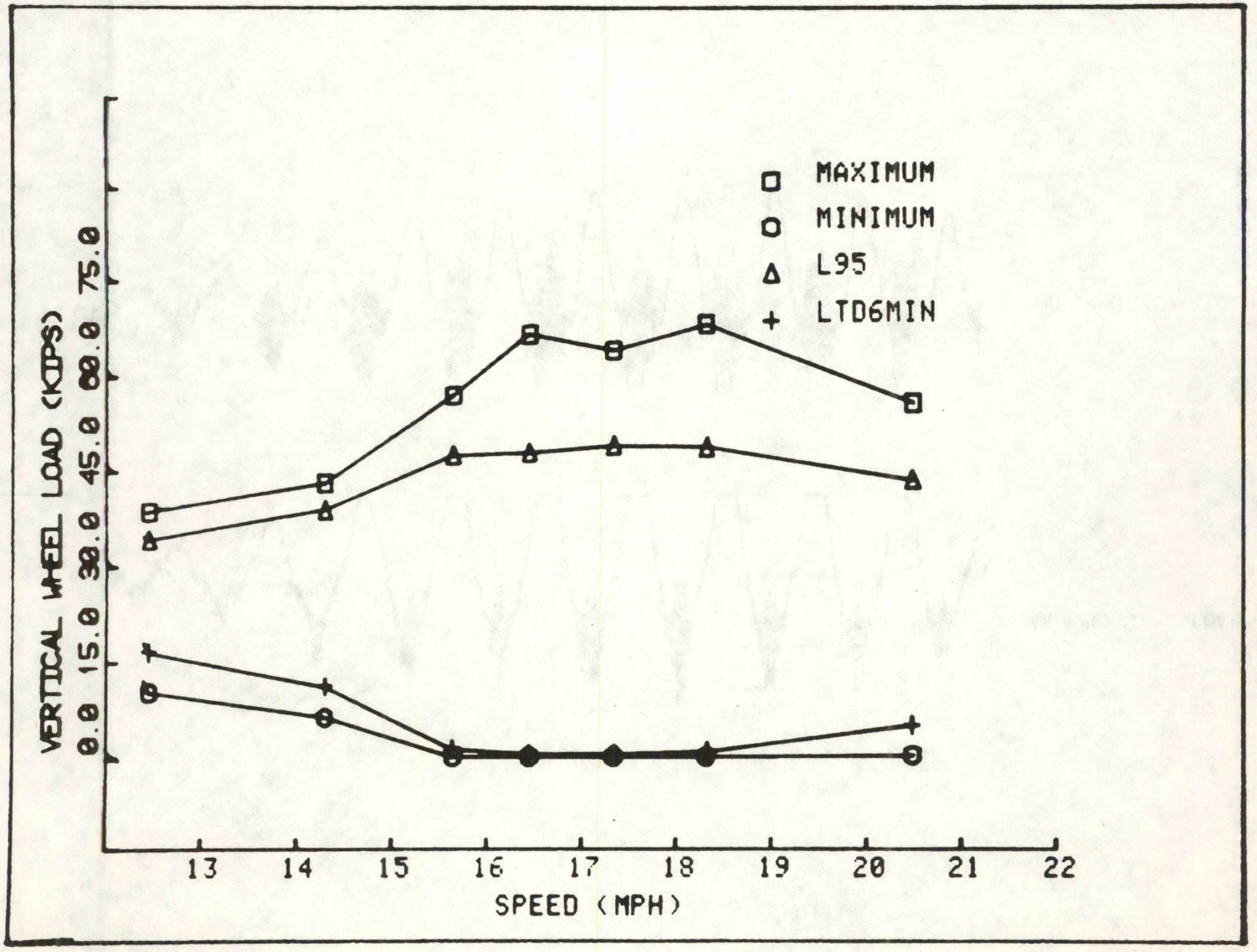

Figure 37. AR4 (High Rail) Vertical Wheel Load vs. Speed, for the Loaded Base Car in the Rock and roll Regime on Curved Track.

As seen in this figure, a 68,500 lb. peak load, occurring at the critical speed, represented a dynamic load factor of 2.1. A maximum of 49,000 lb. was noted for the corresponding L95 load level. At speeds ranging from 15.5 to 18.5 mph, extended wheel lifts were experienced and the wheel unloading, associated with 6-feet of travel, was 100%.

The results of the data reduction and analysis of the wheel loads showed a consistent trend, in which the low rail wheel loads were higher than those for the high rail at most test speeds. On a 7.5 degree curve, due to the offset of the car body center of gravity, along with the increased roll towards the low rail, high dynamic wheel loads were developed on the low rail. As shown in Figure 38, the low rail wheel loads showed an average maximum value of about 66,000 lb. and the average L95 value was approximately 53,000 lb. It should be noted, however, that on a curve with 4.5 inches of superelevation, it is highly unlikely that a loaded car would develop wheel lifts on the low rail side. Wheel lift was noted only at 18.3 mph, near the resonant speed, and the corresponding LTD6MIN value was on the order of 8,000 lb., indicating a response with less sustained wheel unloadings.

To illustrate the severity of the car body roll and its effect on the truck components, a time history plot for the lateral displacement of the leading wheel set, obtained by averaging the outputs from the pair of

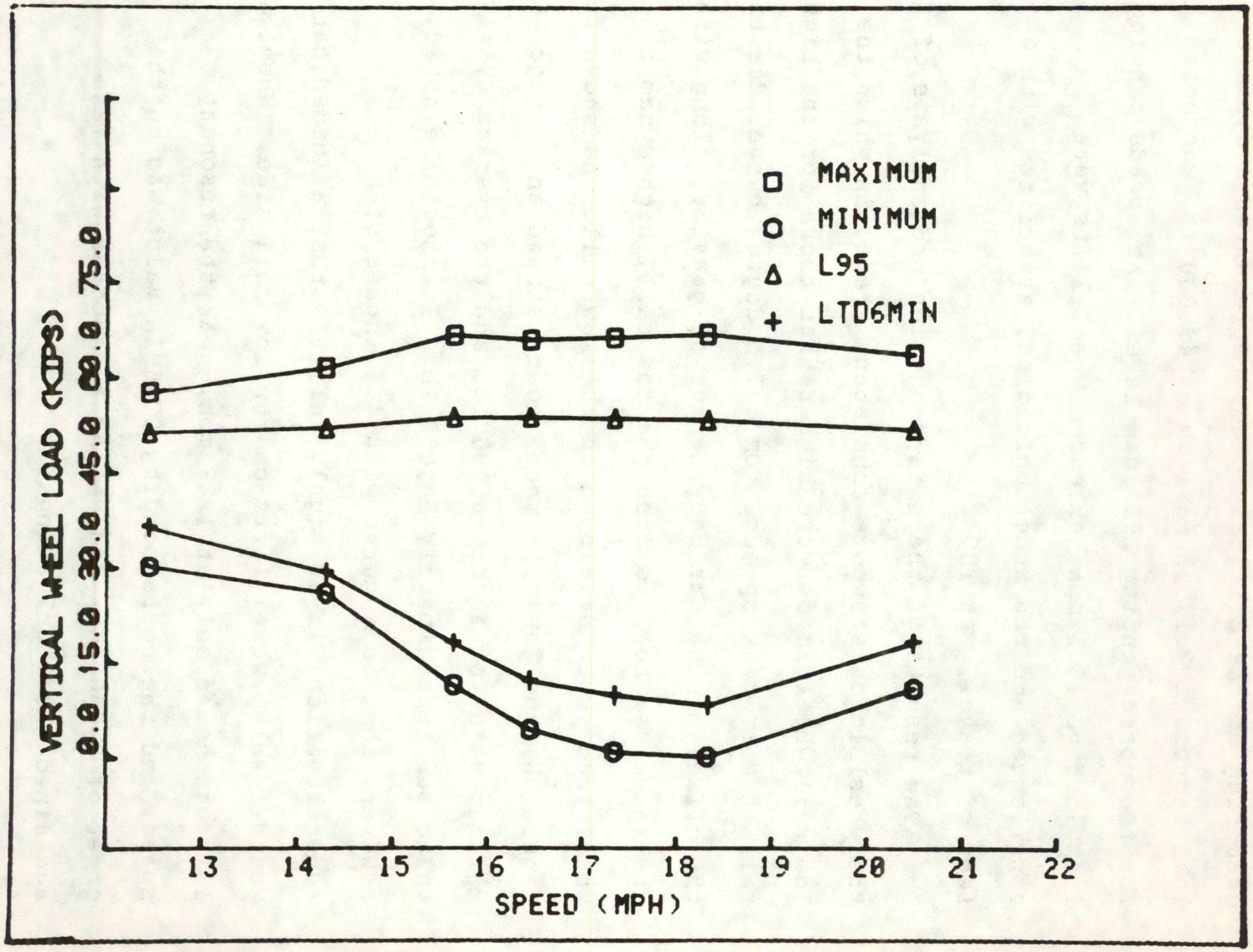

Figure 38. AL4 (Low Rail) Vertical Wheel Load vs. Speed, for the Loaded Base Car in the Rock-and-roll Regime on Curved Track.

wheel/rail displacement probes, is shown in Figure 39. An average lateral displacement of 1.1 inches indicated a serious flange climbing problem. Figure 40 shows the spring deflection time history that was measured on the low rail side at 18.32 mph. It can be seen that a spring compression of more than one inch, which corresponded to spring bottoming, was experienced during six cycles of the motion. The amplitudes of the oscillations in the direction of spring extension, unlike the tangent track response, did not remain at a steady level. The maximum and minimum levels of spring travel, plotted as a function of speed, are shown in Figure 41. Spring bottoming and high levels of spring travel, in compression, can be seen at speeds near the resonant roll speed of the vehicle.

8.3 Conclusions

From the above results, the following conclusions for the roll response of the vehicle were made.

1. Track curvature did not affect the resonant roll speed of the empty base car. The maximum roll response of the empty car was attained near 24 or 25 mph for both the tangent and curved track test runs. At most of the test speeds, the empty car body rolled more on tangent track than on curved track, but in both cases maximum peak-to-peak roll angles of 9.3 degrees were measured on the trailing end of the vehicle.

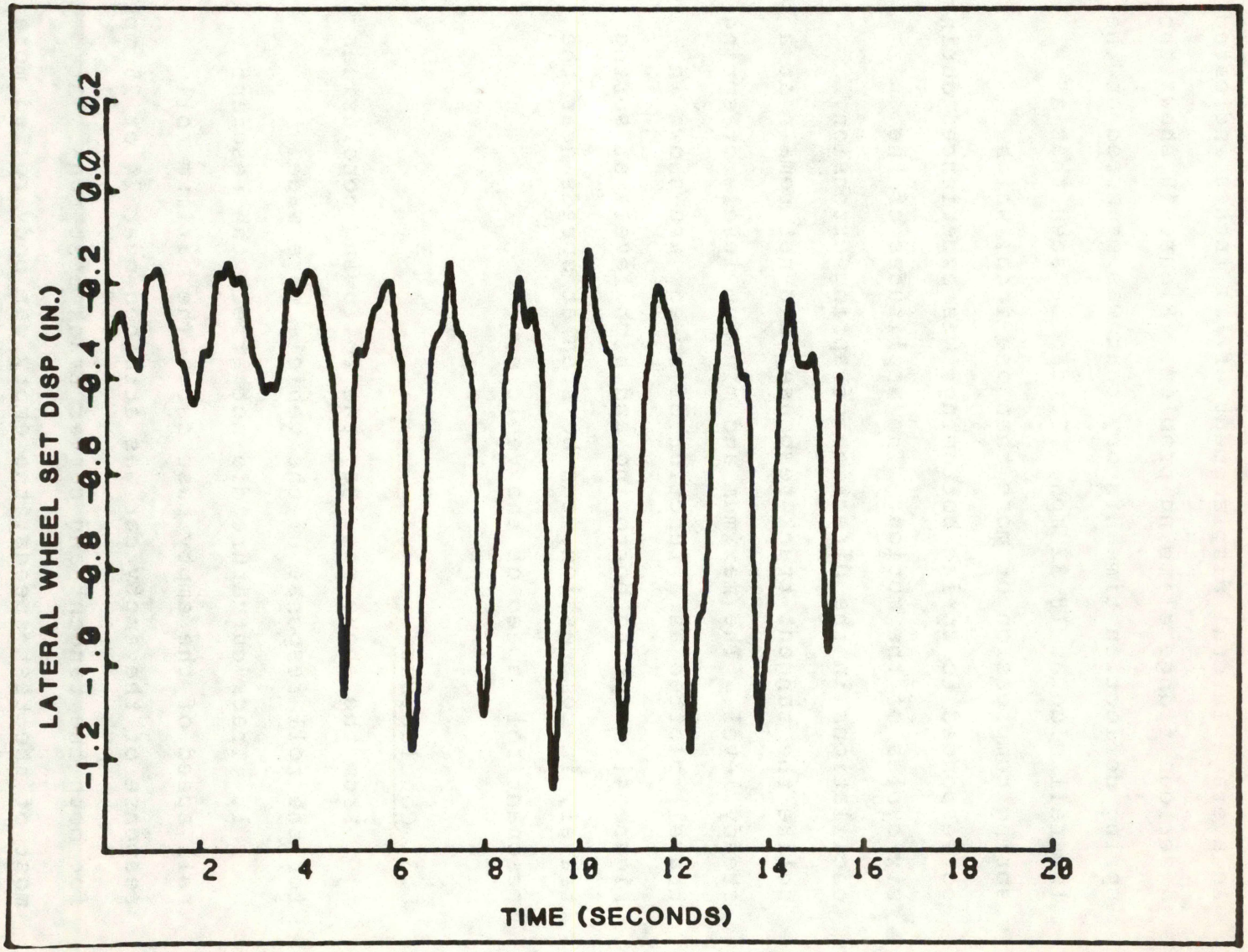

Figure 39. Leading Axle Wheel/Rail Displacement Time History, for the Loaded Base Car at 18.3 mph in the Rock-and-roll Regime on Curved Track.

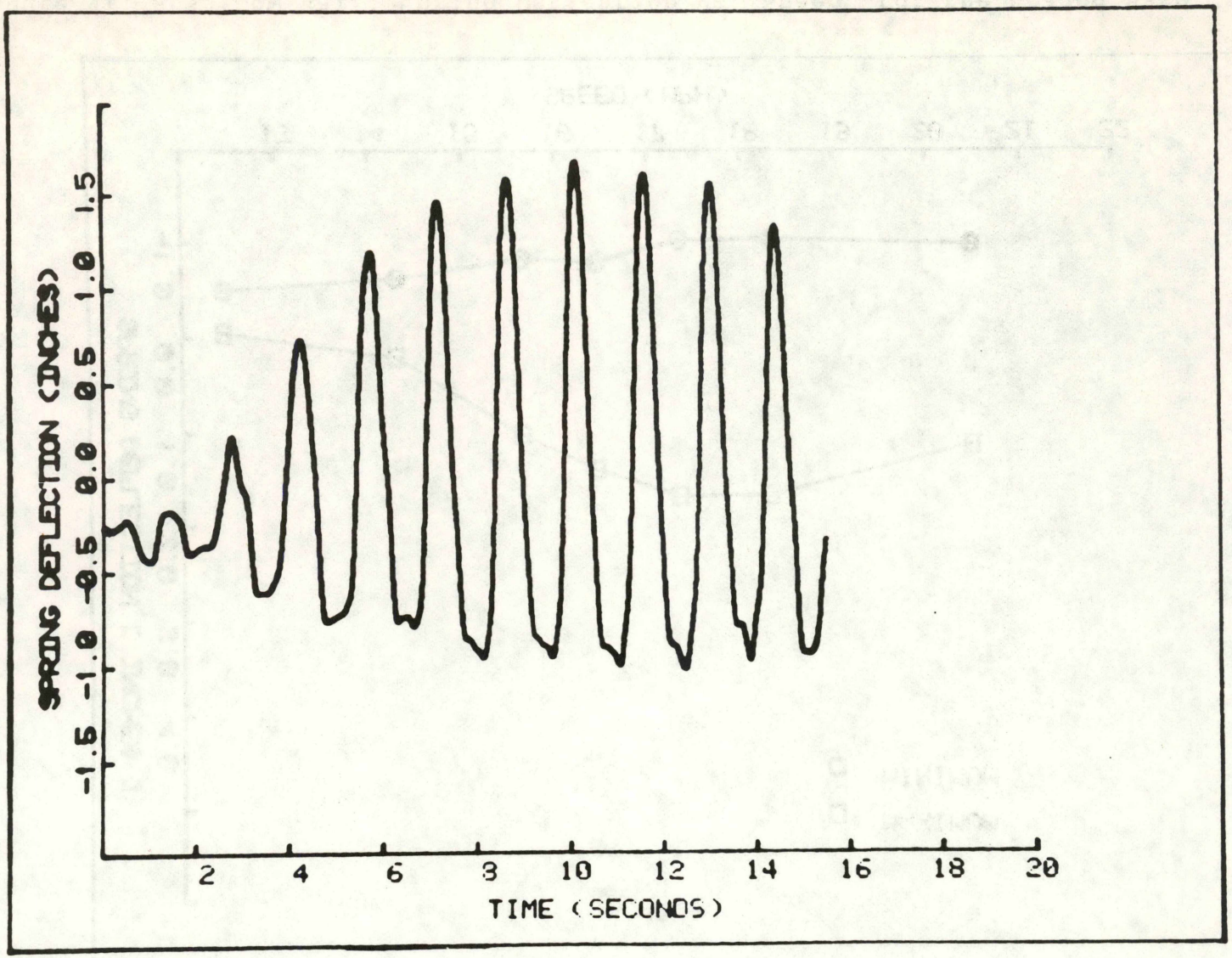

Figure 40. Spring Travel Time History, for the Loaded Base Car at 18.3 mph in the Rock-and-roll Regime on Curved Track.

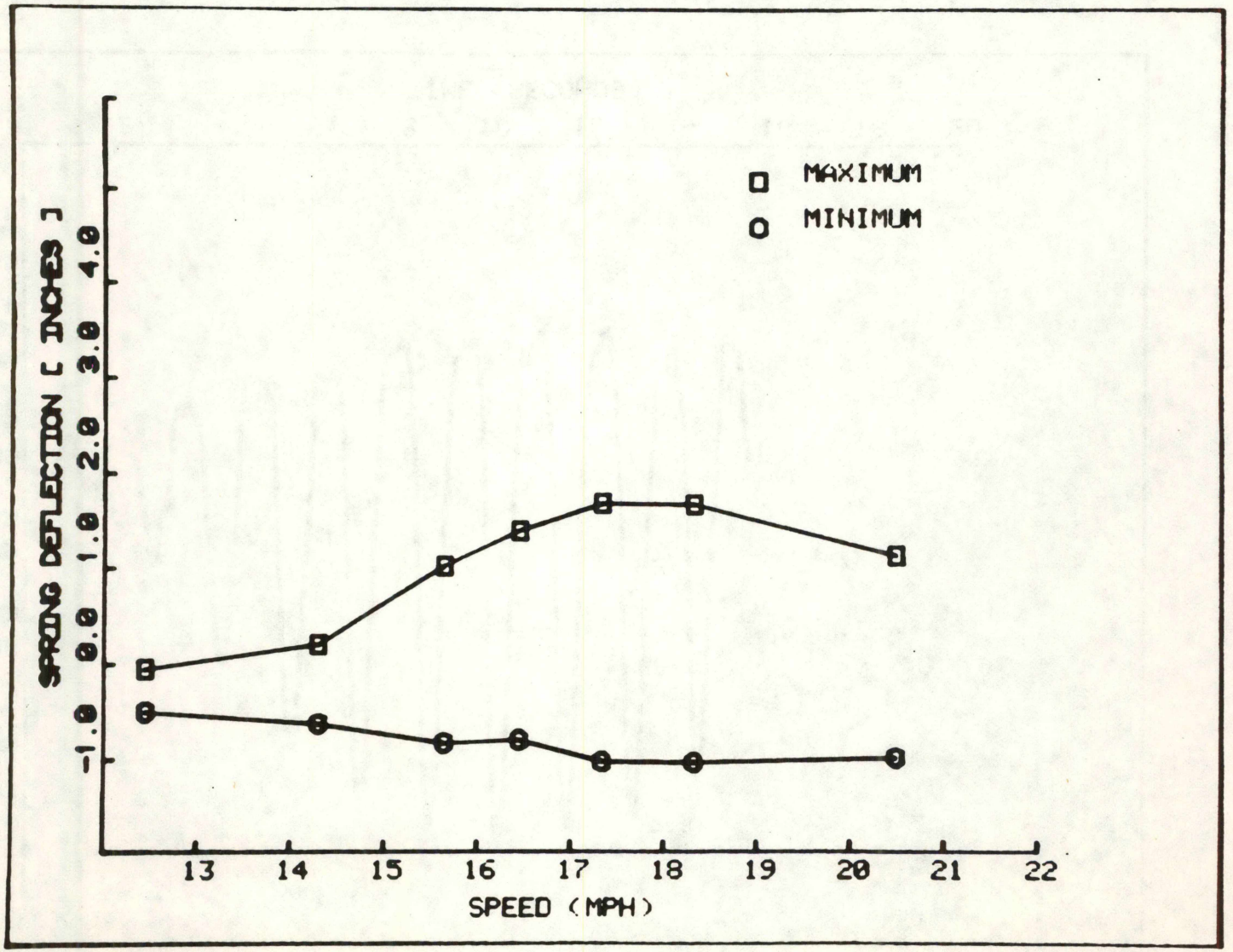

Figure 41. AL3 (Low Rail) Spring Deflection vs. Speed, for the Loaded Base Car in the Rock-and-roll Regime on Curved Track.

In both cases, however, the amplitudes of the roll motions were slightly higher for the trailing end of the car body.

2. The harmonic roll motion of the empty car was not a steady state response, but was highly nonlinear and contained high frequency components. The amplitudes of the motion rapidly increased to a peak value with increasing speed and remained at high levels above the critical speed, indicating a lack of effective damping in the system. This could be attributed to insufficient motion between the truck bolster and side frames, caused by locking action of the friction wedges when they do not slide relative to each other.

3. The vertical wheel loads, measured on the leading wheel set of the empty car, were comparable in both cases. Dynamic load factors, exceeding twice the static wheel load, and wheel lifts of short duration were noted in all of the test runs. The LTD6MIN load levels for the AL4 wheel were, however, much lower on curves than on tangent track. For the curved track, there was insufficient evidence for an increase in wheel loads for the empty car. The peak vertical loads were not developed at the same speeds as the maximum car body roll angles. This was due, in part, to excitations arising from the rail joints and random track irregularities that were present in the test track.

4. In the case of the loaded car, the resonant roll speeds for the tangent and curved track did not coincide, but were close. It should be noted, however, that no measurement was made at 17 mph (the critical speed on tangent track) on the curved track, and the trend of the roll amplitude curve showed that a peak response might exist near 17 mph. Hence, a general statement regarding the resonant roll speed can be made that the critical speed of the base car was not affected by track curvature, and resonance occurred when the car body roll natural frequencies coincided with those of the rail joint input frequency at 0.65 Hertz. Another observation, made from the roll angle time history plots, was that, unlike the empty car, the loaded car roll amplitudes rapidly decreased to lower levels at speeds beyond the critical speed of the vehicle. This was an indication of a high damping capacity in the vehicle suspension system. As noted for the empty car condition, the loaded car body rolled more on tangent track than it did on curved track, at most of the test speeds.

5. Unlike the empty car, the maximum wheel loads for the loaded car occurred at speeds near the resonant speed. The dynamic wheel loads that were measured on tangent track were higher than those on curved track. When comparing the roll response of the base car on tangent and curved track, it should be noted that the tangent track section had a stiffer track ballast

than the curved track section. As a result, higher roll angles and wheel loads could be developed on the track with the stiffer ballast. In both cases, the steady state response of the vehicle was attained a few cycles after entry into the perturbed track test section.

9.0 TEST RESULTS FOR THE PITCH-AND-BOUNCE REGIME

The observations made during the empty car bounce tests indicated no evidence of a clear resonant response of the vehicle at speeds up to 70 mph, which was the maximum speed attained during the tests. Therefore, only the results of the test data for the loaded car in the bounce regime are reported.

Selected parameters, which described the car body in the vertical plane, were used to evaluate the dynamic performance of the vehicle in the bounce regime. Vertical accelerations near the center plate locations at both ends of the car body were used to determine the critical speed of the vehicle. The leading wheel set wheel loads were used to quantify the dynamic effects of unstaggered perturbations on tangent track.

The car body acceleration response was evaluated over a frequency range of 0 to 20 Hertz, by low pass filtering the acceleration time histories at 20 Hertz.

9.1 Pitch-and-Bounce on Tangent Track

Figures 42 and 43 show the maximum car body accelerations for the A and B ends, respectively, as a function of speed. The B-end (rear) accelerations were higher than those at the A-end, and peaks of 0.9 and 1.2 g were noted at 56.3 mph for the A- and B-ends, respectively.

These curves imply that the peak response, which occurred at 56.3 mph, was near one of the car body natural frequencies in the vertical plane. An obvious assumption would be to associate this peak with the critical bounce speed. It could be seen from some of the acceleration plots that the vehicle seemed to be pitching, which could be expected for a car having a truck center distance of more than 45 feet.

To better understand the coupling of the bounce and pitch modes, a more detailed investigation was needed. In the first step, the pitch and bounce accelerations of the car body were calculated by combining the leading and trailing end accelerations, using the principles of rigid-body dynamics, as follows:

Bounce acceleration = $0.5\ (a_{43} + a_{44})$....g

Pitch acceleration = $32.2\ (a_{43} - a_{44})$ /L..rad/sec^2

where a_{43} = vertical acceleration at the A-end.

a_{44} = vertical acceleration at the B-end.

L = distance between accelerometers.

Note that this is reasonable, particular at low frequencies, because the car body of a covered hopper is

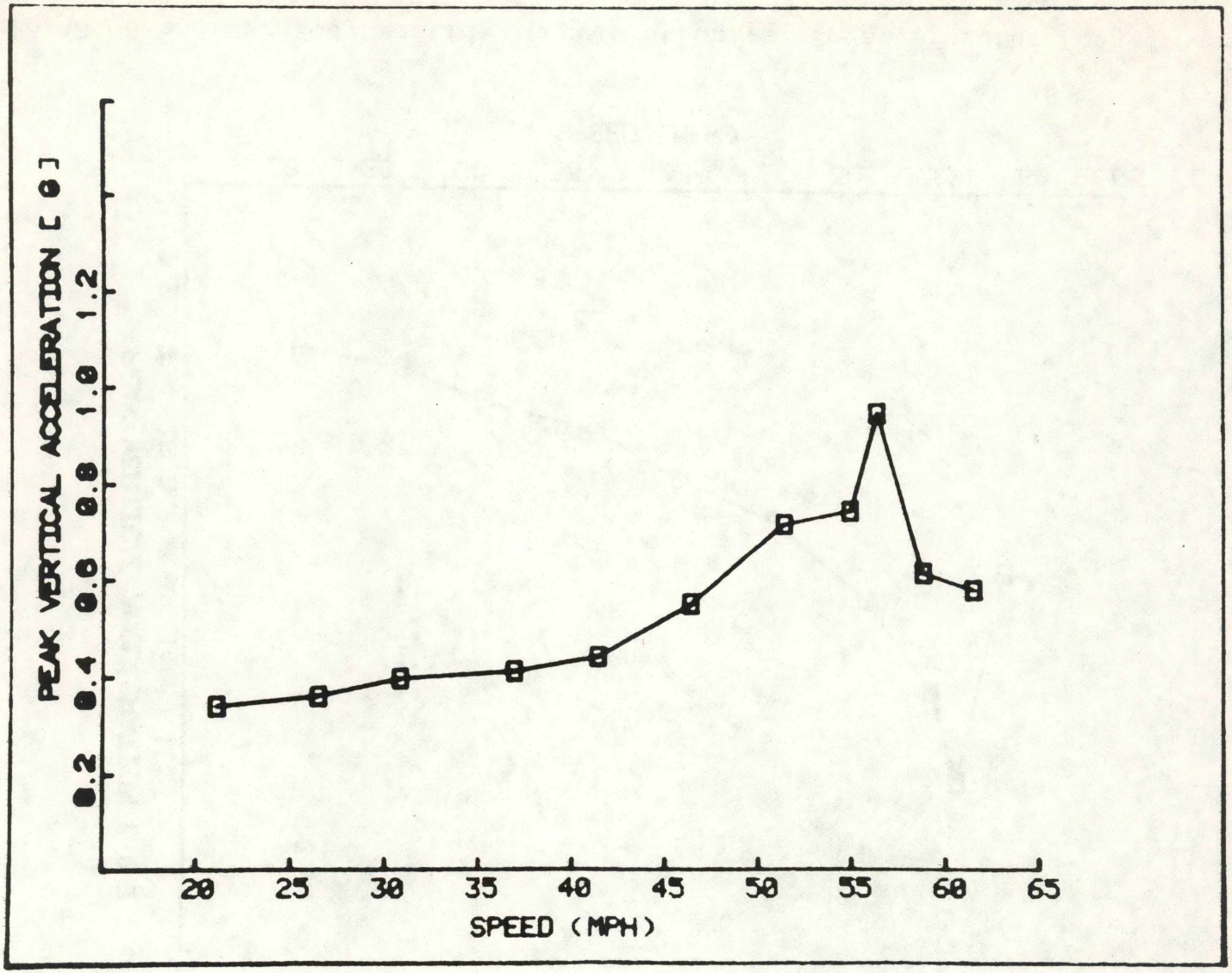

Figure 42. A-end Car Body Vertical Acceleration vs. Speed, for the Loaded Base Car in the Pitch-and-bounce Regime on Tangent Track.

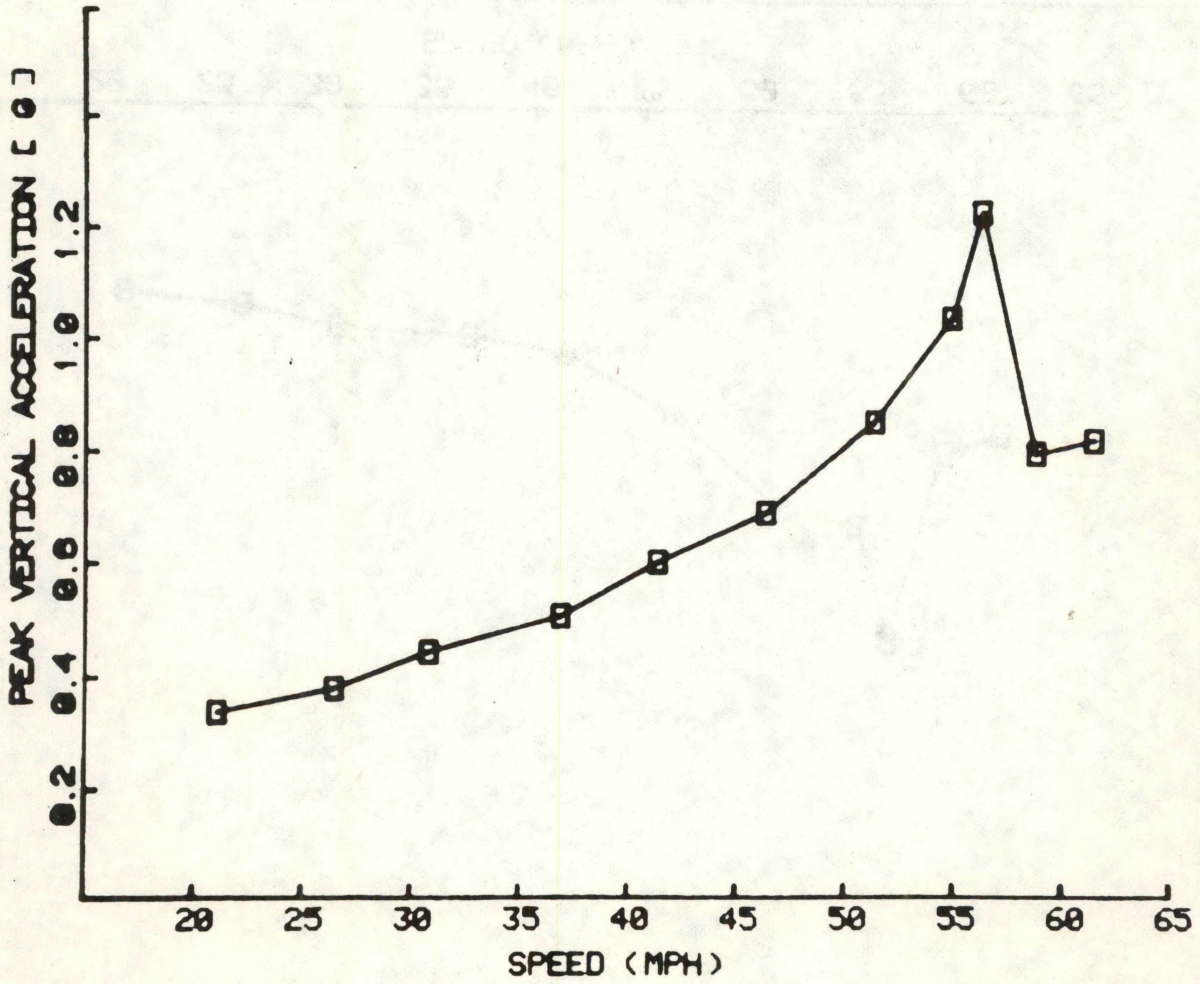

Figure 43. B-end Car Body Vertical Acceleration vs. Speed, for the Loaded Base Car in the Pitch-and-bounce Regime on Tangent Track.

stiff. Figure 44 shows the rms values of the resulting car body bounce accelerations as a function of speed. The rms bounce accelerations remained relatively constant at around 0.25 g, for speeds ranging from 20 to 45 mph, then increased to a peak value of 0.39 g at 56.3 mph. This peak clearly indicated the resonant bounce condition, in which the vehicle experienced its maximum amplitude response.

Figure 45 shows the calculated rms values of car body pitch acceleration as a function of vehicle speed. The rms pitch accelerations peaked as the vehicle speed approached the 56 mph resonant speed, and then decreased. Note that the peak pitch response speed coincided with the critical bounce speed. The vertical acceleration data clearly show the existence of the rigid body modes of pitch and bounce.

Power spectral densities of the vertical accelerations were calculated for many of the test speeds, and revealed a strong relationship between the track input and the resulting vertical car body vibrations. In general, the test track that was configured to simulate unstaggered rail joint conditions contained many periodic components. The resultant input spectra appeared, in effect, to be of a wide-band random process, with many discrete frequencies arising from these components. Each power spectrum contained dominant peaks at the corresponding rail joint frequencies and their higher harmonics. In examining

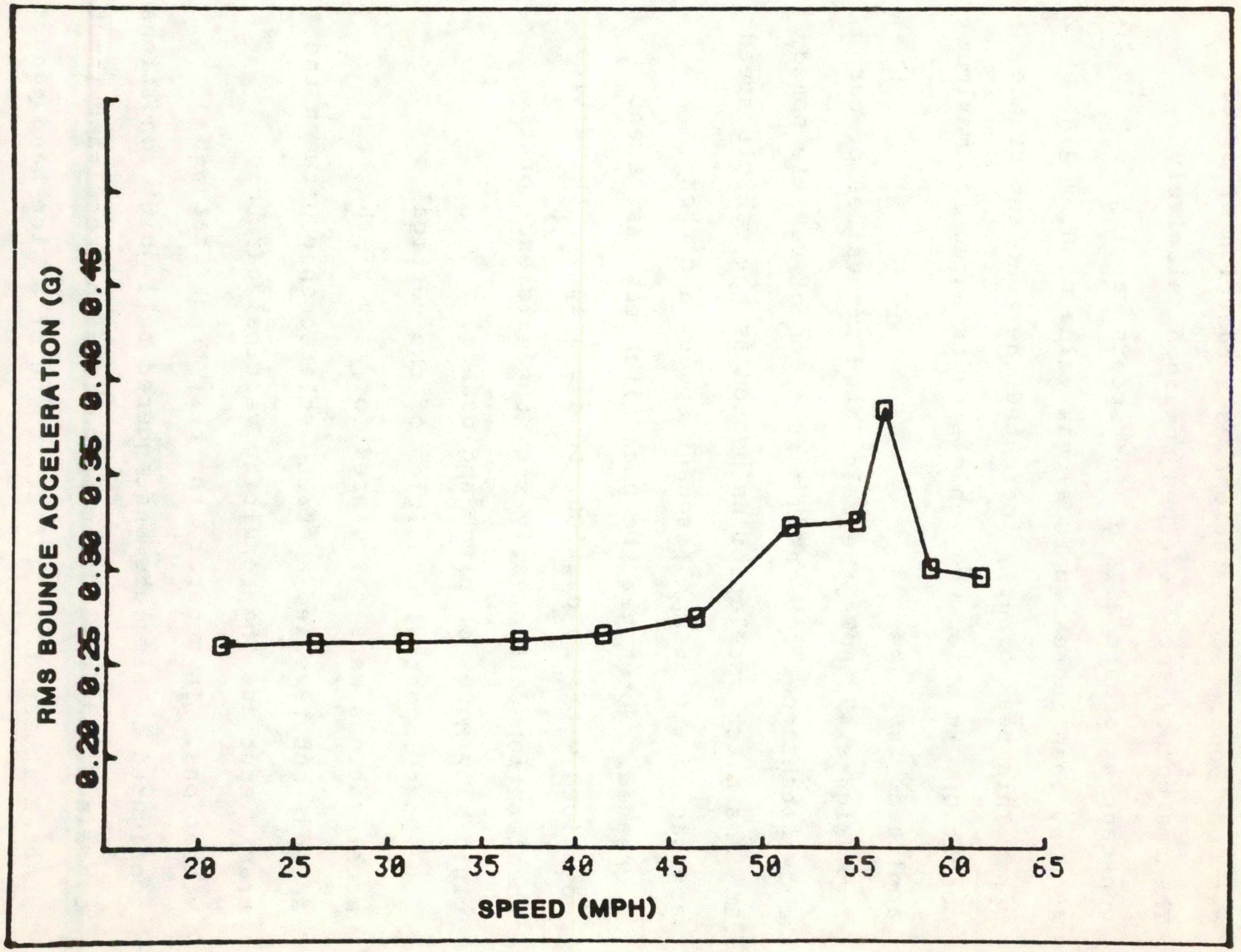

Figure 44. Calculated Root-mean-square Car Body Bounce Acceleration vs. Speed, for the Loaded Base Car in the Pitch-and-bounce Regime on Tangent Track.

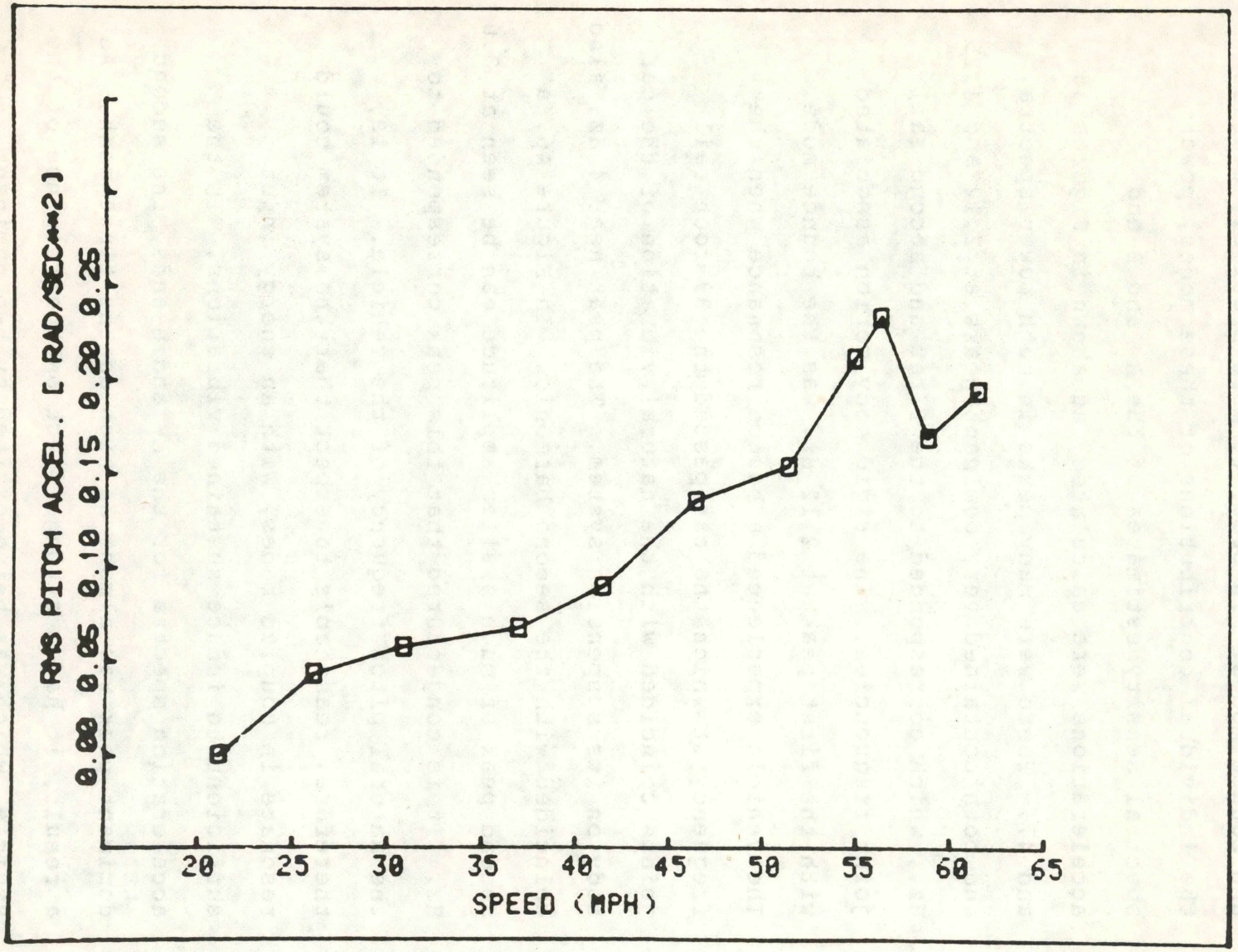

Figure 45. Calculated Root-mean-square Car Body Pitch Acceleration vs. Speed, for the Loaded Base Car in the Pitch-and-bounce Regime on Tangent Track.

the acceleration time history plots, two distinct components around the peak acceleration values could be seen, most probably from the contributions of the pitch and bounce modes. In order to more precisely evaluate the individual contributions of these modes, power spectral density estimates of the A- and B-end accelerations were calculated, as shown in Figures 46 and 47. There were many peaks in both power spectra, and both contained very dominant peaks at 2.12 and 4.25 Hz., which corresponded to the first and second rail joint frequencies. The rigid body motion associated with the first peak at 2.12 Hz. was the bounce mode. The vehicle experienced a bounce resonance when the frequency at which the car passed the 39-foot rail joints coincided with the natural vibration of the car body on its suspension system. The peak near 4 Hz. also coincided with the second harmonic. In Figure 46, a second peak of much smaller amplitude can be seen at 3.0 Hz. It is conjectured that this peak corresponded to the natural pitch frequency of the vehicle. It is, therefore, reasonable to expect that the system could resonate in coupled modes, with an energy input sufficient to induce sustained vibrations. In the acceleration spectra for the A- and B-ends, the second dominant peak was almost as high as the first peak. As a result, it had a strong effect on the response of the vehicle, which was being excited by two dominant frequencies at the same time.

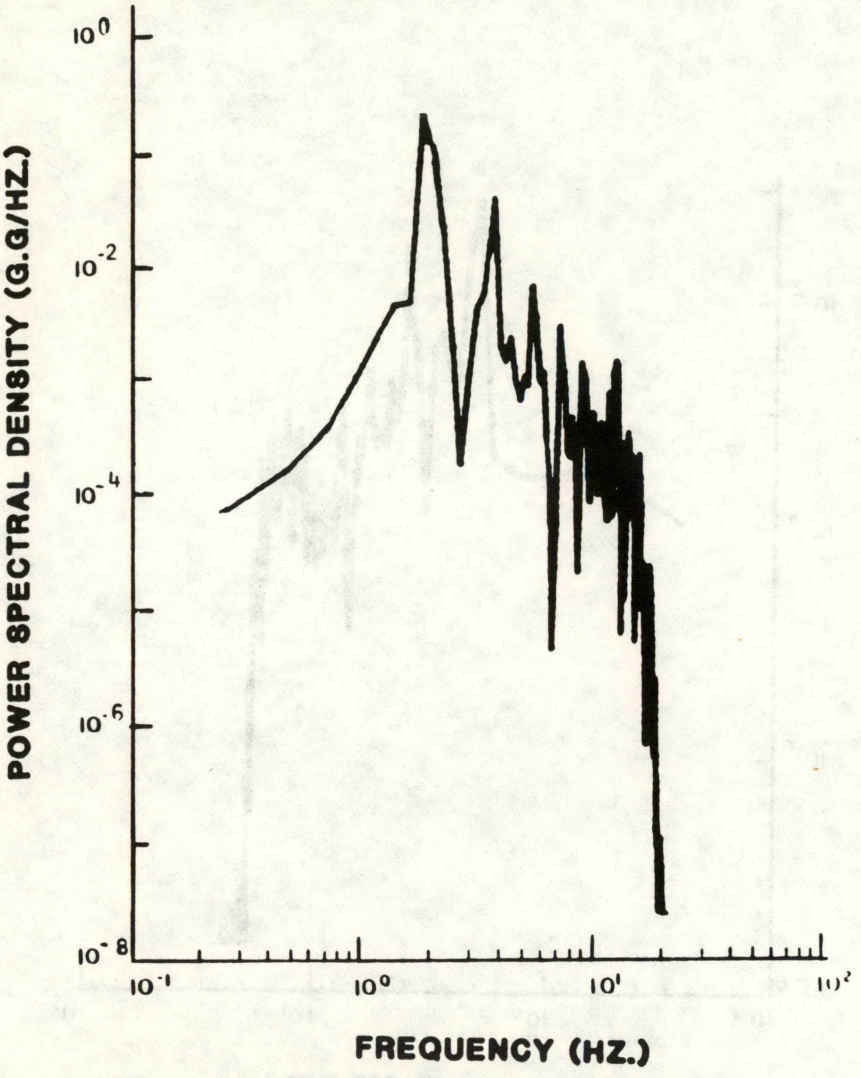

Figure 46. A-end Car Body Acceleration Power Spectral Density, for the Loaded Base Car at 56.3 mph in the Pitch-and-bounce Regime on Tangent Track.

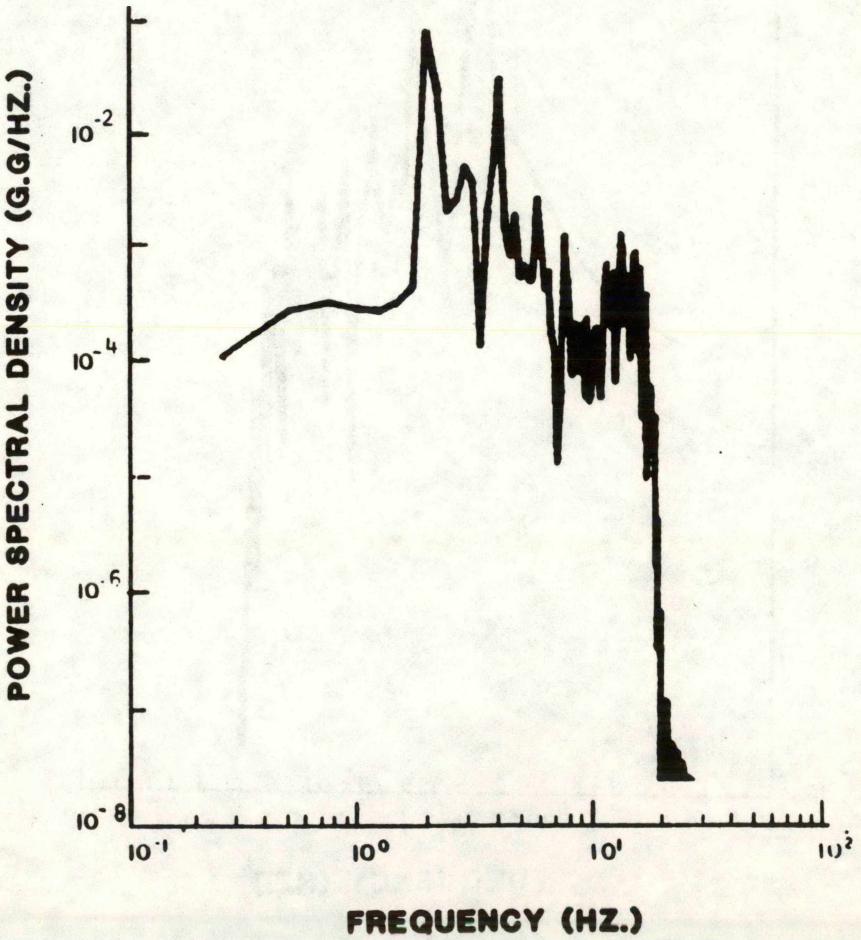

Figure 47. B-end Car Body Acceleration Power Spectral Density, for the Loaded Base Car at 56.3 mph in the Pitch-and-bounce Regime on Tangent Track.

The AR4 and AL4 vertical wheel load time histories at the resonant speed of the vehicle are shown in Figure 48. The amplitudes of the loads gradually increased, until the steady state response was achieved, and then decreased to the static load level as the vehicle moved out of the perturbed track test section.

Figure 49 illustrates the AR4 maximum and minimum wheel loadings as a function of train speed, and shows maximum loads of approximately 40,000 lb. at speeds from 20 to 45 mph, where there is no evidence of excessive vertical vibrations. As the vehicle approached its resonant speed, the wheel loads exhibited high dynamic effects. The maximum load on the right wheel increased with increasing speed to a maximum value of 58,000 lb. at 61.5 mph, representing a dynamic load factor of approximately 1.8. It can be seen in this figure that the location of the peak L95 of 46,000 lb. coincided with the resonant speed of the vehicle. The AR4 minimum wheel loads shown on the same graph decreased with increasing speeds, indicating a general increase in the peak developed by the increased dynamic effect. The minimum value of 9,500 lb. was also recorded at the resonant speed. As seen in Figure 50, the wheel loads developed on the left wheel were somewhat higher than those on the right wheel, for speeds from 20 to 50 mph, but they were comparable at the resonant speed. A maximum value of 58,000 lb. for the AL4 wheel occurred at 55 mph. The minimum loads for the same wheel

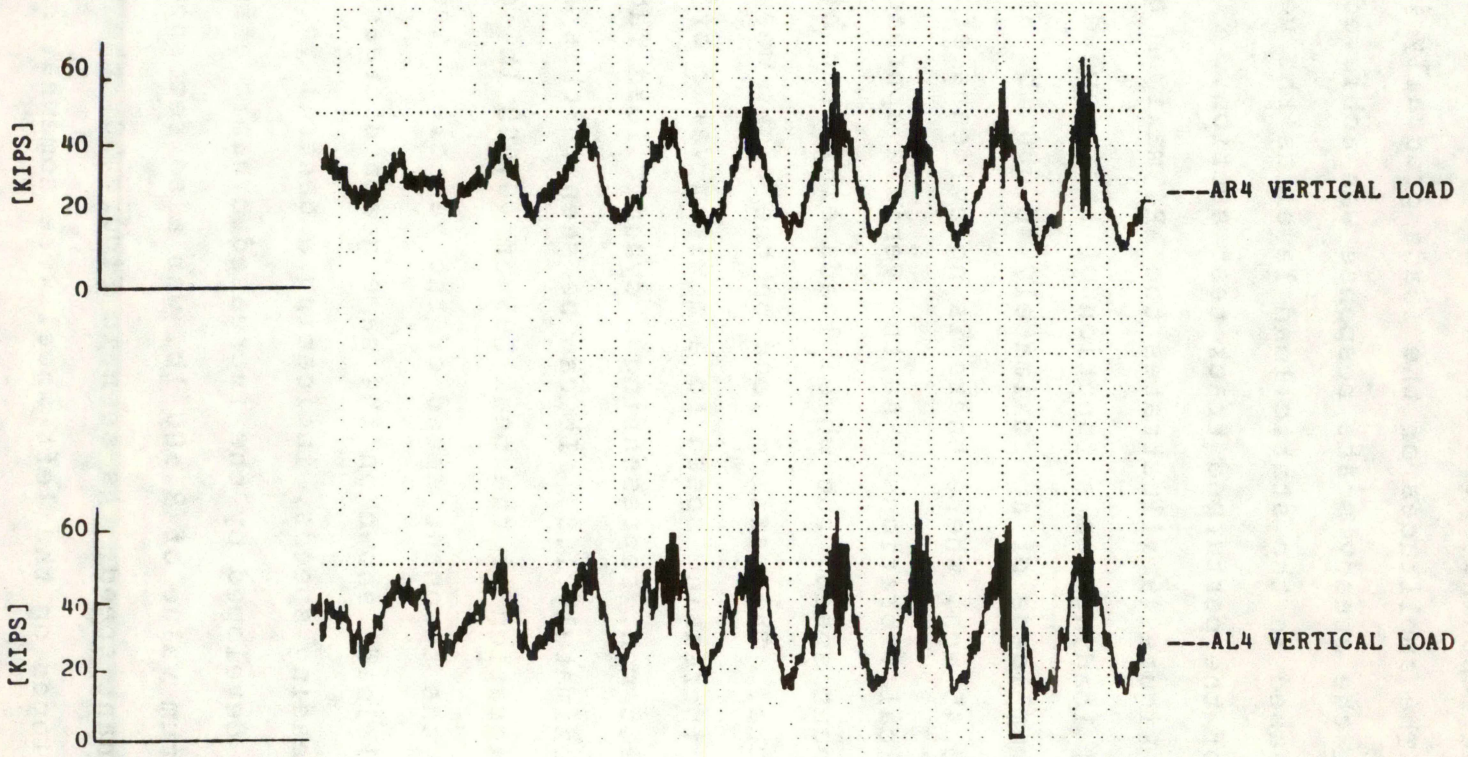

Figure 48. AR4 and AL4 Vertical Wheel Load Time Histories, for the Loaded Base Car at 56.3 mph in the Pitch-and-bounce Regime on Tangent Track.

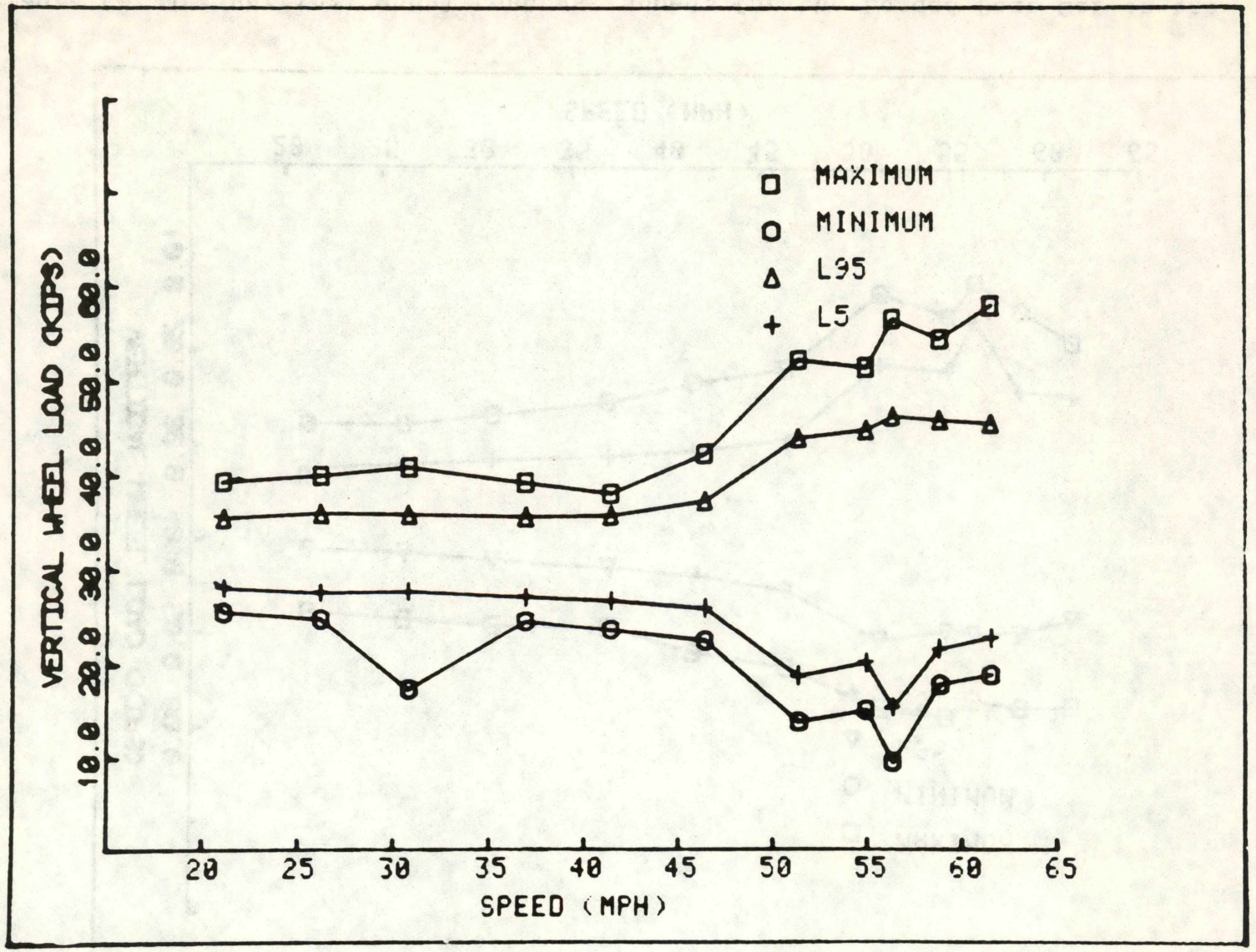

Figure 49. AR4 Vertical Wheel Load vs. Speed, for the Loaded Base Car in the Pitch-and-bounce Regime on Tangent Track.

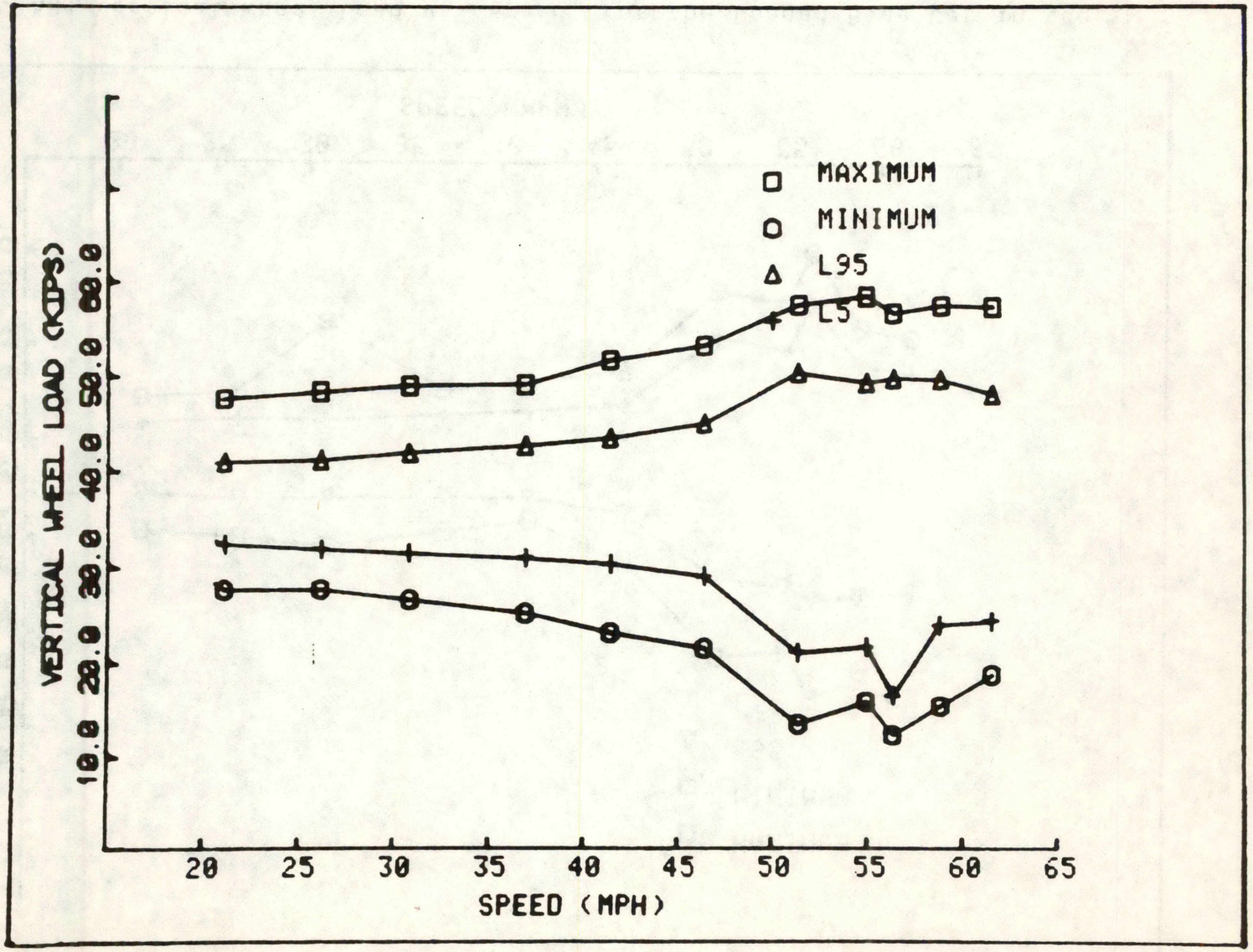

Figure 50. AL4 Vertical Wheel Load vs. Speed, for the Loaded Base Car in the Pitch-and-bounce Regime on Tangent Track.

decreased with increasing speed, reaching a minimum value of 12,000 lb. at the critical speed.

Figure 51 shows the spring deflection time history recorded on the left side of the leading truck at 56.3 mph, where the -1.13 inches of spring deflection corresponded to spring bottoming. The characteristic resonance condition, involving a gradual increase in the amplitude of oscillations in each cycle of motion, can be seen. The maximum and minimum spring travels are plotted as a function of speed in Figure 52. In the speed range of 51 to 56 mph, spring bottoming occurred, and approximately 3 inches of total spring travel occurred at 56.3 mph. Figures 51 and 52 clearly illustrate the resonance condition with the corresponding suspension spring response.

9.2 Conclusions

From the results, the following conclusions were made about the dynamic performance of the vehicle in the pitch-and-bounce regime.

1. The loaded car body vibrated at its input excitation frequencies and their higher harmonics. At speeds of 20 to 45 mph, the vertical vibrations of the car body had lower amplitudes, but were accentuated when the frequency of the rail joint inputs approached the natural frequency of the vehicle in the vertical plane. The critical bounce speed for the vehicle was 56.3 mph, which also coincided with the critical pitch speed. The

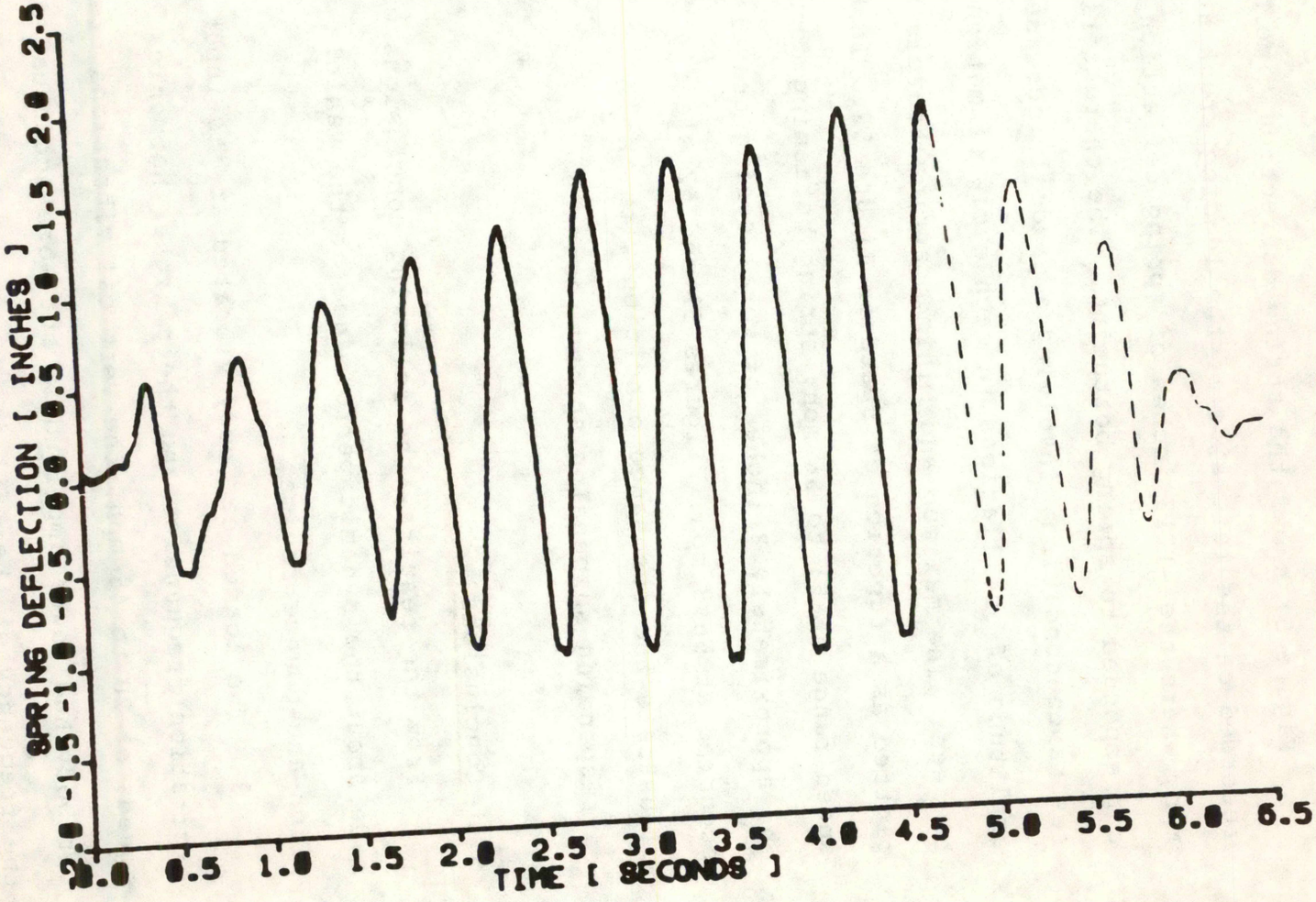

Figure 51. AL4 Spring Deflection Time History, for the Loaded Base Car at 56.3 mph in the Pitch-and-bounce Regime on Tangent Track.

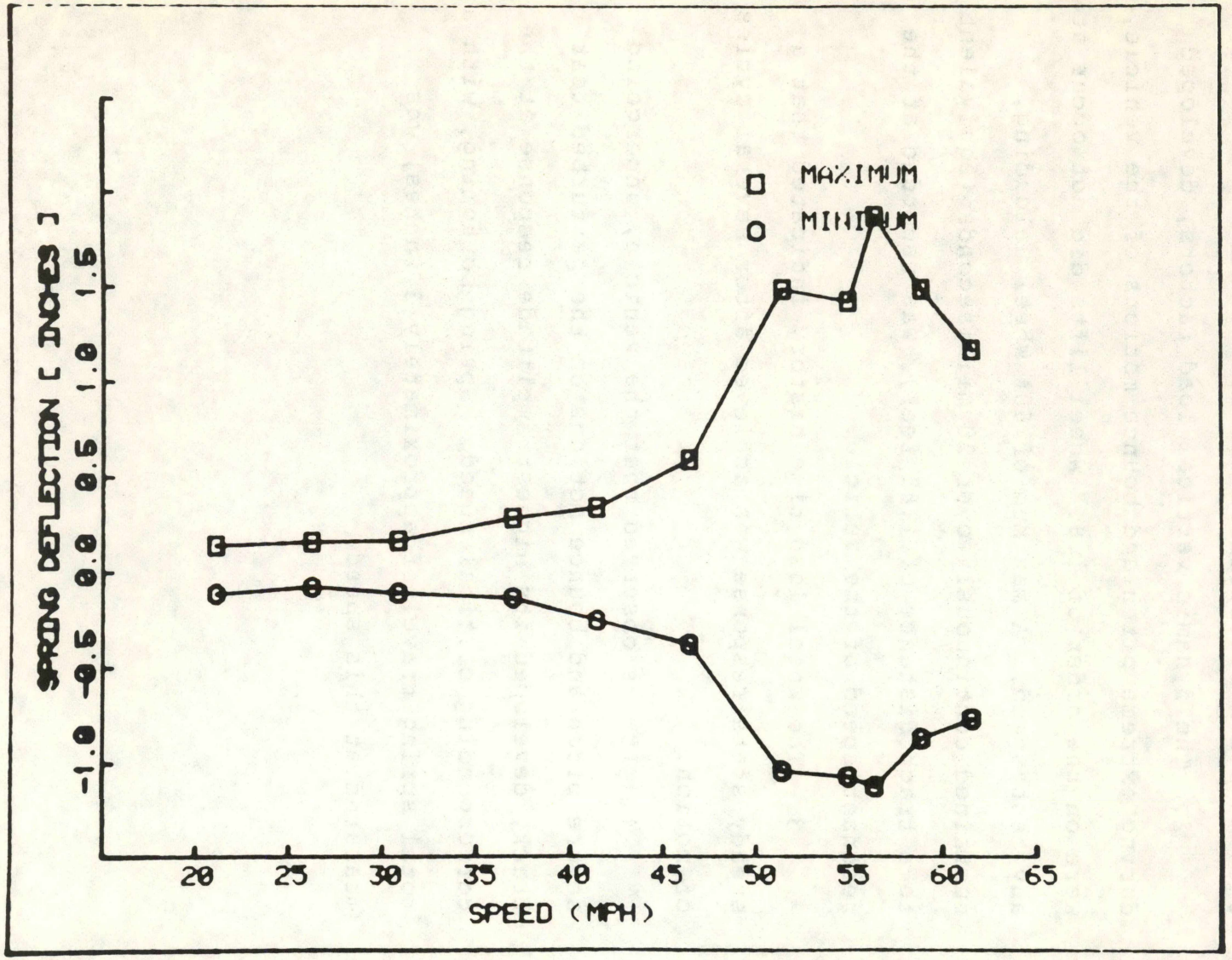

Figure 52. Maximum and Minimum AL4 Spring Deflection vs. Speed, for the Loaded Base Car in the Pitch-and-bounce Regime on Tangent Track.

maximum rms bounce acceleration of the car body was approximately 0.39 g, calculated in the frequency range of 0 to 20 Hertz. The corresponding maximum value for the rms pitch acceleration was 0.24 rad/sec^2.

2. The dynamic vertical load factors, developed during extreme pitch and bounce motions of the vehicle, were on the order of 1.8. Wheel lifts did not occur at any test speed. A maximum of 60% wheel unloading, sustained continuously over 20 milliseconds (equivalent to a track distance of 1.65 feet), was recorded at the resonant speed of the vehicle.

3. The wheel load time history indicated that a steady state response was achieved after several cycles of motion.

4. It was observed that the vehicle, undergoing severe pitch and bounce motions on the perturbed test track, developed its highest amplitude response at the corresponding critical speed. Spring bottoming, with a total spring travel of approximately 3 inches, was measured at this speed.

10.0 REFERENCES

1. Manos, W. P., and Johnstone, B., "Performance Guidelines - High Performance/High Cube Covered Hopper Car," Association of American Railroads, Report No. R-423, Chicago, Illinois, June, 1980.

2. Kalaycioglu, S. F., and Punwani, S. K., "High Performance/High Cube Covered Hopper Program, Base Car Dynamic Performance Tests. Volume 2 - Hunting," Association of American Railroads, Report No. R-568, Chicago, Illinois, April, 1984.

3. Kalaycioglu, S. F., and Punwani, S. K., "High Performance/High Cube Covered Hopper Program, Base Car Dynamic Performance Tests. Volume 3 - Curving," Association of American Railroads, Report No. R-572, Chicago, Illinois, April, 1984.

4. Kalaycioglu, S. F., and Punwani, S. K., "High Performance/High Cube Covered Hopper Program, Base Car Dynamic Performance Tests. Volume 4 - Summary" Association of American Railroads, Report No. R-581, Chicago, Illinois, June, 1984.

5. Punwani, S. K., Johnson, M. R., Joyce, R. P., and Mancillas, C., "Measurement of Wheel/Rail Forces on the High Cube, High Performance Covered Hopper Car Project," Proceedings of the ASME Rail Transportation Conference, Chicago, Illinois, Spring, 1984.

6. A. D. Little, Inc., "SDP-40F Test on the Burlington Northern Railroad," Report No. ADL 82746, Cambridge, Massachusetts, February, 1980.

7. Ramachandran, P. V., and ElMadany, M. M., "Performance Characteristics of Conventional Freight Vehicle Systems," ASME Paper No. 81-WA/RT-3, November, 1981.

8. Bendat, J. S., and Piersol, A. G., Random Data: Analysis and Measurement Procedures, Wiley - Interscience, 1971.

9. Otnes, K. R., and Enochson L., Applied Time Series Analysis, John Wiley & Sons, Inc., New York, New York, 1982.

10. Newland, D. E., Random Vibrations and Spectral Analysis, Longman, Inc., New York, New York, 1975.

11. Arslan, A. V., "The Development and Evaluation of a Six-Axle Tangent Track Locomotive Model," Proceeding of the 8th International Association for Vehicle System Dynamics (IAVSD) Symposium, Massachusetts Institute of Technology, Cambridge, Massachusetts, August, 1983.

11.0 APPENDIX A - DATA ANALYSIS METHODS

A.1 Data Pre-procesing Routines

A.1.1 Trend Removal

A.1.2 Editing of Wild Points

A.1.3 Check for Stationarity

A.2 Data Analysis Parameters

APPENDIX A - DATA ANALYSIS METHODS

The analysis of less-than-perfect physical data created by digitization, instrumentation and computer errors requires many supplementary programs for editing. In order to avoid redundancy, some of these programs are not described, and only the contents of the most often used programs are presented.

In a time series analysis, statistical concepts are generally applied. In this report, the statistical parameters that describe the basic properties of the data are the mean square and variance values, the probability density and the power spectral density functions. The mean square value describes the magnitude of the data, whereas the probability density function gives information about the data in the amplitude domain. The power spectral density function supplies similar information in the frequency domain.

The discussions assume that the data being considered are ergodic and stationary, so that its properties can be determined from time averages of individual records [8, 9, 10].

A.1 Data Pre-Processing Routines

Data often contains unwanted noise, level shifts and wild points. These errors can lead to certain inaccuracies in computing the various parameters from time series data. Some of the techniques which are used to prepare the data for appropriate analysis are discussed below.

A.1.1 Trend Removal

A least-squares procedure was used to remove trends that were inherent in the data. The general expression is given by:

$$\sum_{k=0}^{k} b_k \sum_{n=1}^{N} (n\Delta\tau)^{k+\ell} = \sum_{n=1}^{N} \bar{x}_n (n\Delta\tau)^{\ell} \quad \ell=0,1,2\ldots,k \qquad (1)$$

where:

$\bar{x}_n$ is the original sample record,

$n = 1,2,..,N$ are the data values,

$\Delta\tau$ is the sampling interval, and

b_k is the least squares coefficients.

For $K=1$ and $\ell = 1$, the above equation gives the result:

$$b_1 = \frac{12\sum_{n=1}^{N} nx_n - 6(N+1)\sum_{n=1}^{N} x_n}{\Delta\tau\, N\,(N-1)\,(N+1)} \qquad (2)$$

Hence, the removal of a linear trend can be accomplished by use of the equation:

$$\bar{x}(\tau) = x(\tau) - b_1\tau \qquad (3)$$

A.1.2 Editing of Wild Points

Wild points in the data were detected by comparing the first differences of consecutive pairs of data points, as well as by visual inspection of the time traces. Depending upon the wild point content of the data, either direct editing of the time series or smoothing by cubic-spline-fit techniques were employed.

A.1.3 Check for Stationarity

A random process is said to be stationary if its statistical properties are time invariant. These properties can be estimated from a simple sample record, rather than by the ensemble averaging of many sample records, if the data sequence is ergodic.

In the processing of the base car test data, the stationarity of the data was determined by either visual inspections, or by statistical tests when non-stationarity was suspected. The data sequence was divided into many time intervals of equal lengths, the mean square values of each data segment were then computed and the resulting sequence run tested for the presence of time variance. Inspection of the probability density and power spectral density plots revealed the normality and periodicity, if present, in the sample records.

A2. Data Analysis Parameters

The statistical descriptors used in the analysis of individual test records are outlined, as follows:

Maximum value: the positive peak value of the time series after smoothing.

Minimum value: the negative peak value of the time series after smoothing.

Mean value: the average value of the data sequence, given by:

$$\mu_x = \frac{1}{N} \sum_{n=1}^{N} x(n) \qquad (4)$$

Mean square value: the average of the squared values of the time series and computed by using the equation:

$$\psi_x^2 = \frac{1}{N} \sum_{n=1}^{N} x^2(n) \qquad (5)$$

In this report, the positive square root value of the mean square value is called the rms value.

Variance: the mean square value about the mean. In equation form it is given by:

$$\sigma_x^2 = \psi_x^2 - \mu_x^2 \qquad (6)$$

In this report, the positive square root value of the variance is called the standard deviation.

Power Spectral Density

A power spectral density function (PSD) gives the distribution of mean square values of a variable with respect to frequency. The power spectral estimate of a time history is obtained by means of a Blackman-Tukey Fast Fourier Transform (FFT) procedure [8]. The entire procedure is briefly described as follows:

1. Time Averaging.

   The stationary data sequence is divided into segments, such that the number of points in each segment is a power of two. The data in each section are then transformed to the zero mean value.

2. Cosine Tapering.

Each resulting sequence is multiplied by a data window to suppress the large side lobes obtained by means the FFT transformation in the frequency domain. This is the tapering employed to round off the potential discontinuities at each end of the finite segment of the time history being analyzed, when looked at from the time domain standpoint.

3. Fourier Component Calculations.

The Fourier components are calculated at the following discrete frequency values:

$$F_k = \frac{k}{n\Delta\tau} \quad k=0,1,2,\ldots,N-1 \tag{7}$$

The Fourier components are then calculated from the equation:

$$x = \sum_{n=1}^{N-1} x_n \exp\left[-j\frac{2\pi kn}{N}\right] \tag{8}$$

4. Power Spectrum Estimates.

The power spectrum estimates are calculated and adjusted for the tapering scale factor, as follows:

$$\tilde{S}_k = \frac{1}{0.875}\,\frac{2\Delta\tau}{N}|x_k|^2 \quad \text{for } k=0,1,2,\ldots,N-1 \tag{9}$$

5. Estimate Smoothing

The power spectrum estimates are smoothed by segment averaging, using the following equation:

$$\tilde{S}_k = \frac{1}{q} [\tilde{S}_{k,1} + \tilde{S}_{k,2} + \ldots + S_{k,q}] \qquad (10)$$

where q denotes the number of segments used in the PSD averaging.

L95 and L5 Values

Figure A-1 shows a sample time history for a random process, with the times for which $x \leq x(t) \leq x+dx$

If there are N sample values, dn of these values lie in the band x to x+dx; then, the probability density function is given by:

$$p(x)dx = \frac{dn}{N} , \qquad (11)$$

where p(x)dx is the fraction of total number of samples that lie in the band from x to x+dx.

The L95 and L5 values of a parameter are determined by using this principle. An interval over the range of x, say $a \leq x \leq b$, is divided into 1000 subintervals of equal length. All of the data are examined and the number of occurrences in each interval is determined. Then an estimate of p (x) is obtained by dividing the number of occurrences in each interval by the sample size N, as shown above. This is equivalent to summing all of the time spent in each interval of x and dividing by the total elapsed time.

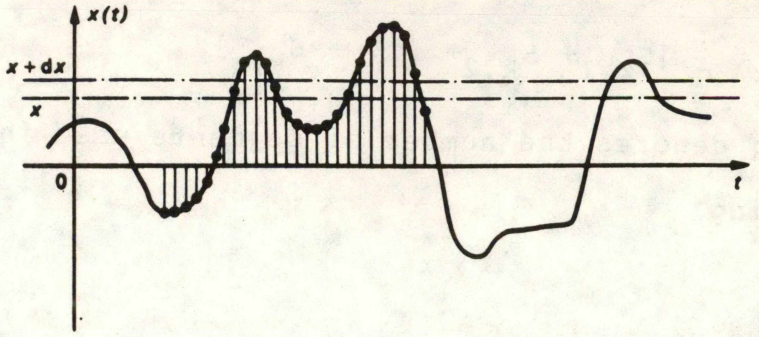

Figure A-1. Digitized Sample Time History for a Random Process, Illustrating the Methodology for Calculating the Probability Density.

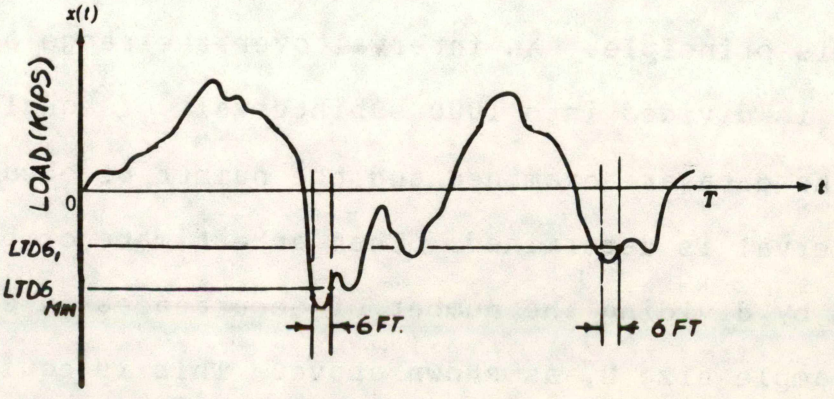

Figure A-2. Calculation of the LTD6 Value for a Random Process.

The probability that x is less than or equal to a certain value x_i, for example, the level representing the 95th percentile value, is obtained from the probability density function p (x) by summing the probabilities of all x's up to and including x_i.

LTD6 Values

In a time series analysis, the time duration of the extreme values of a parameter of interest, for example the wheel loads, are of great importance. According to the Performance Guidelines, the extreme values of the wheel loads which are continuously sustained over six feet of track are used to quantify the dynamic load performance of the vehicle.

An algorithm was developed [11] and a digital computer program written to determine the minimum load level, called LTD6MIN, which was used to quantify the wheel unloadings in the rock-and-roll regime, and in which the load was continuously sustained over six feet of a track segment.

Consider a test run made at 14 mph. Over a 6 foot distance, and at a sampling rate of 256 per second, the number of data points digitized would be approximately 75. Therefore, the program searches for the minimum level within the time history of the variable for which 75 data points continuously exist. See Figure A-2.

High Performance, High Cube Covered Hopper Program Base Car Dynamic Performance Tests: Volume 1 - Rock-and-Roll & Bounce(TTD), 1984- Association of American Railroads, SF Kalaycioglu, SK Punwani